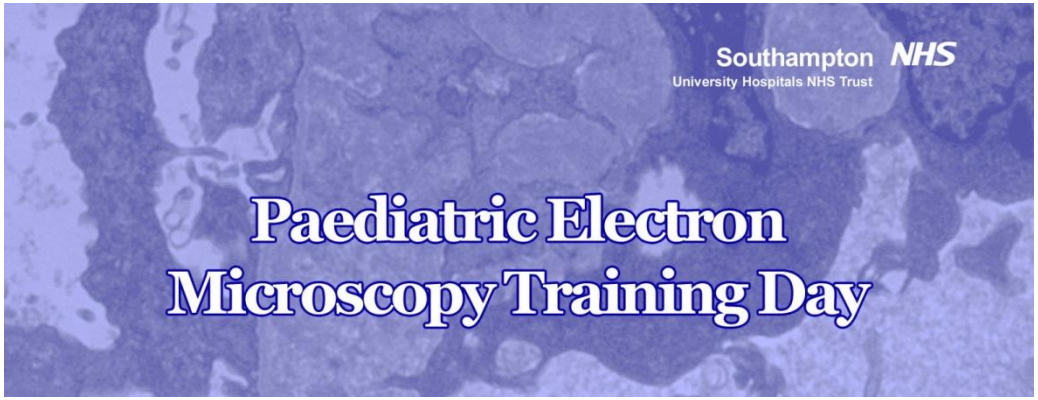

Pitfalls in Paediatric EM
or
Mistakes, I've made a few.

Friday 4th October 2013

Bart Wagner
Chief Biomedical Scientist
Histopathology Department
Royal Hallamshire Hospital
Sheffield
UK
bart.wagner@sth.nhs.uk

Hopefully this lecture will help you avoid a few of those

from

to

moments

Cases..

- Renal
- GI tract
- Blood

- 5 minute break

- Skin
- Heart
- Platelet review

Renal biopsy (1990)

- Patient: 14 year old boy with haematuria
- Clinical suspicion: IgA
- IF: Negative
- Histology: Normal
- EM: Thin GBM’s. No deposits.
- Diagnosis: Benign familial haematuria
- Prognosis: Good

Thin GBM

14 year old boy with persistent haematuria

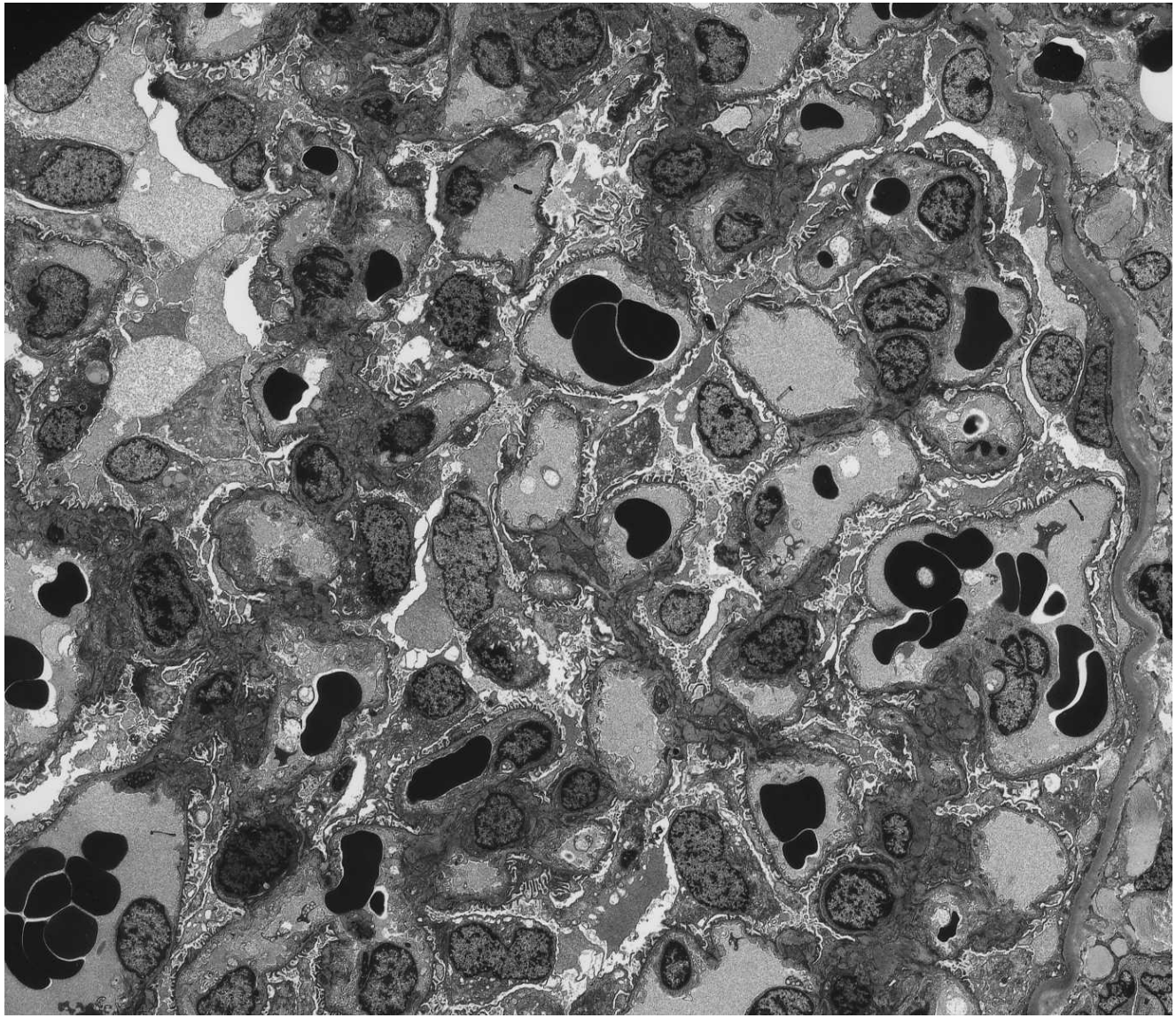

Normal on histology

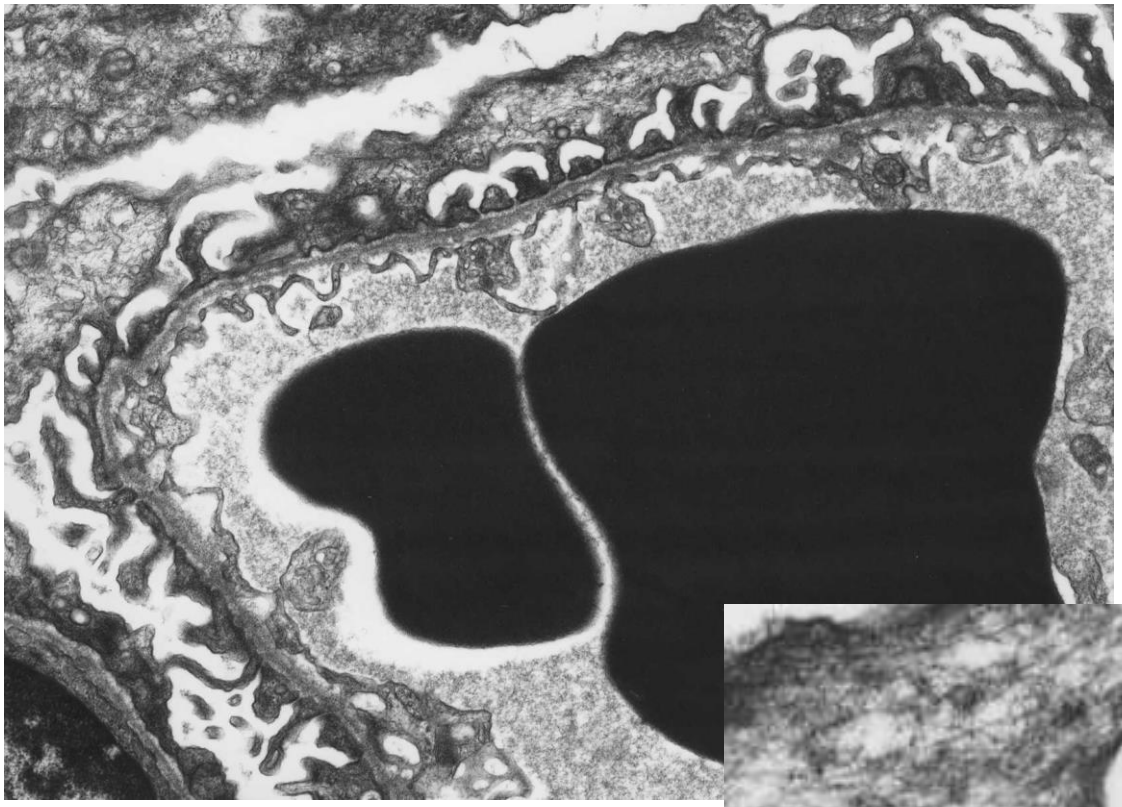

Thin GBM
14 year old boy with
persistent haematuria

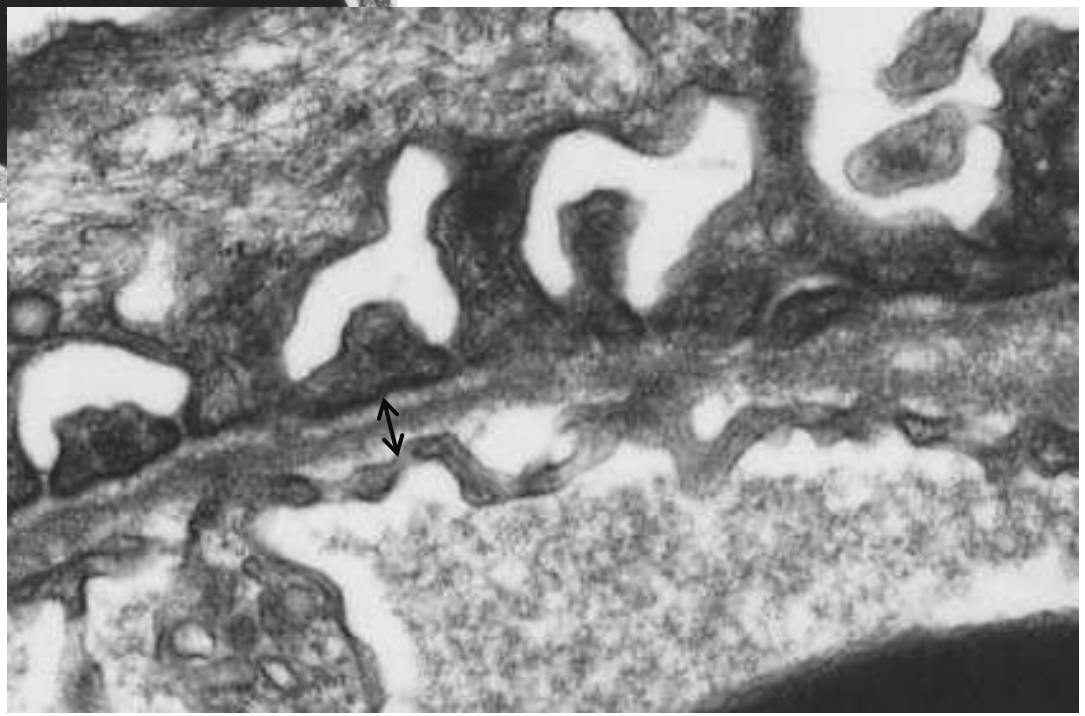

Mean GBM diameter 140nm
(Normal for age 270nm)

Histopathology. 1990 Apr;16(4):331-7.

Thin basement membrane nephropathy as a cause of recurrent haematuria in childhood.

Lang S, Stevenson B, Risdon RA.

Source
Department of Histopathology, Great Ormond Street Hospital for Sick Children, London, UK.

Abstract
A survey of 69 children presenting with recurrent or persistent haematuria and submitted to percutaneous renal biopsy at this hospital over a 17-year period, was performed to establish the incidence of thin basement membrane nephropathy (TBMN). A diagnosis of primary glomerular disease was established in 44 (IgA nephropathy in 16, Alport syndrome in 13 and other varieties of glomerulonephritis in 15). Of the remaining 25 patients in whom light microscopical and immunochemical examination revealed no abnormalities, material for electron microscopy was available in 11. In eight of these (five of whom had a family history), TBMN was diagnosed on the basis of ultrastructural morphometric evaluation of glomerular basement membrane thickness. Assuming a similar proportion of the remaining 14 patients with renal biopsy specimens normal by light microscopy had TBMN, the probable frequency of this abnormality in the whole series would be 26%, very similar to that of IgA nephropathy. **In the eight TBMN patients the mean glomerular basement membrane thickness ranged between 181 and 236 nm, whilst in 'control' biopsies from children with 'minimal change' nephrotic syndrome or IgA nephropathy, the mean thickness ranged between 242 and 333 nm.**

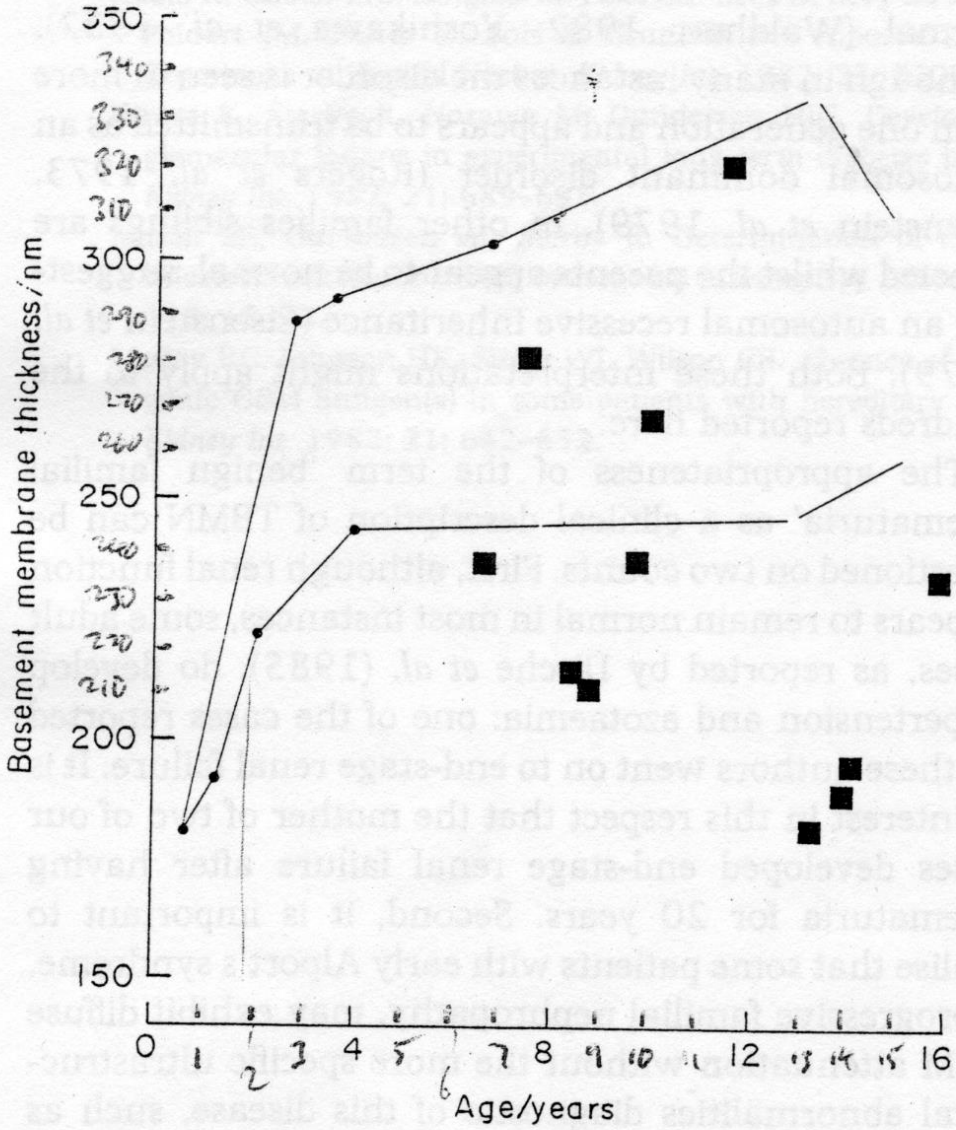

Figure 3. Harmonic mean of glomerular basement membrane thickness in the test cases (■) plotted against age. The lines indicate the maximum and minimum values in the controls (see Figure 2).

Histopathology. 1990 Apr;16(4):331-7.
Thin basement membrane nephropathy as a cause of recurrent haematuria in childhood.
Lang S, Stevenson B, Risdon RA.

Back to thin GBM disease case

- 7 years later (age 21)
- Increasing head aches.
- Collapse
- Chronic renal failure.
- Accelerated phase hypertension.
- Dialysis.
- Renal transplant soon after.
- Diagnosis reviewed.
- X-linked Alport's (ie COL4A5)

Thin GBM disease case, the silver lining...

- The patient later married the nurse who looked after him on the renal unit
- They now have a healthy son

Reminder:
Classical Alport nephritis EM as seen in adults

Alport nephritis:

21 year old male
Nephrotic syndrome
Haematuria
Normal creatinine clearance

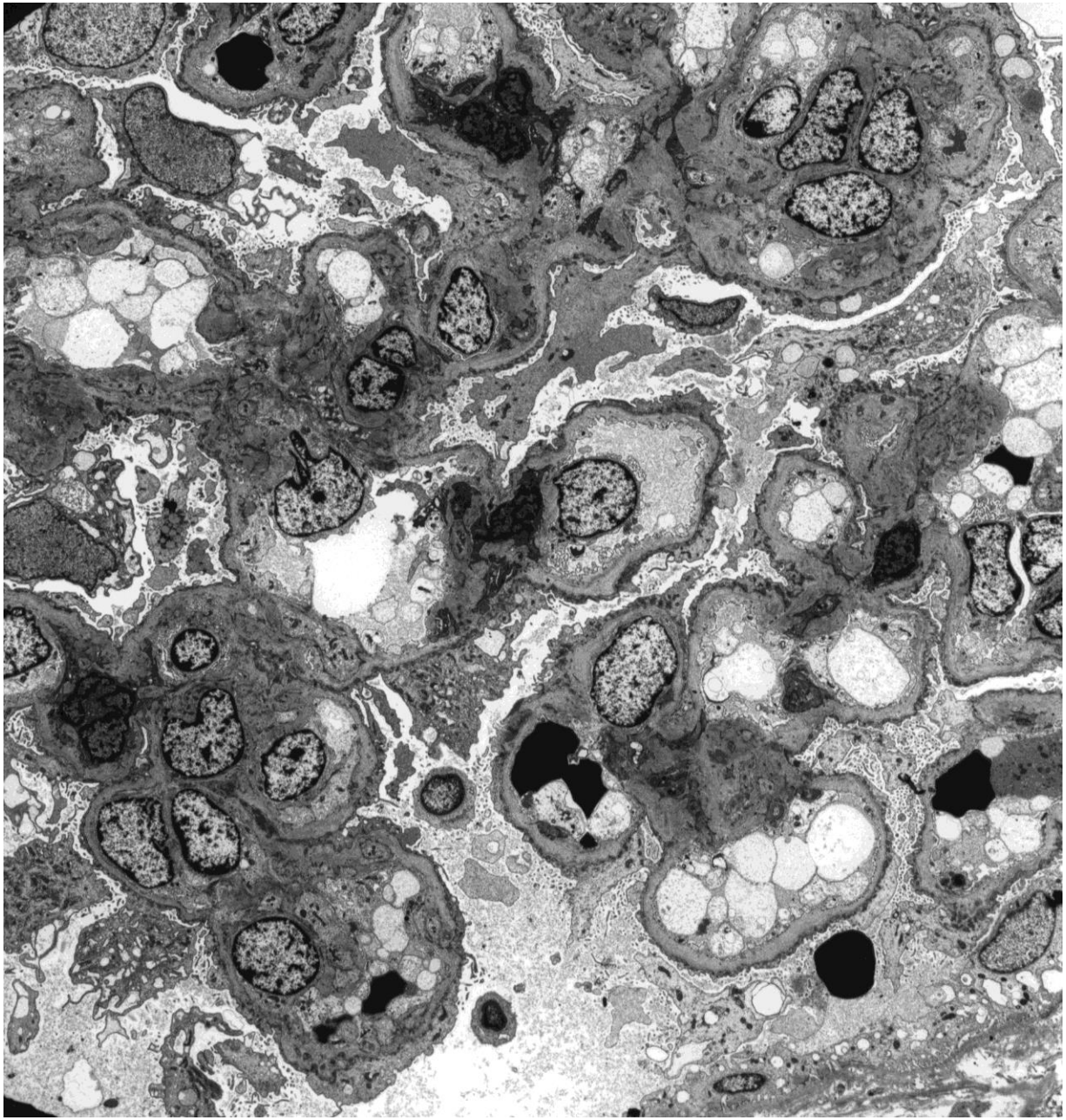

Typical x-linked Alport nephritis case
21 year old male
Nephrotic syndrome and haematuria
Normal creatinine clearance

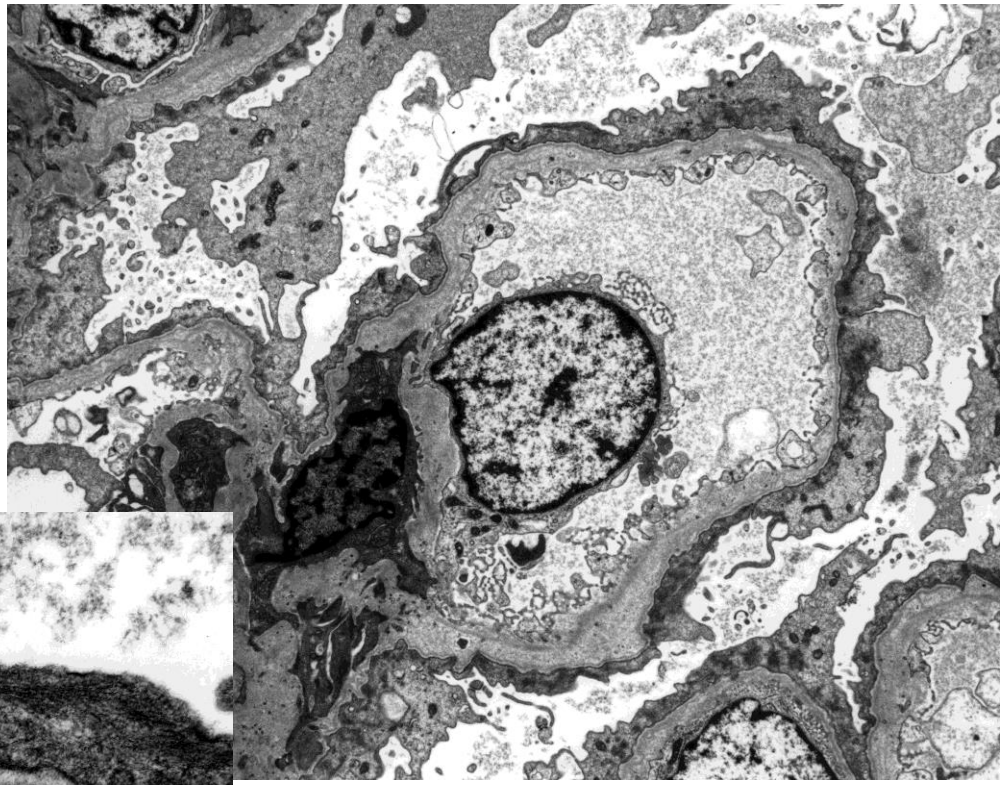

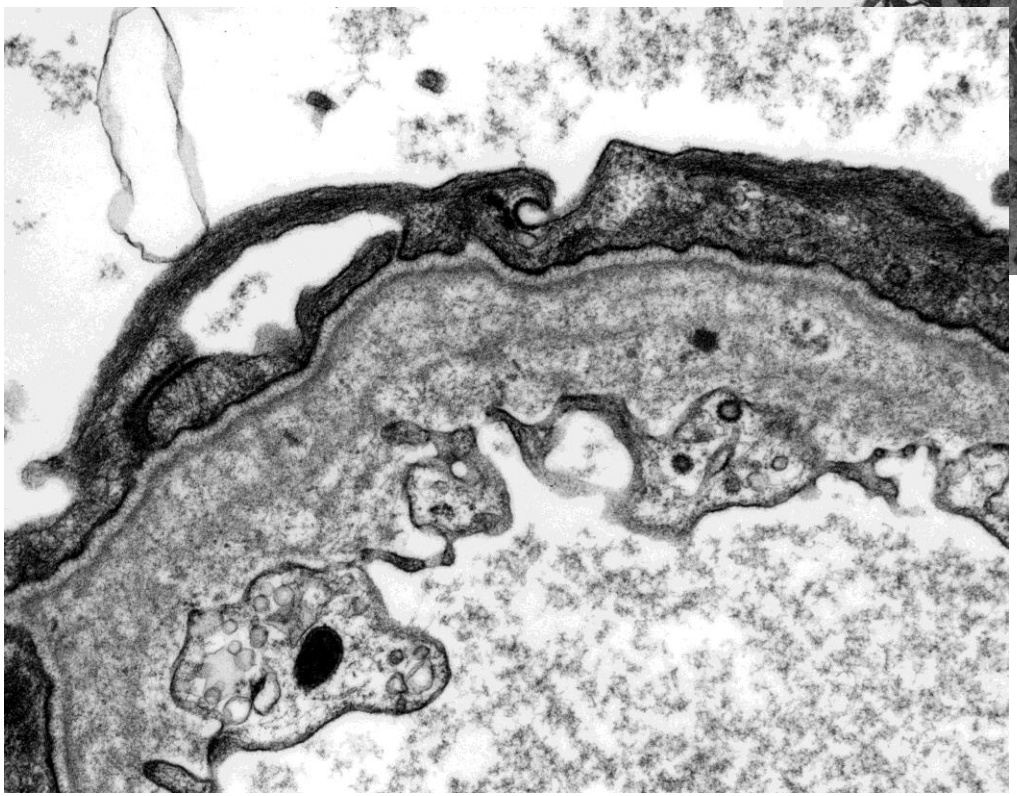

GBM's not thin -
but would have been when young.
GBM reduplication/lamination/basket weave.
Severe podocyte foot process effacement.

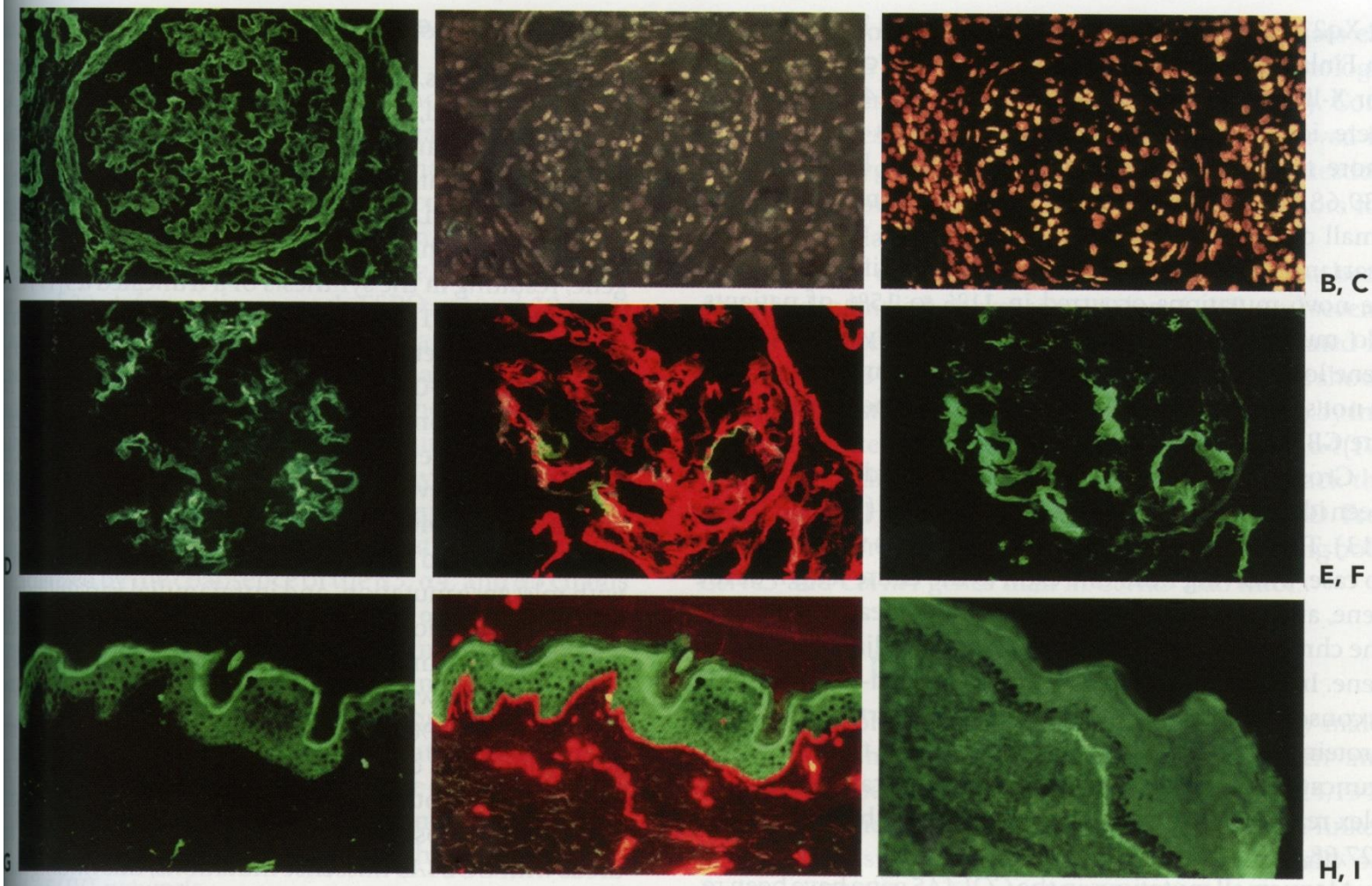

Figure 11.7 Immunofluorescence distribution of type IV collagen chains in renal (**A–F**) and epidermal (**G–I**) basement membranes of patients affected with X-linked Alport's syndrome. In a male patient (**A–C**), no α3 or α5(IV) labeling (**B, C**), contrasting with the strong linear α1(IV) labeling of the GBM (**A**). In a female patient (**D–F**), discontinuous α5(IV) GBM labeling (**D, F**), with strong α2(IV) labeling of α5(IV)-negative GBM segments (**E**). No EBM α5(IV) staining in a male patient (**G**), with preservation of α2(IV) labeling (**H**). Segmental α5(IV) labeling in a female patient (**I**). (α1, α3, α5: FITC; α2: Texas red.)

X linked Alport Male

No COL4A3 orA5

X linked Alport Female

Discontinuous COL4A5

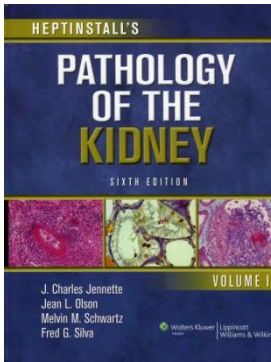

J Am Soc Nephrol. 2013 Feb;24(3):364-75. doi: 10.1681/ASN.2012020148. Epub 2013 Jan 24.

Expert guidelines for the management of Alport syndrome and thin basement membrane nephropathy.

Savige J, Gregory M, Gross O, Kashtan C, Ding J, Flinter F.

Source

Department of Medicine (Northern Health), University of Melbourne, Melbourne, Australia. jasavige@unimelb.edu.au

Abstract

Few prospective, randomized controlled clinical trials address the diagnosis and management of patients with Alport syndrome or thin basement membrane nephropathy. **Adult and pediatric nephrologists** and geneticists from four continents whose clinical practice focuses on these conditions have developed the following guidelines. The 18 recommendations are based on Level D (Expert opinion without explicit critical appraisal, or based on physiology, bench research, or first principles-National Health Service category) or Level III (Opinions of respected authorities, based on clinical experience, descriptive studies, or reports of expert committees-U.S. Preventive Services Task Force) evidence. **The recommendations include the use of genetic testing as the gold standard for the diagnosis of Alport syndrome and the demonstration of its mode of inheritance**; the need to identify and follow all affected members of a family with X-linked Alport syndrome, including most mothers of affected males; the treatment of males with X-linked Alport syndrome and individuals with autosomal recessive disease with renin-angiotensin system blockade, possibly even before the onset of proteinuria; discouraging the affected mothers of males with X-linked Alport syndrome from renal donation because of their own risk of kidney failure; **and consideration of genetic testing to exclude X-linked Alport syndrome in some individuals with thin basement membrane nephropathy.** The authors recognize that as evidence emerges, including data from patient registries, these guidelines will evolve further.

Learning point

- In 1990 we didn't know that in childhood, Alport's nephritis starts off looking like benign hereditary thin GBM disease ultrastructurally.

Any questions?

Next case

Rectal biopsy (1997)

- 11 year old girl
- Constipation requiring constant treatment
- Urinary tract infections only prevented by prophylactic antibiotics
- Rectal biopsy to support clinical diagnosis of:
  hollow visceral myopathy

  pseudo-obstruction

  gut dysmotility disoder

  enteric smooth muscle disease

  gastro-enteric neuromuscular diseases

  inherited visceral myopathy

Table from Morson and Dawson's GI Path book

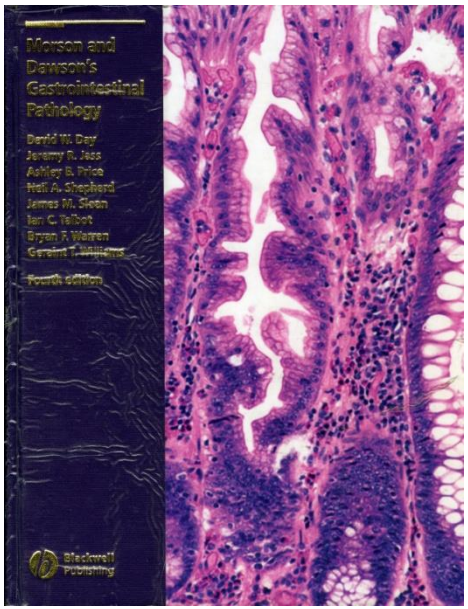

Table 35.1 Causes of chronic colonic pseudo-obstruction and megacolon.

SMOOTH MUSCLE DISORDERS

Primary

Inherited visceral myopathy:

1 autosomal dominant

2 autosomal recessive

Sporadic visceral myopathy

Secondary

Collagen diseases:

1 scleroderma

2 dermatomyositis

Myotonic dystrophy

Progressive muscular dystrophy

Amyloidosis

NEUROLOGICAL DISORDERS

Primary

Inherited disorders:

1 familial visceral neuropathies (autosomal recessive)

2 neurofibromatosis

3 ganglioneuromatosis in multiple endocrine neoplasia type IIb

Developmental disorders:

1 Hirschsprung's disease

2 hypoganglionosis

3 hyperganglionosis (neuronal colonic dysplasia)

Sporadic visceral neuropathy:

1 Shy–Drager syndrome

2003

Patient thought to have one of these.

One type is thought to be cause by a mutation in an smooth muscle actin gene

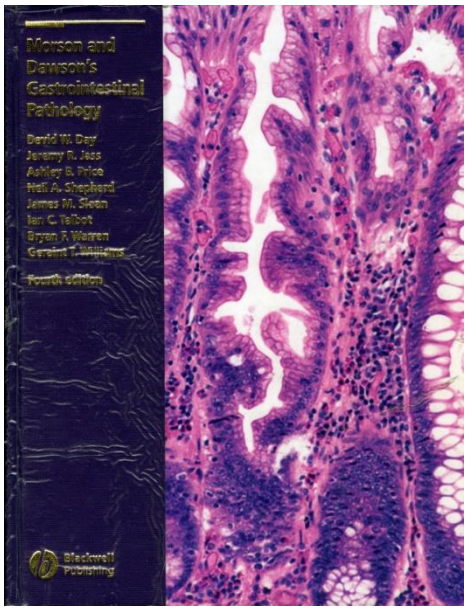

Table 35.1 Causes of chronic colonic pseudo-obstruction and megacolon.

SMOOTH MUSCLE DISORDERS

Primary

Inherited visceral myopathy:

1 autosomal dominant

2 autosomal recessive

Sporadic visceral myopathy

Secondary

Collagen diseases:

1 scleroderma

2 dermatomyositis

Myotonic dystrophy

Progressive muscular dystrophy

Amyloidosis

NEUROLOGICAL DISORDERS

Primary

Inherited disorders:

1 familial visceral neuropathies (autosomal recessive)

2 neurofibromatosis

3 ganglioneuromatosis in multiple endocrine neoplasia type IIb

Developmental disorders:

1 Hirschsprung's disease

2 hypoganglionosis

3 hyperganglionosis (neuronal colonic dysplasia)

Sporadic visceral neuropathy:

1 Shy–Drager syndrome

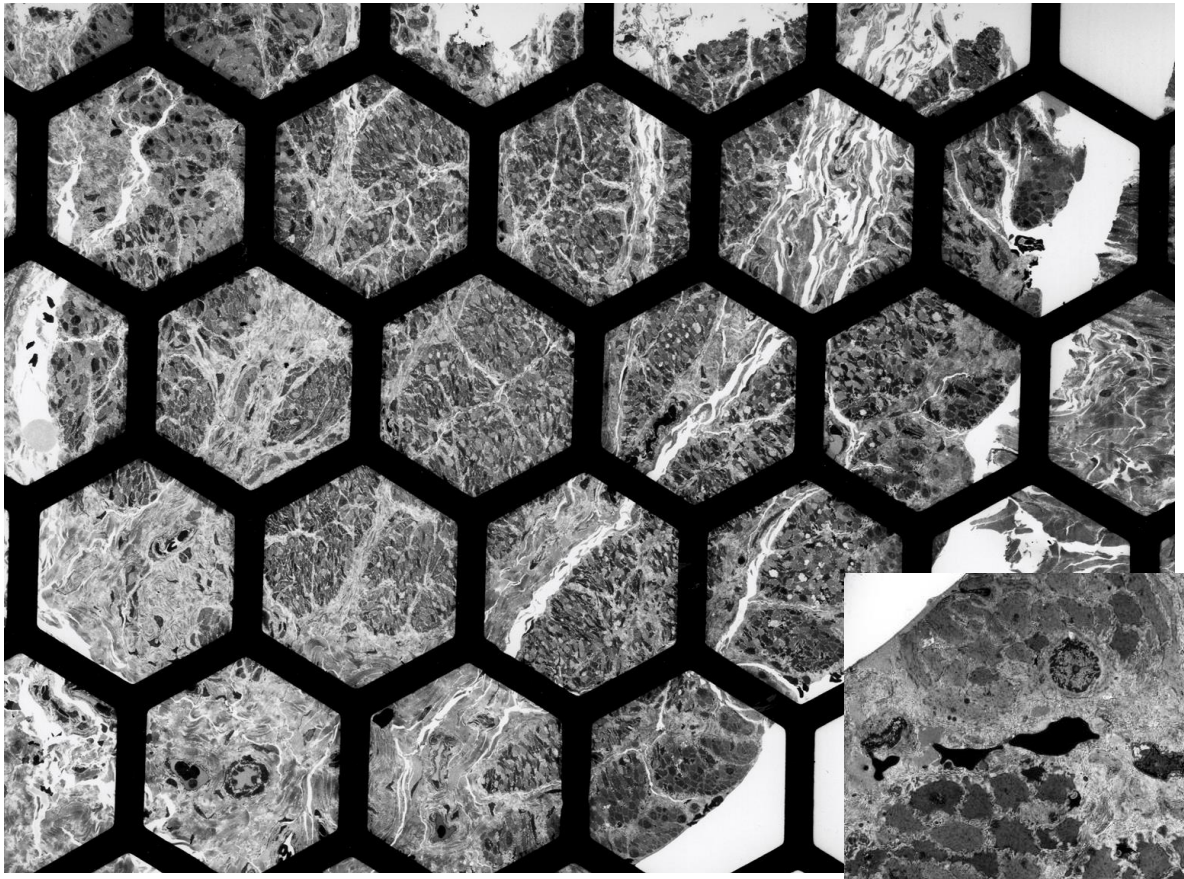

11 year old girl with possible hollow visceral myopathy.

Rectal biopsy. Muscularis propria

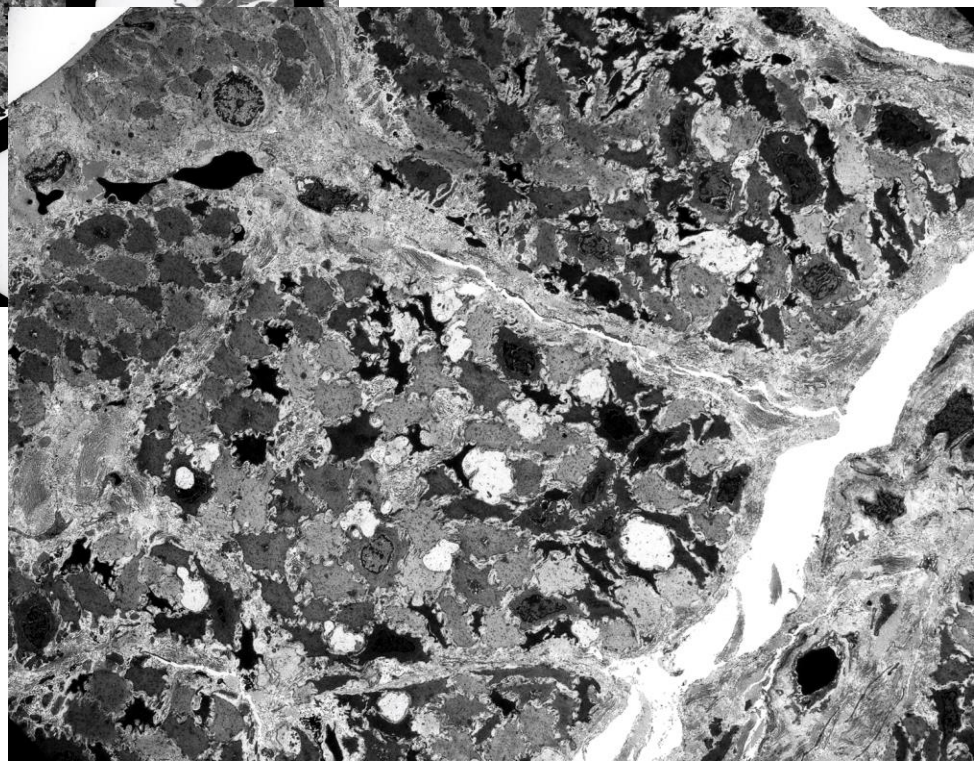

Myocyte vacuolation

Visible histologically

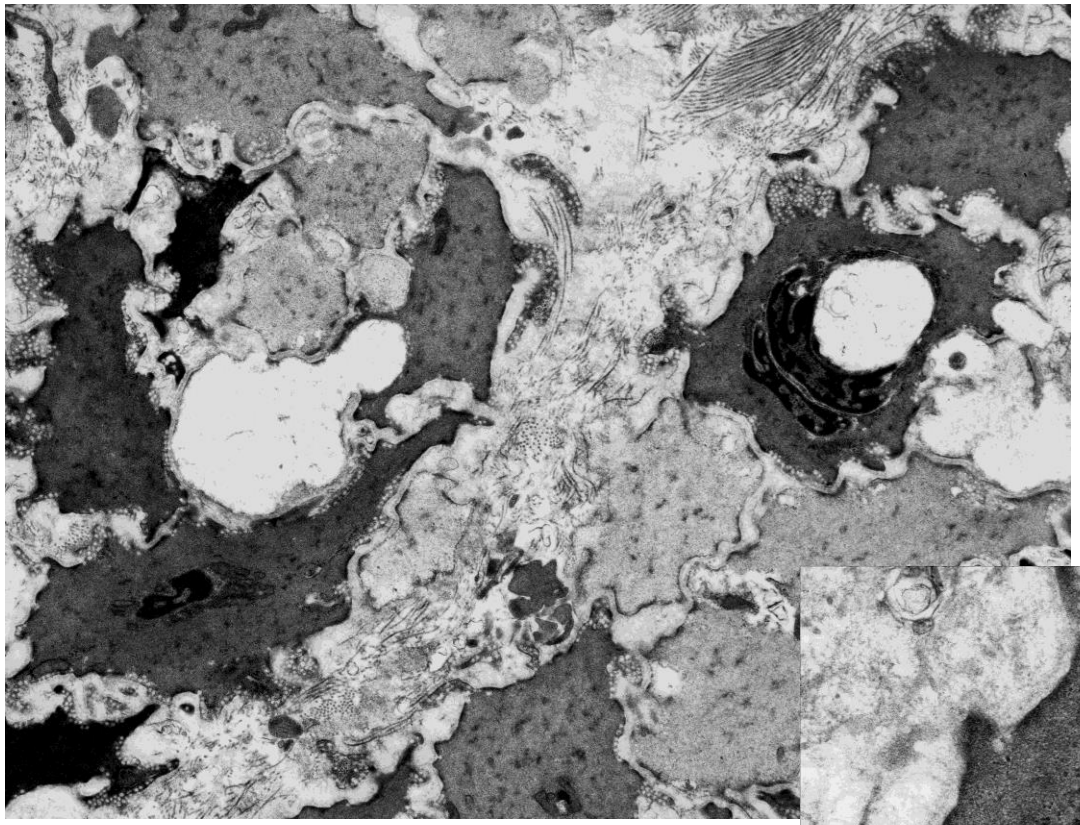

11 year old girl with possible hollow visceral myopathy. Rectal biopsy. Muscularis propria

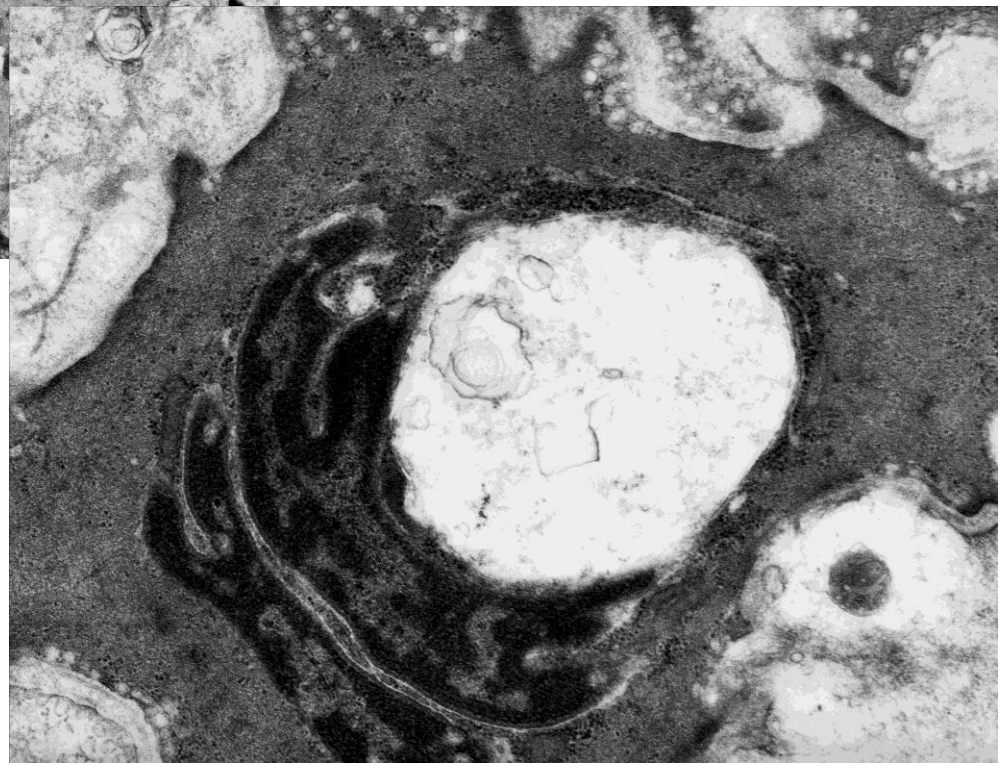

Myocyte vacuolation

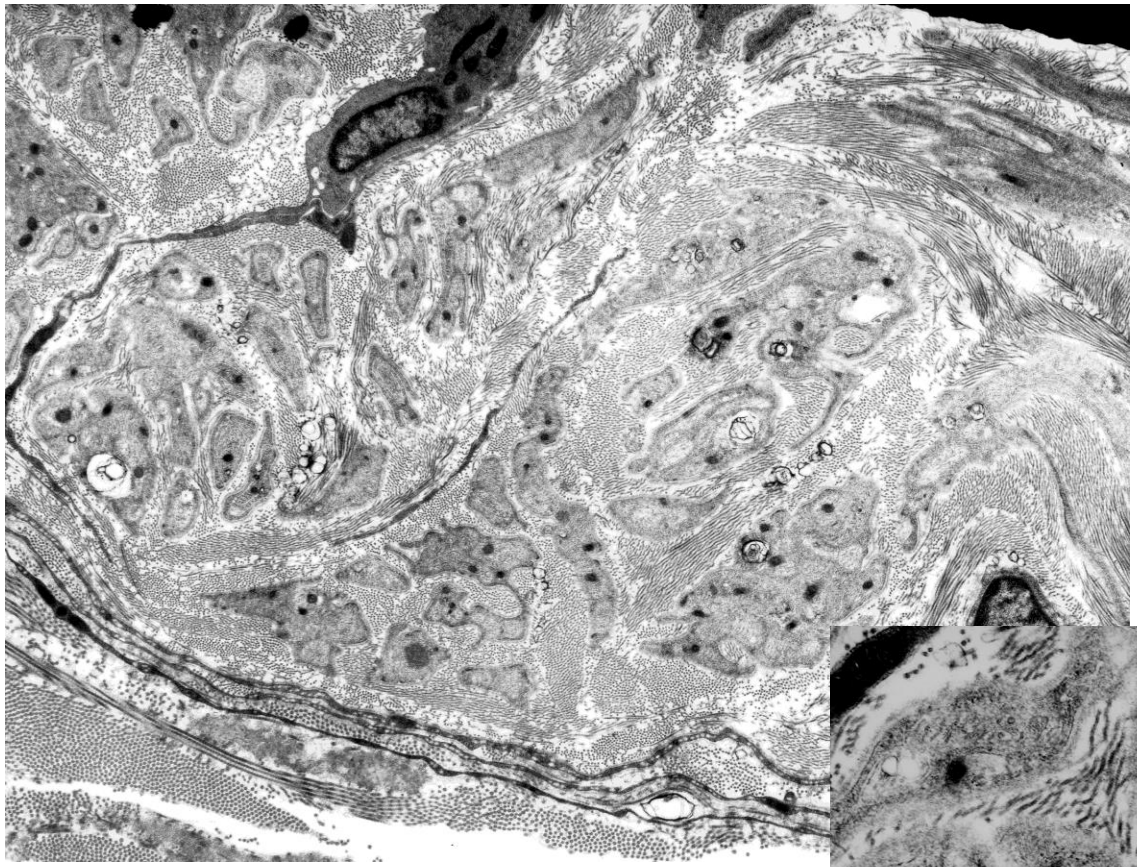

Peripheral, unmyelinated, nerve – appears normal

Rectal biopsy. Patient with suspected hollow visceral myopathy.

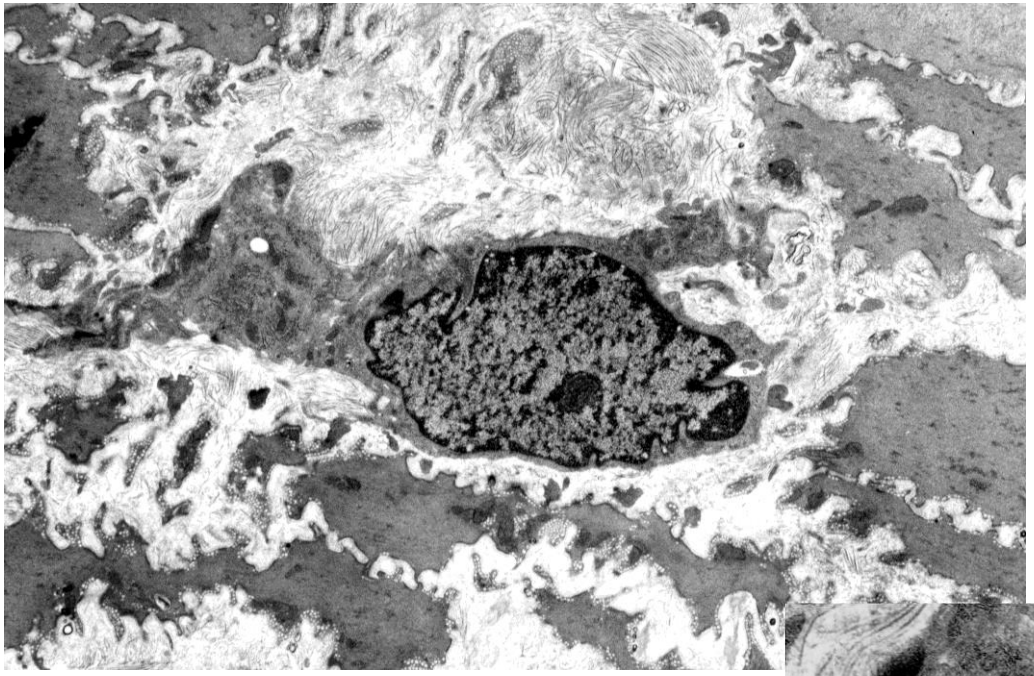

Interstitial cell of Cajal.
Normal complement of these cells immuno-histochemically using c-Kit/CD117 antibody

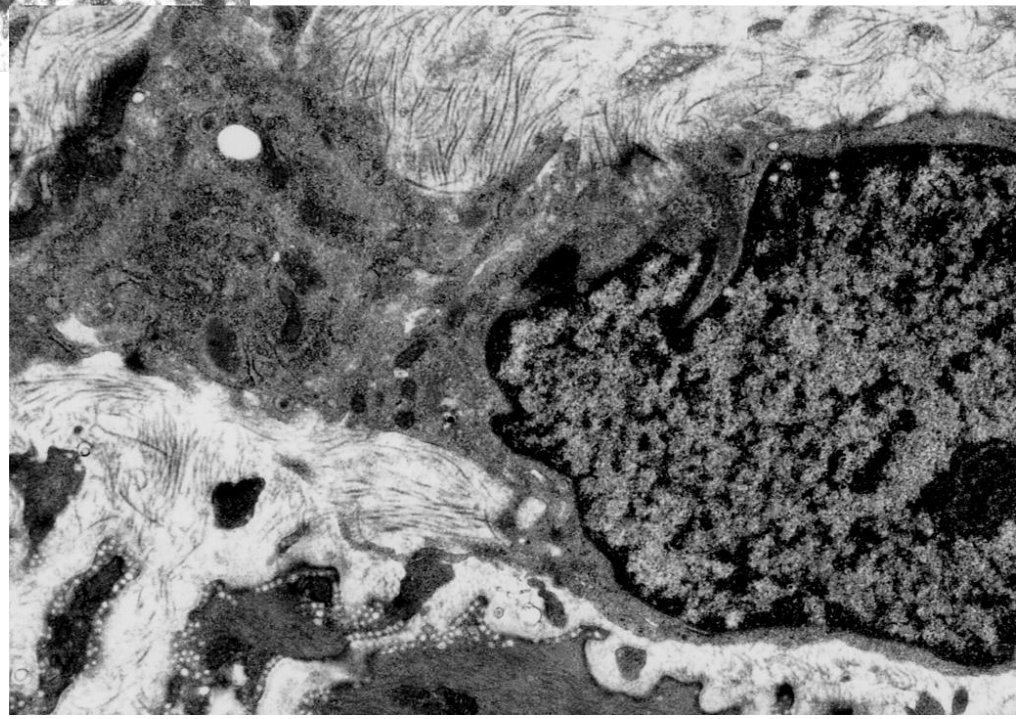

Rectal biopsy. Patient with suspected hollow visceral myopathy.

Histopathology. 1997 Aug;31(2):112-22.

Histological phenotypes of enteric smooth muscle disease causing functional intestinal obstruction in childhood.

Smith VV, Milla PJ.

Source
Great Ormond Street Hospital for Children NHS Trust, London, UK.

Abstract
AIMS:
Functional intestinal obstruction or chronic idiopathic intestinal pseudo-obstruction is due to defects either in the enteric innervation or in intestinal smooth muscle. We have studied full-thickness intestinal biopsies from 27 patients with functional intestinal obstruction due to enteric smooth muscle disease by routine histology and electron microscopy together with histochemical and immunohistochemical techniques to detect changes in the intestinal smooth muscle.

METHODS AND RESULTS:
Two patients appeared to have an acquired intestinal myopathy as a result of an **autoimmune process**. In 25 the disorders were congenital, of these seven had segmental abnormalities limited to the rectum and distal colon and 18 had a diffuse disease affecting both the small and large bowel. We identified **five apparent histological phenotypes of enteric muscle disease**, three of which represent abnormalities in morphogenesis resulting in **alterations in intestinal muscle layering** and two exemplify **intrinsic myocyte defects** and/or changes in the extracellular matrix.

CONCLUSIONS:
Careful phenotyping of these patients is important in devising optimal treatment and in understanding the underlying defect as well as the possible genetic mechanisms resulting in these abnormalities. Recognition of autoimmune smooth muscle disease is helpful, since making the diagnosis influences the patient's management.

Histopathology. 1997 Aug;31(2):112-22.
Histological phenotypes of enteric smooth muscle disease causing functional intestinal obstruction in childhood.
Smith VV, Milla PJ.

muscle coat[6] being described. In others the abnormality is at the cellular level consisting of fibrosis and myocyte vacuolation detected by light microscopy on conventionally stained histological sections[7-25]. Smooth muscle in the urinary tract may also be affected resulting in megacystis and/or megaureter[24], thus enteric smooth muscle disease is often referred to as hollow visceral myopathy.

However, routine histology in these disorders only identifies the most severe degrees of fibrosis, myocyte atrophy and smooth muscle vacuolation, and more subtle morphological abnormalities or intrinsic cellular defects may remain undetected unless ultrastructural or immunohistochemical studies are performed[7,11,15,17-19,26-31].

Glutaraldehyde fixed skin biopsy (taken for sub-typing of Ehlers-Danlos Syndrome)
Normal arrector pili (2004)

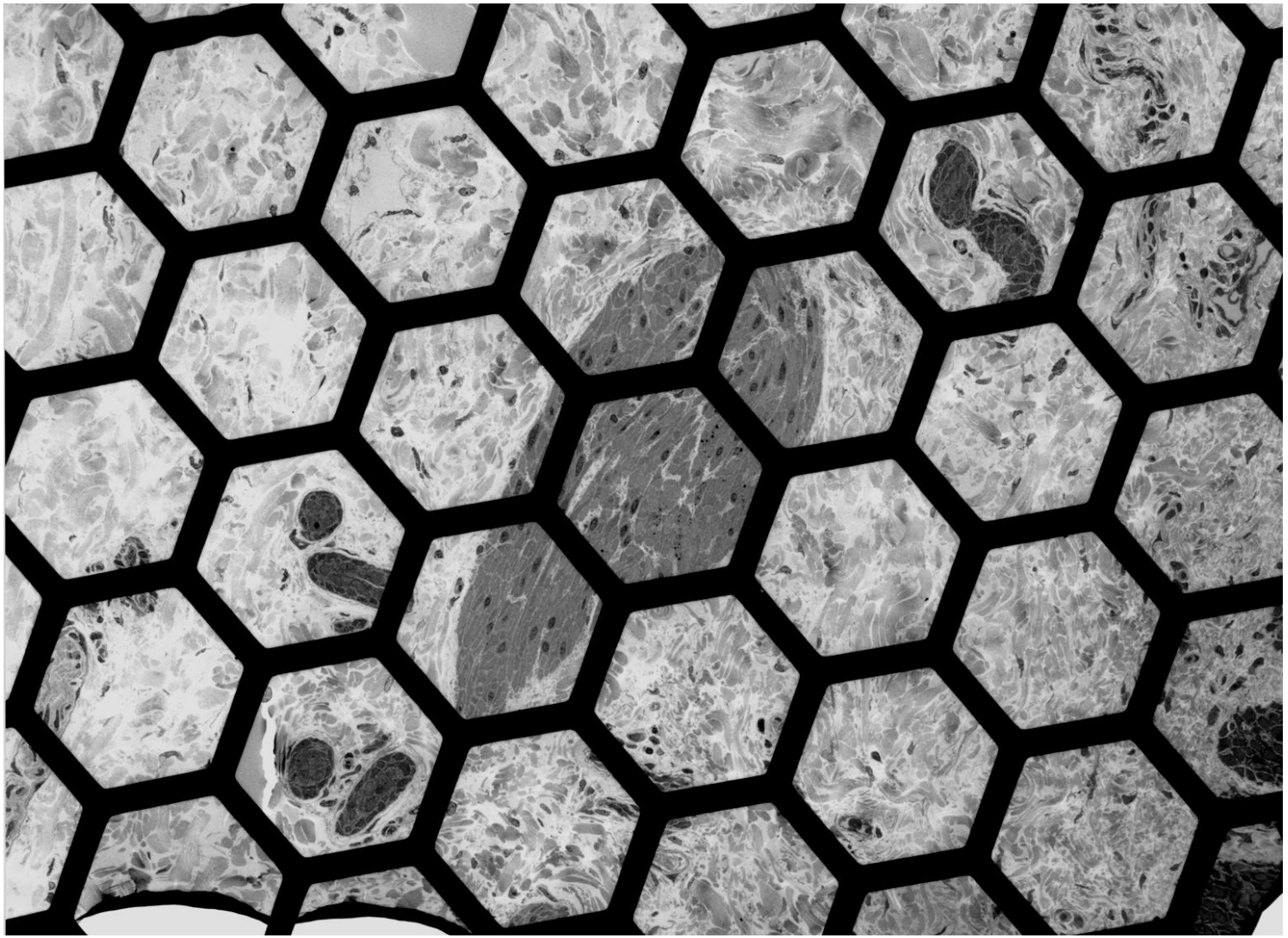

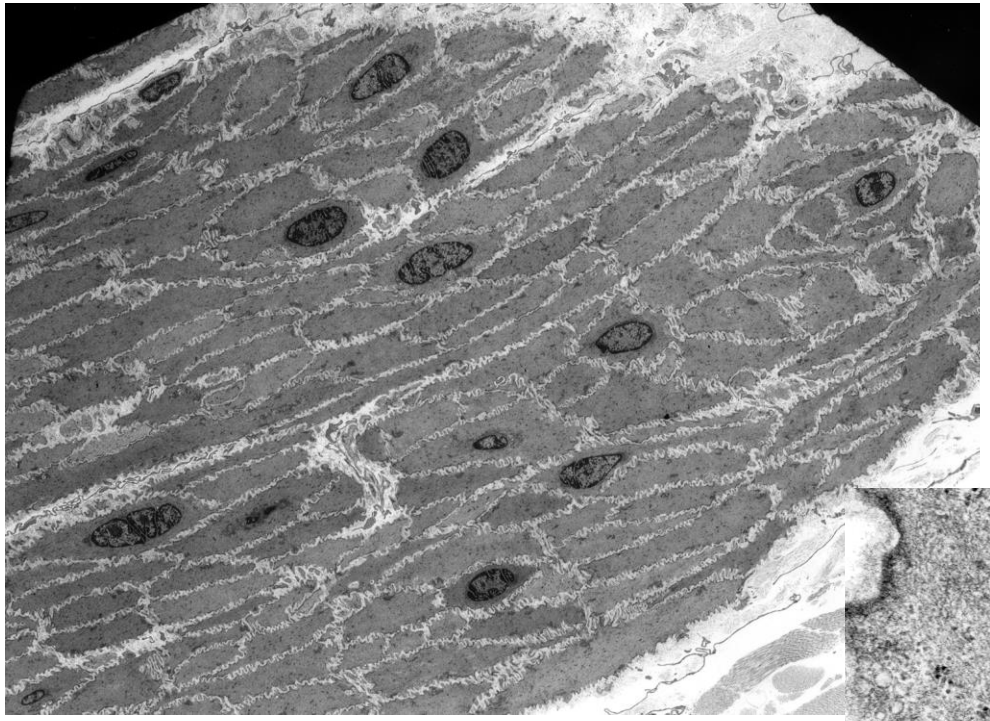

Glutaraldehyde fixed skin biopsy.
Normal arrector pili (2004)

No vacuolation

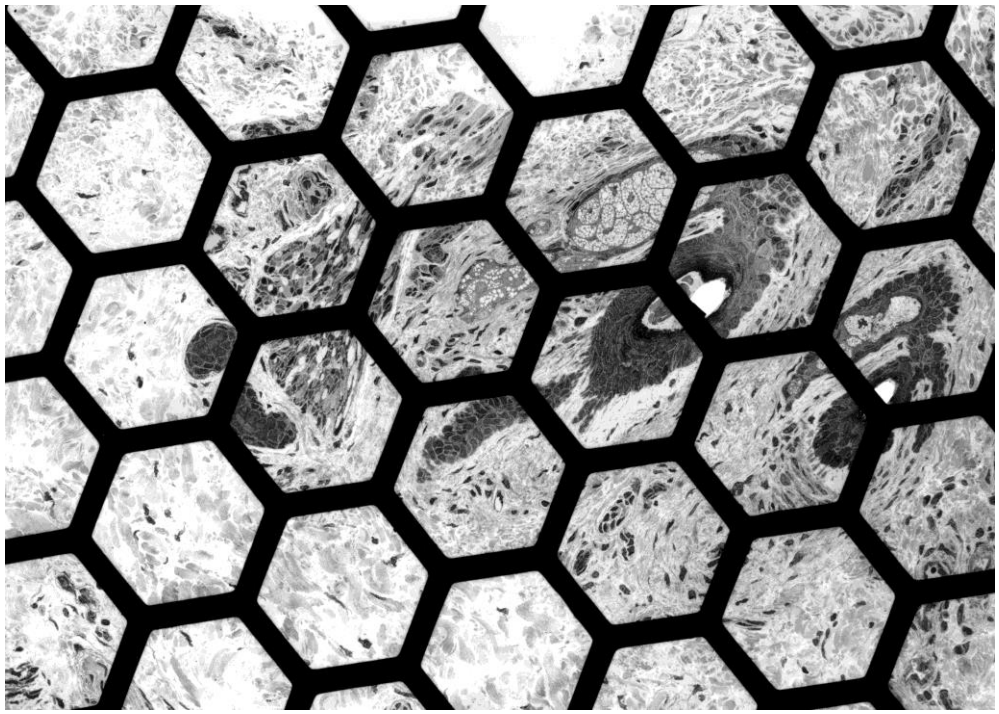

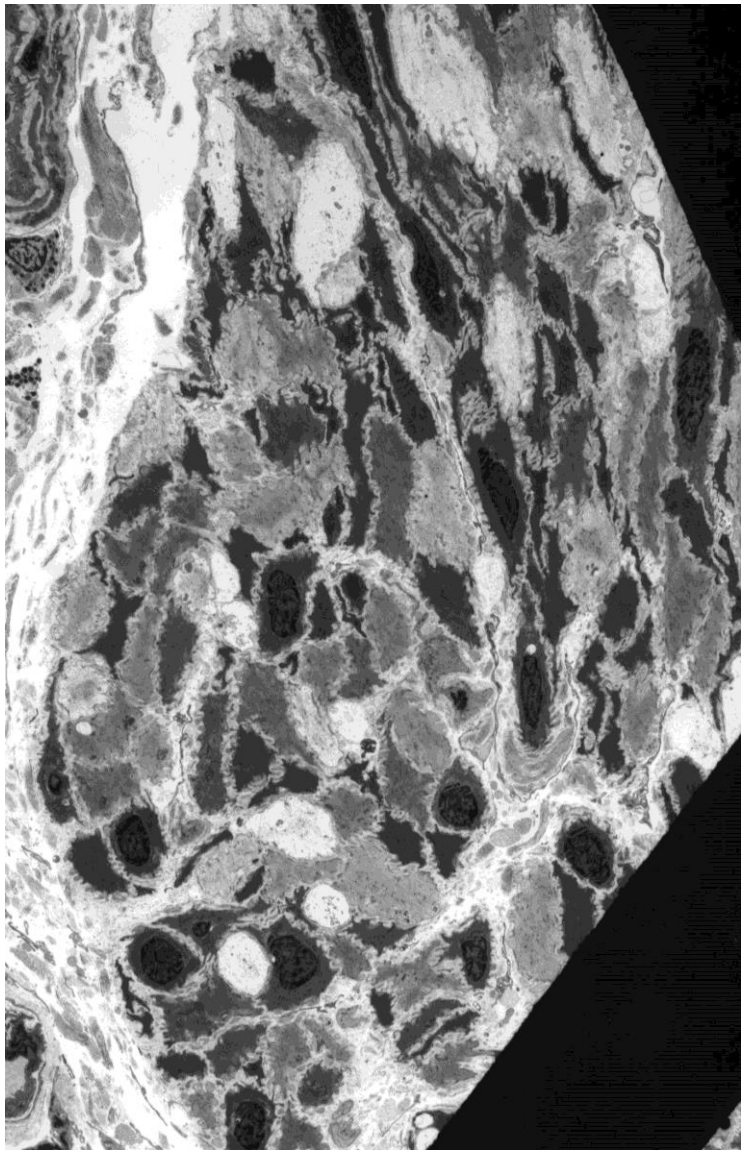

Same glutaraldehyde fixed skin
biopsy as previous slide.
Arrector pili with contraction artefact

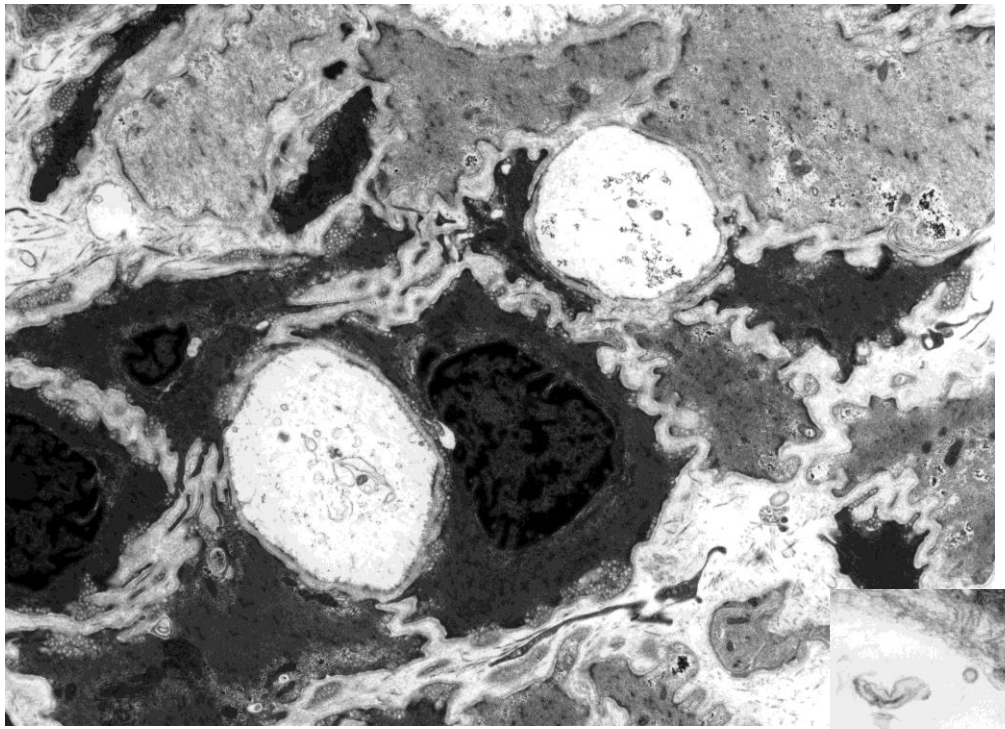

Same glutaraldehyde fixed skin biopsy as previous slide.
Arrector pili with contraction artefact

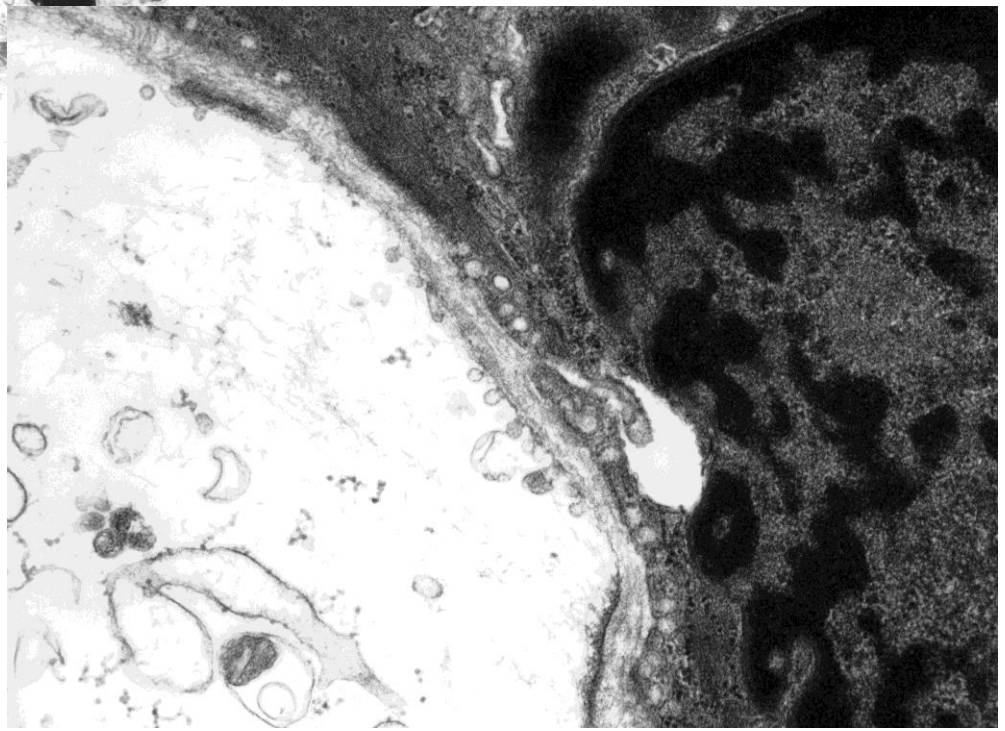

11 year old girl with possible hollow visceral myopathy.
Rectal biopsy. Muscularis propria

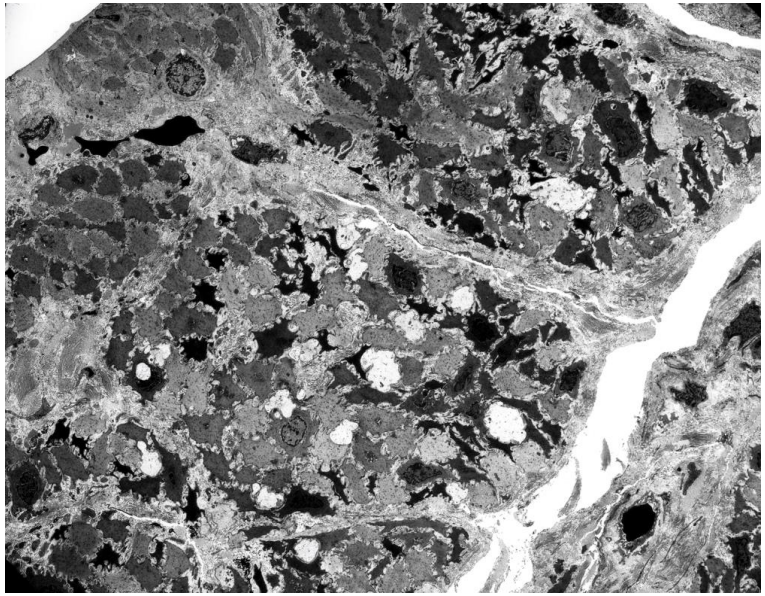

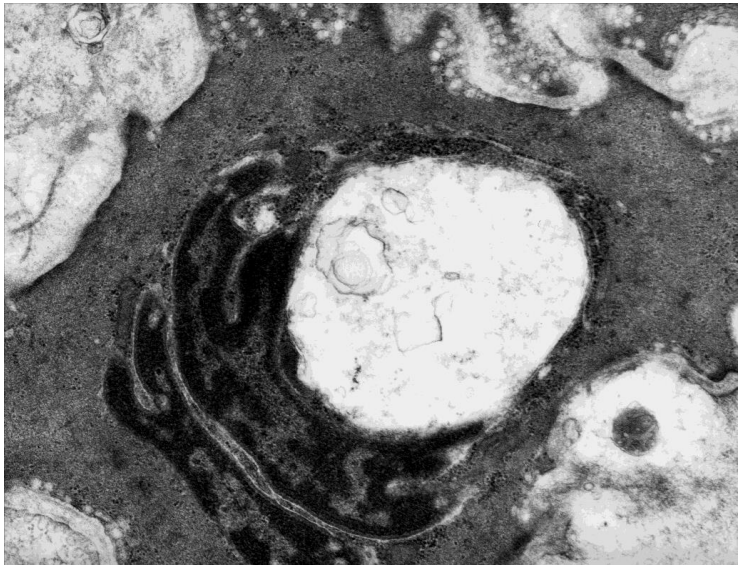

Contraction artefact present. Therefore, possibly, ultrastructural evidence of hollow visceral myopathy/familial visceral myopathy not confirmed.

I wanted to be educated on the subject so invited an expert to speak at an ACEM meeting, albeit a few years later

Leeds University -Thursday 3rd July 2008.

Association of Clinical Electron Microscopists. 11th annual scientific meeting

Satellite meeting to The Pathological Society of Great Britain and Ireland.

www.pathsoc.org.uk

www.acem.org.uk

9.00am

Registration

9.30 – 10.20am

Gadolinium in skin

Josef Schroeder, Regensberg

Chair: Bart Wagner

10.20 – 10.30am

Group photo

10.30 – 11.00am

Coffee break

11.10 – 11.50pm

CADASIL diagnosis – Ultrastructural and immunohistochemical

Mr Ray Moss,

St George's Hospital, London

Chair: Ian Shore

12.00 – 1.00pm

Technical EM - EQA feed back.

Mrs Tracey de Haro,

Leicester Royal Infirmary

Chair: Bart Wagner

1.00 - 2.00pm

Lunch break.

2.05 – 2.50pm

Gut dysmotility – Histopathology and ultrastructure

Professor Jo Martin, Consultant Neuropathologist

The Royal London Hospital

Chair: Glenn Anderson

2.55 – 3.30pm

Renal biopsy case presentation with review of literature

Mr Bart Wagner,

Northern General Hospital, Sheffield

Chair: Trish Dopping-Hepenstal

3.30 – 4.00pm

Tea break

4.00 – 5.00pm

AGM – open to ACEM members and non-members.

After giving the talk she published on the topic

World J Gastroenterol. 2009 Jan 14;15(2):192-7.

New techniques in the tissue diagnosis of gastrointestinal neuromuscular diseases.

Knowles CH, Martin JE.
Source

Neurogastroenterology Group, Centres for Academic Surgery and Pathology, Institute of Cellular and Molecular Science, Barts and the London, Queen Mary's School of Medicine and Dentistry, Whitechapel, London, United Kingdom. c.h.knowles@qmul.ac.uk

Abstract
Gastrointestinal neuromuscular diseases are a clinically heterogeneous group of disorders of children and adults in which symptoms are presumed or proven to arise as a result of neuromuscular (including interstitial cell of Cajal) dysfunction. Common to most of these diseases are symptoms of impaired motor activity which manifest as slowed or obstructed transit with or without evidence of transient or persistent radiological visceral dilatation. A variety of histopathological techniques and allied investigations are being increasingly applied to tissue biopsies from such patients. This review outlines some of the more recent advances in this field, particularly in the most contentious area of small bowel disease manifesting as intestinal pseudo-obstruction.

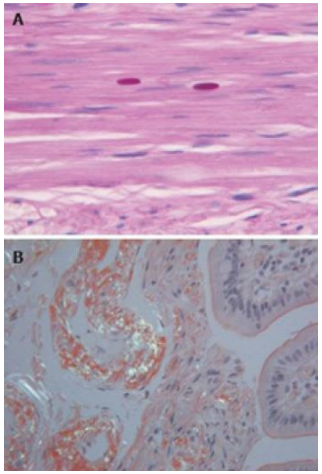

PAS +ve inclusions

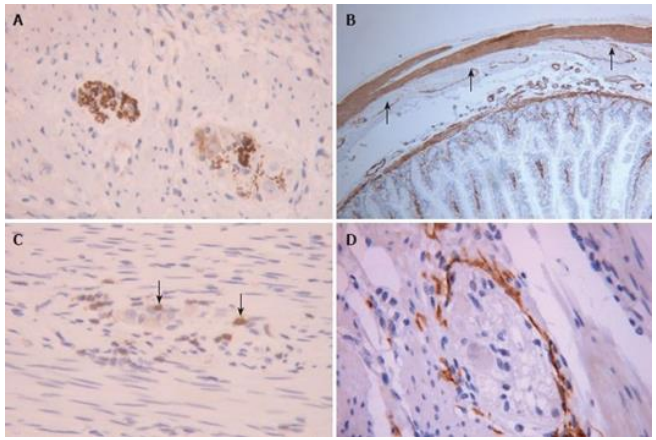

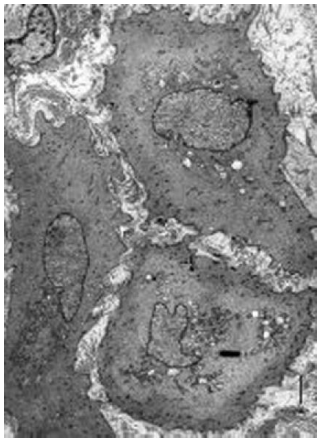

World J Gastroenterol. 2009 Jan 14;15(2):192-7.

New techniques in the tissue diagnosis of gastrointestinal neuromuscular diseases.

Knowles CH, Martin JE.

Page 195

Electron microscopy

Ultrastructural examination of neurons, muscle and interstitial cells of Cajal can be a useful adjunct to the above assessments in certain patients. These include some rare childhood myopathies where H&E findings are absent or equivocal (e.g. subtle fibrosis, atrophy of myocytes or myocyte vacuolation)[30], the identification of rare inclusion bodies[31] suggestive of mitochondrial disorders and some ultrastructural changes of ICC[32] and myocytes, including a transformation to more secretory phenotypes.

30. Smith VV, Milla PJ.
Histological phenotypes of enteric smooth muscle disease causing functional intestinal obstruction in childhood. Histopathology. 1997 Aug;31(2):112-22.

31. Barnett JL, McDonnell WM, Appelman HD, Dobbins WO.
Familial visceral neuropathy with neuronal intranuclear inclusions: diagnosis by rectal biopsy. *Gastroenterology* 1992; 102: 684-691

32. Ohlsson B, Veress B, Lindgren S, Sundkvist G.
Enteric ganglioneuritis and abnormal interstitial cells of Cajal: features of inflammatory bowel disease. *Inflamm Bowel Dis* 2007; 13: 721-726

Learning points
Hollow Visceral Myopathy case

- When assessing smooth muscle cells try to either avoid examining areas showing contraction artefact, or if not possible, disregard features associated with it.

Any questions?

Next case

Venous blood sample for ? Batten disease (1999)

- 6 year old girl

6 year old girl
Blood sample EM

Numerous
normal looking
lymphocytes

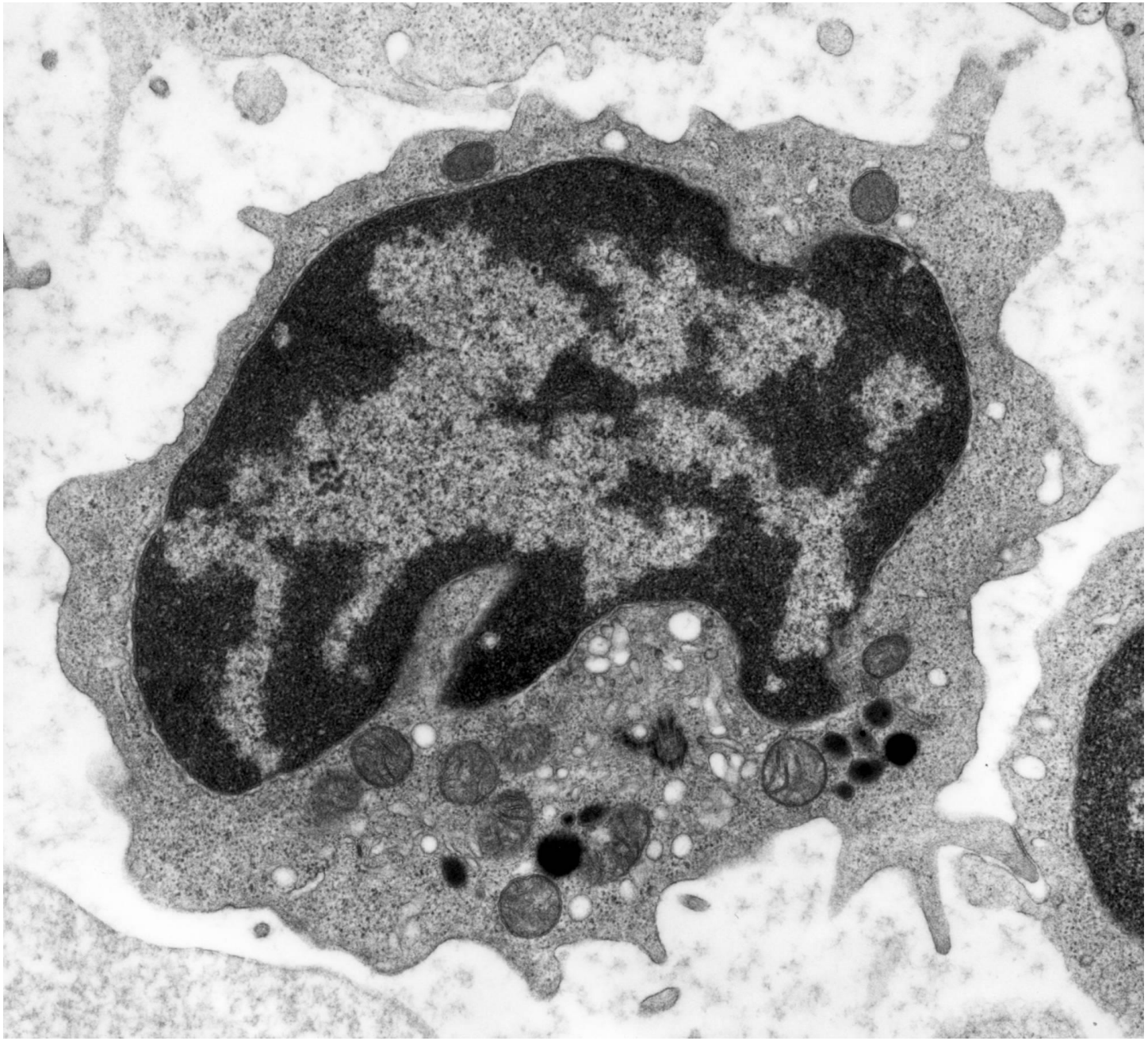

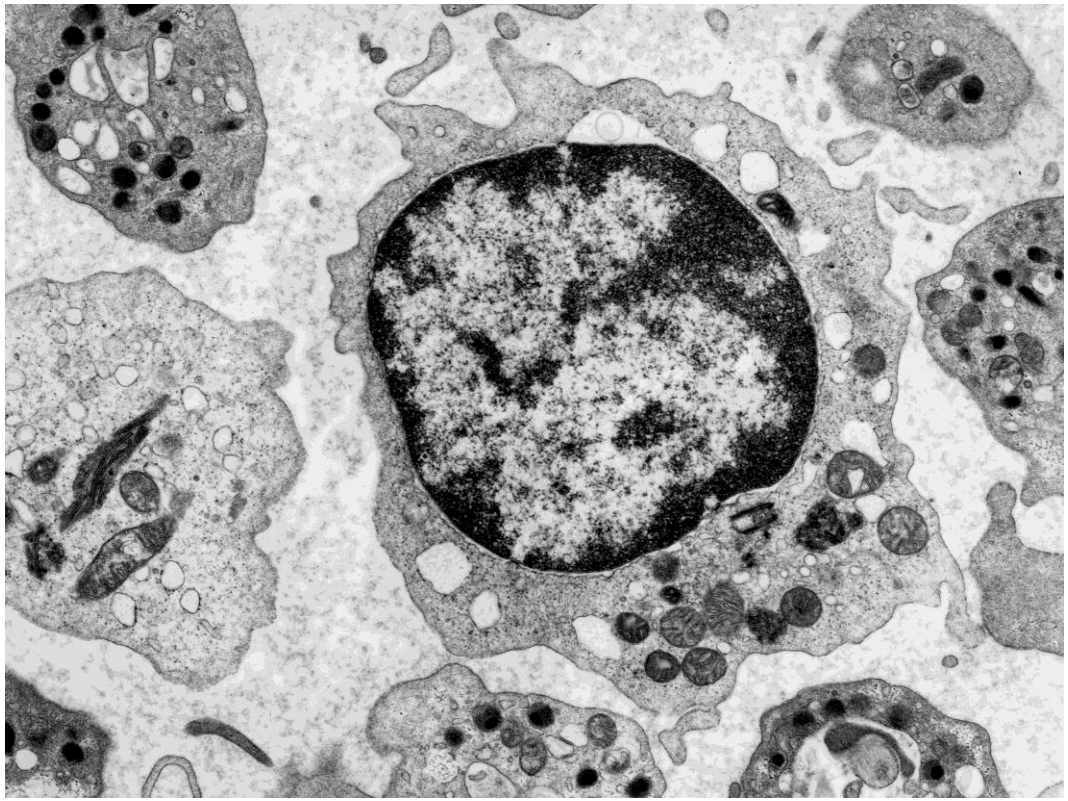

6 year old girl
Blood sample EM

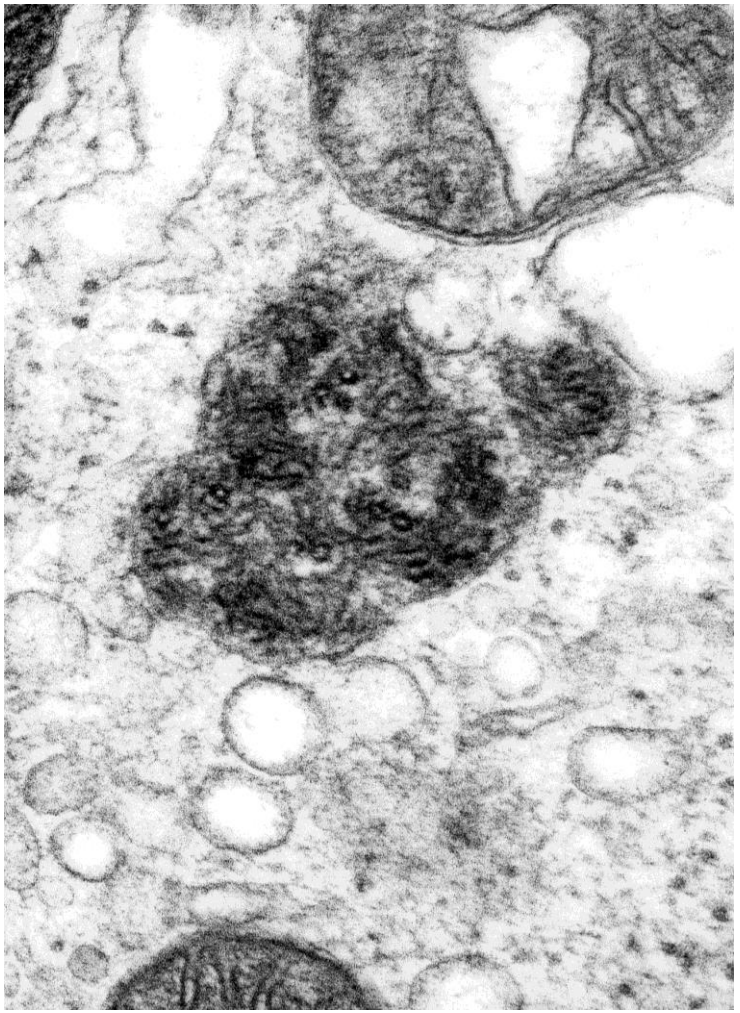

Lymphocyte granules with tubular substructure

6 year old girl
Blood sample EM

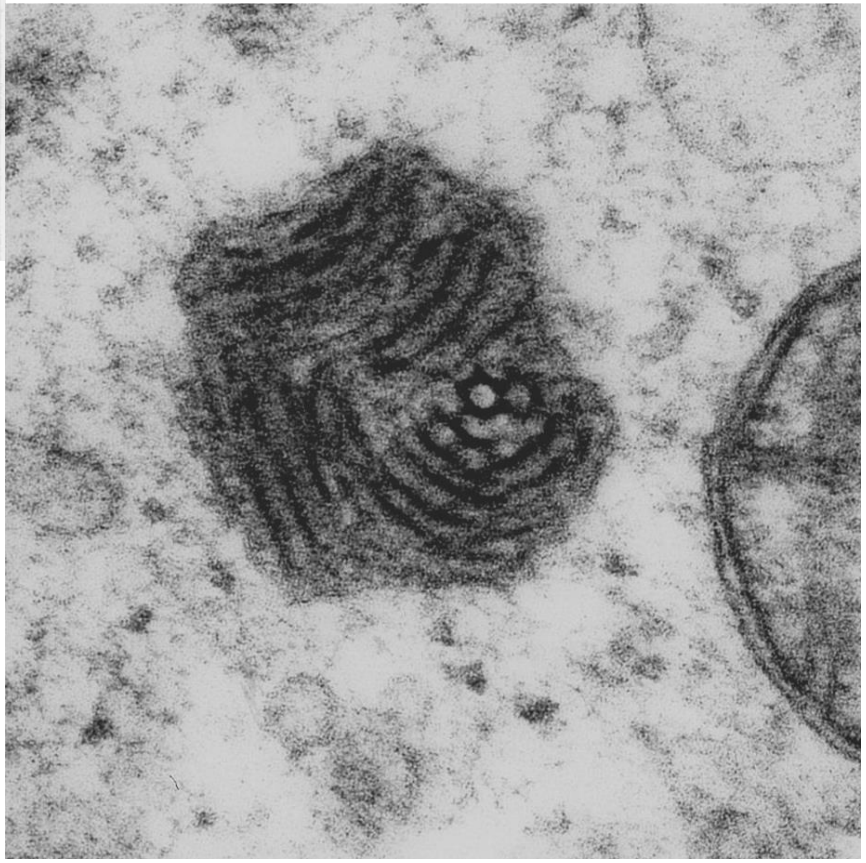

Lymphocyte granules with
tubular substructure

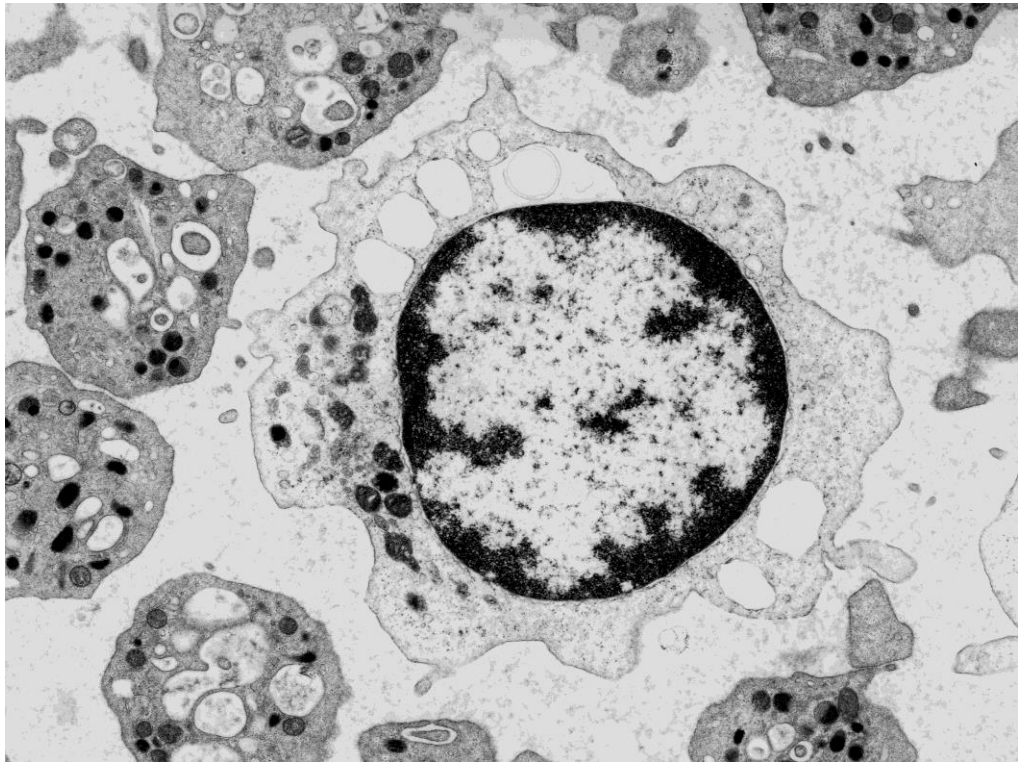

6 year old girl
Blood sample EM

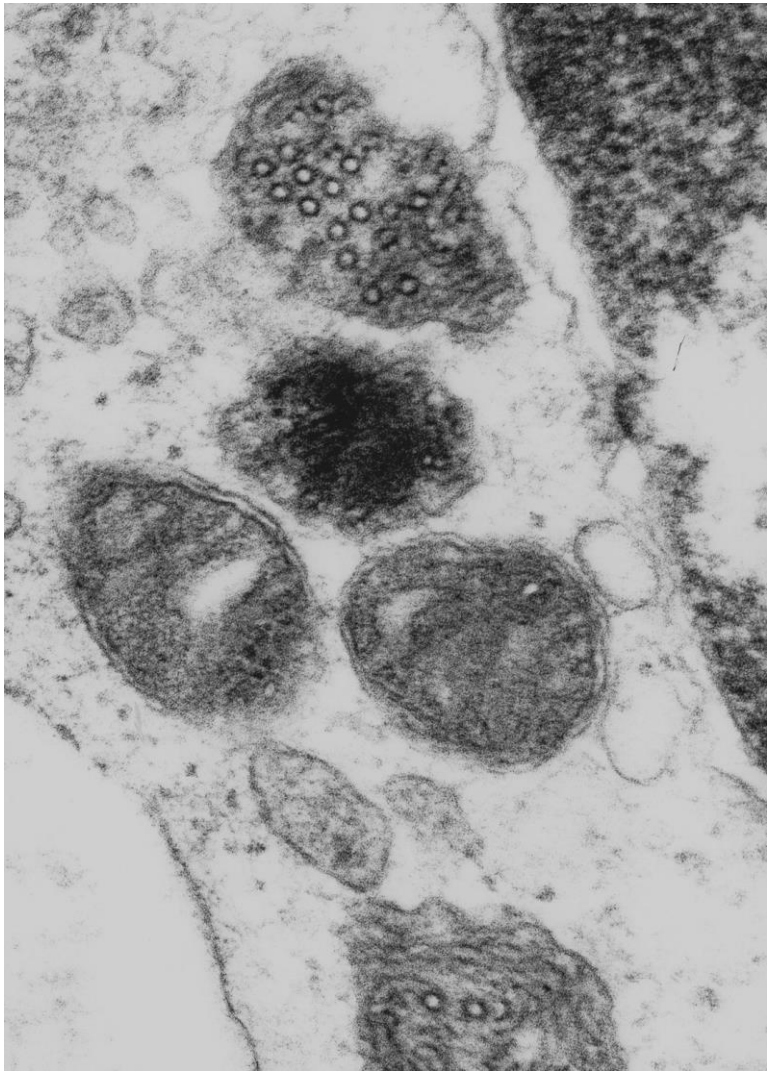

Lymphocyte granules with
tubular substructure

Renal biopsy – different case

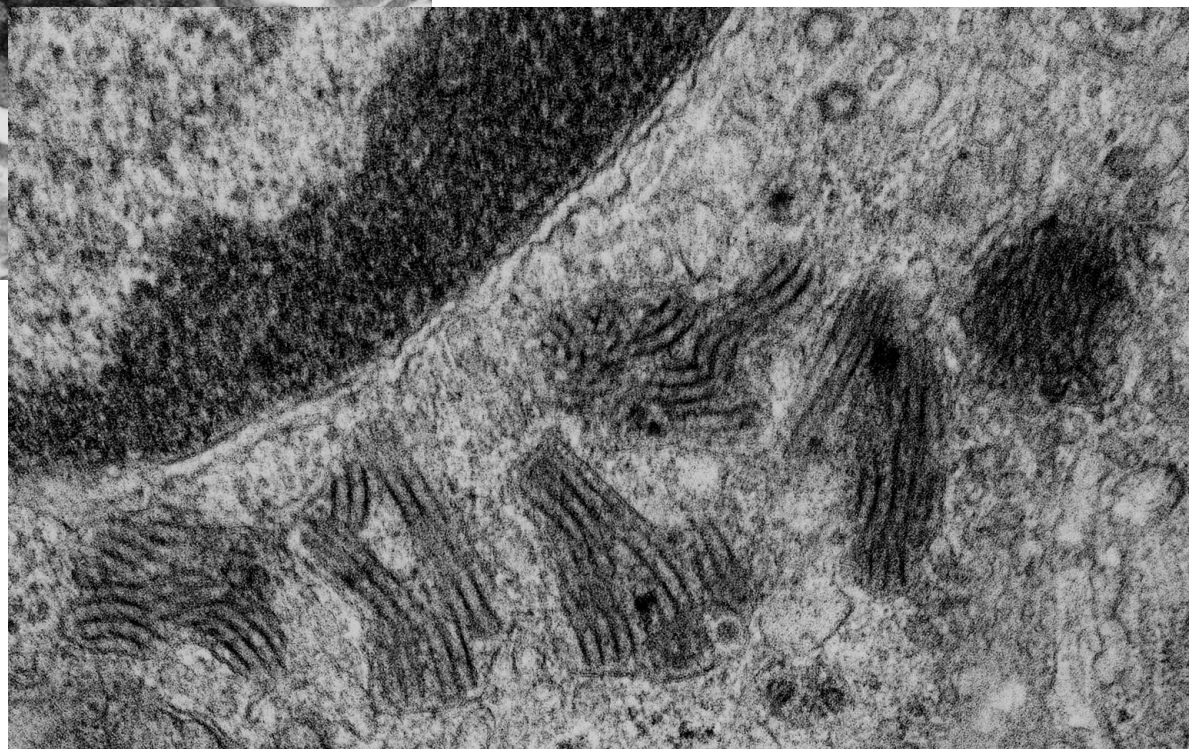

Lymphocyte with granules with tubular substructure in glomerular capillary

(1976)

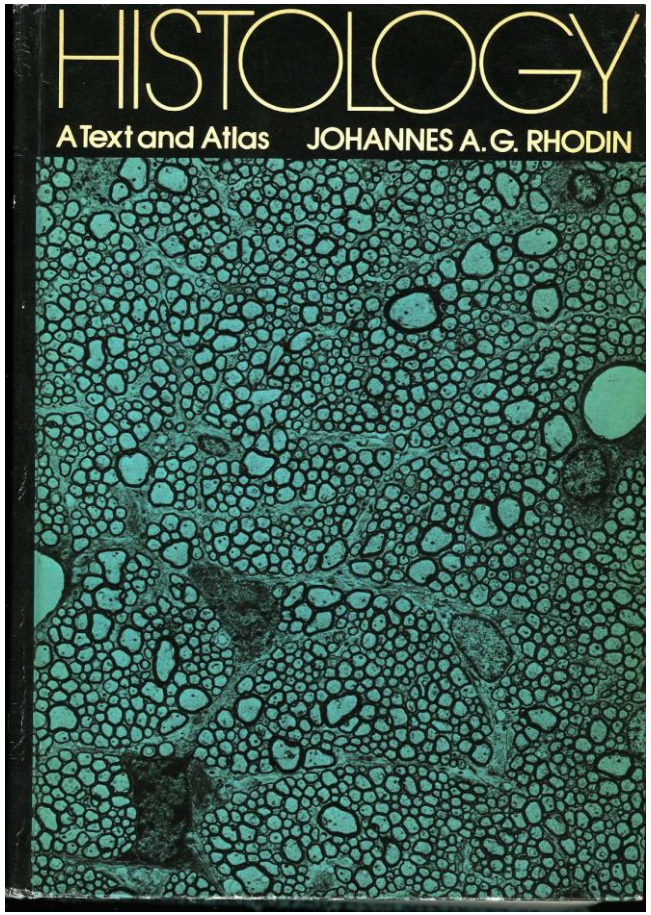

No pictures of a cell such as this in these books

(2005)
Not available at time in question

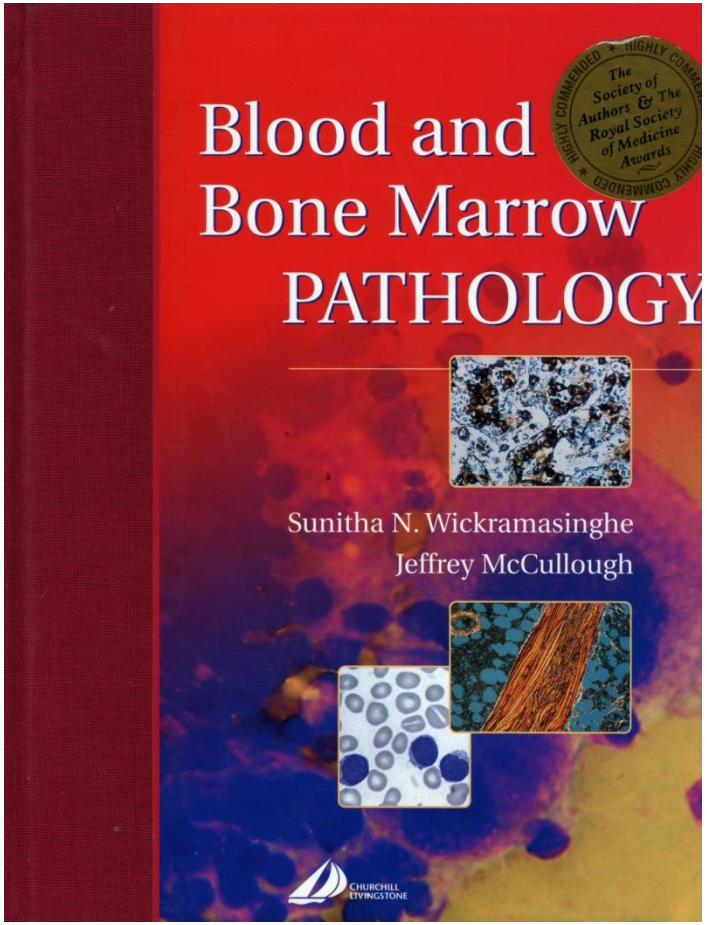

The lysosomal storage disorder with a microtubular substructure is Gaucher disease

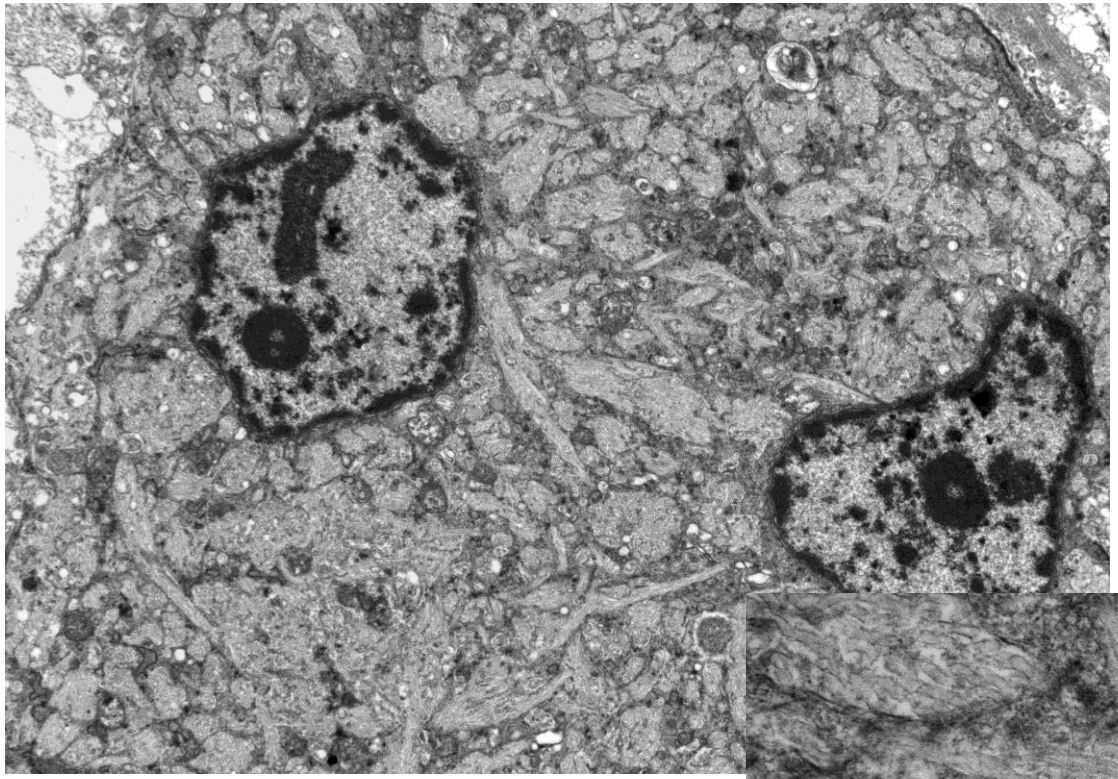

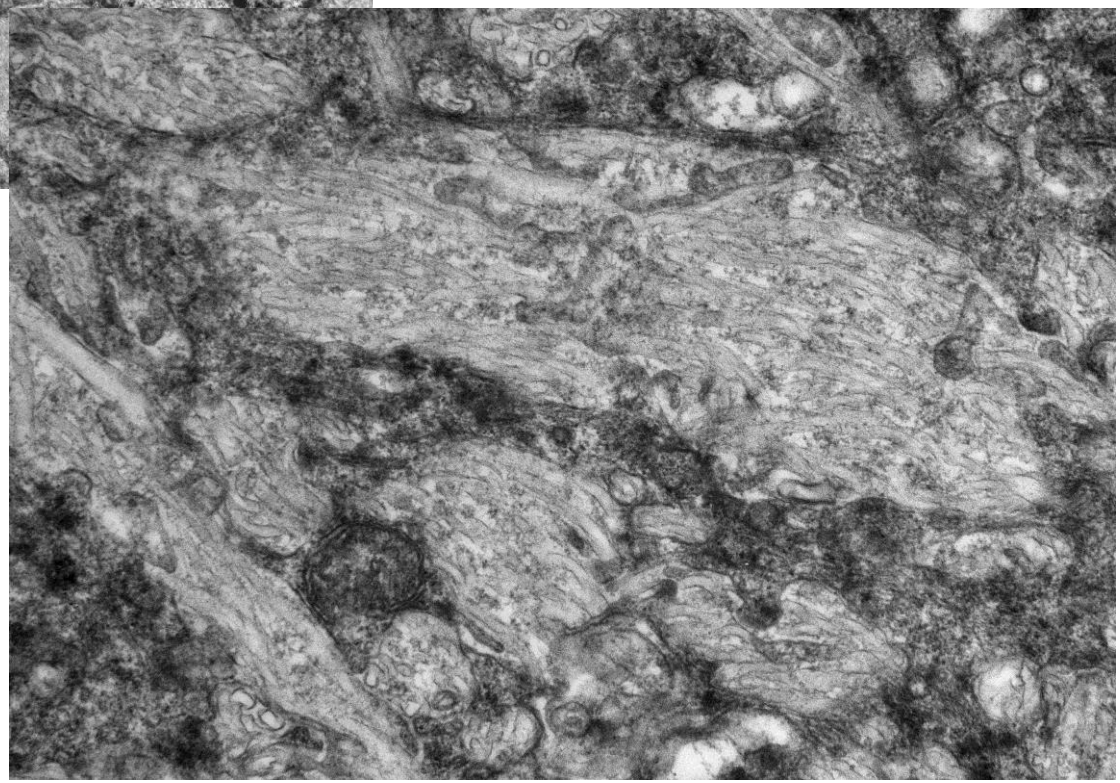

Splenectomy specimen
15 year old girl
Gaucher disease
(sample from 1989)

Spleen 15 year old girl (sample from 1989). Gaucher disease

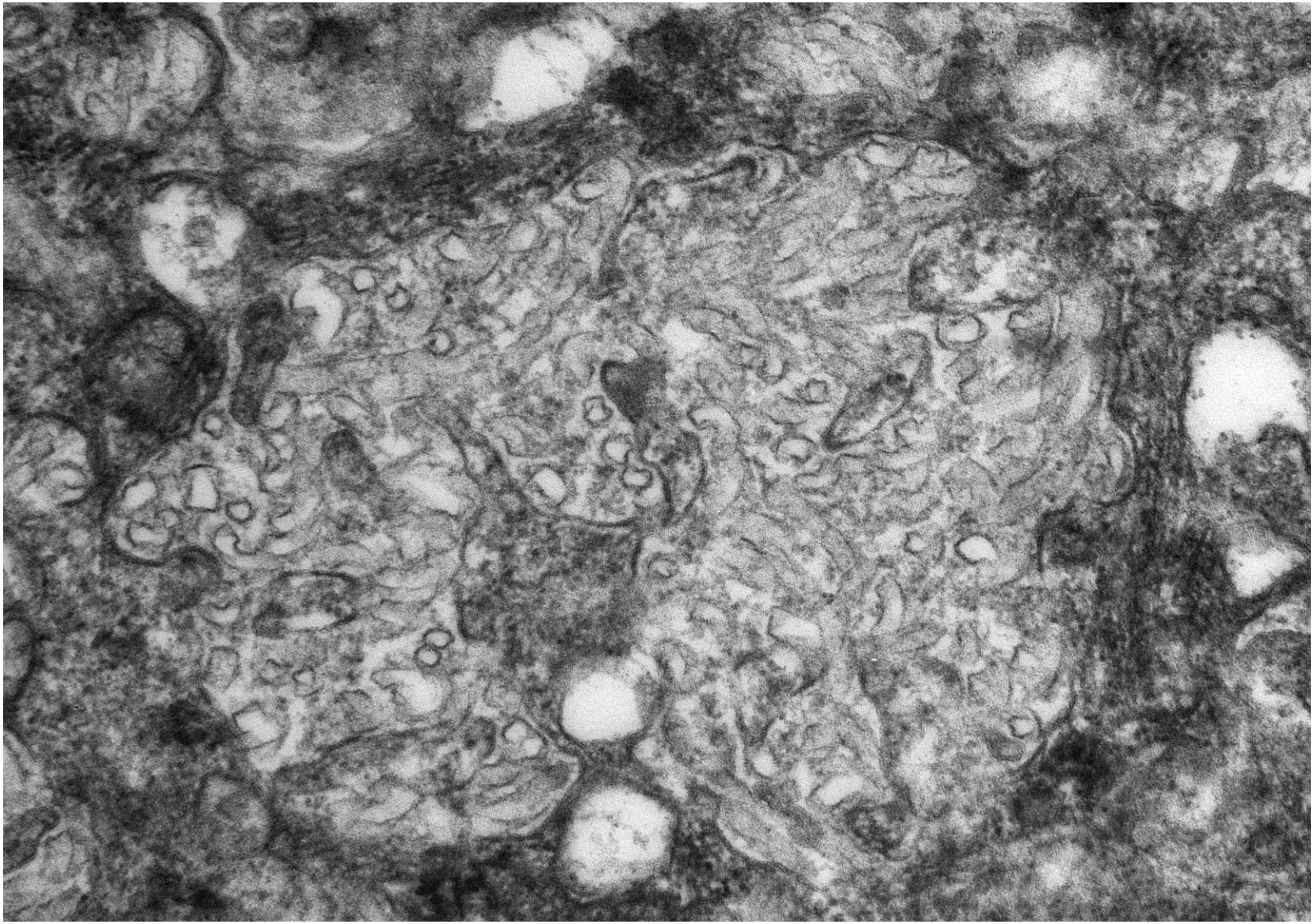

Enlarged lysosome with tubular
substructure in macrophage in spleen

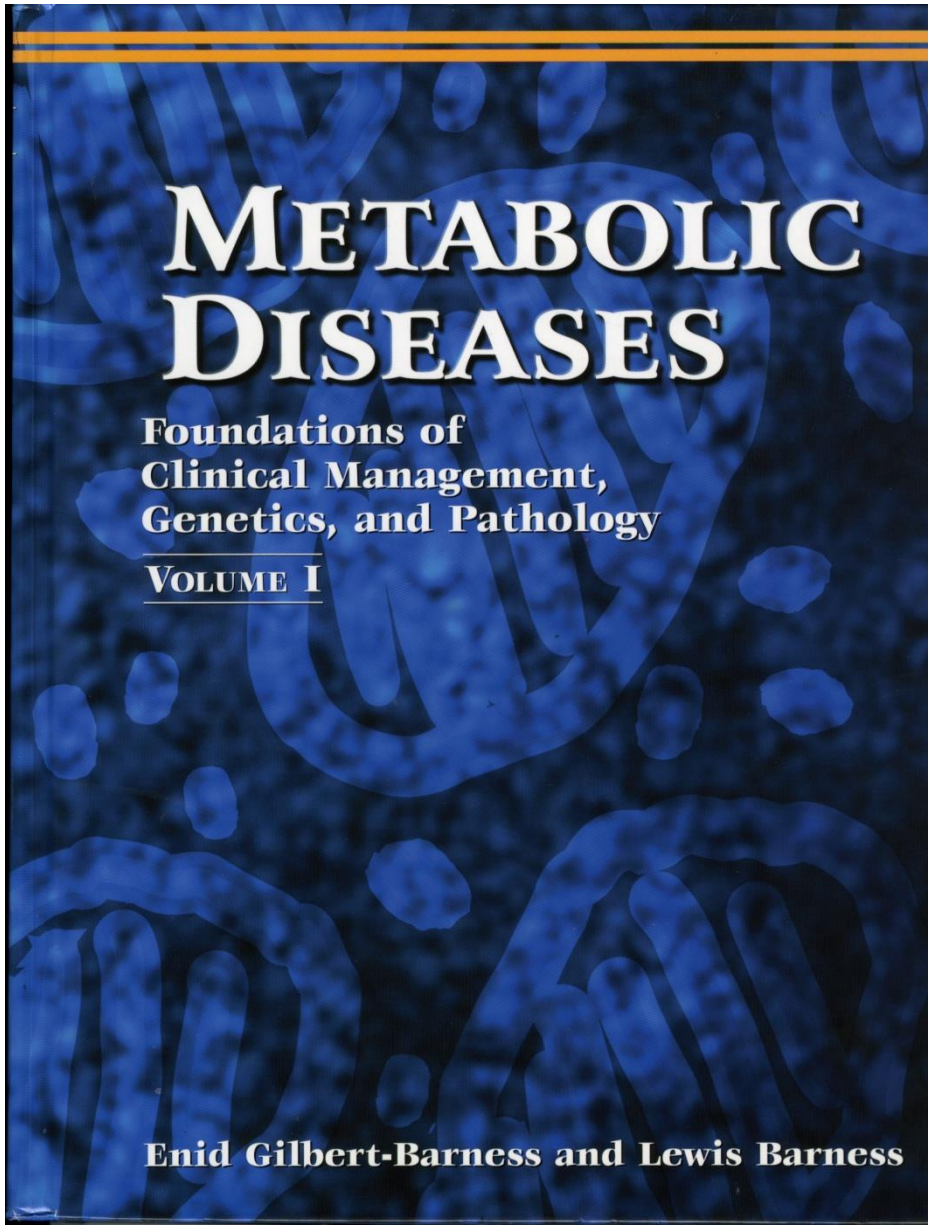
METABOLIC DISEASES
Foundations of Clinical Management, Genetics, and Pathology
VOLUME I
Enid Gilbert-Barness and Lewis Barness

(2000)

Table 4. Inherited Metabolic Disorders with Recognized Peripheral Blood, Bone Marrow, and Conjunctival/Skin Pathology

Disease	Peripheral WBC	Bone Marrow Foamy Histiocytes	Conjunctival/Skin Biopsy	
			Inclusion Type	Site
Niemann-Pick disease	VL	+	Pleomorphic, dense-lucent, lamellar	Ep, En, M, N
Gaucher disease		+		
Krabbe disease			Crystal-like	N
Metachromatic leukodystrophy			Herringbone	N
Farber disease		+	Tubular, "banana bodies" granular membranous	M, En, N
Glycogen storage disease type II				
GM Gangliosidosis	VL	+	Fibrillogranular, membranous	Ep, En, M, N
Tay-Sachs disease			Membranous, granular	N,En, M
Sandhoff disease			Membranous, granular	N, En, M
Fabry disease	-	+	Lamellar	En, M
Wolman disease	VL	+		
Mucopolysaccharidoses I, II, III	NG,VL	+	Fibrillogranular, membranous	Ep,M,N,En
Sialic acid storage disease	VL	+	Granular, sparse	En,M
Mucolipidosis II	VL		Fibrillogranular, lamellar	M,En,N
Mucolipidosis III	VL		Fibrillogranular, lamellar	M,En,N
Mucolipidosis IV	VL		Fibrillogranular, lamellar	Ep,En,M,N
Fucosidosis	VL	+	Fine granular, sparse	Ep,En, M, N
Mannosidosis	VL	+	Fibrillogranular	M,En,N
Aspartylglucosaminuria	VL		Fibrillogranular	En,M,N
Galactosialidosis	VL		Fibrillogranular, sparse	Ep, M
Cystinosis		+	Crystals	M

WBC, white blood cells; Ep, epithelial; En, endothelial; M, mesenchymal (histiocytes); N, neural; NG, neutrophil granules; VL, vacuolated lymphocytes

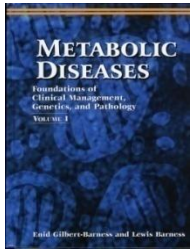

Gaucher disease not evident in lymphocytes, and is associated with splenomegaly. Splenomegaly not part of phenotype of the 6 year girl whose blood sample I had looked at.

Some time later – not sure but could have been months –
I read the relevant pages in Ghadially's text book

1997

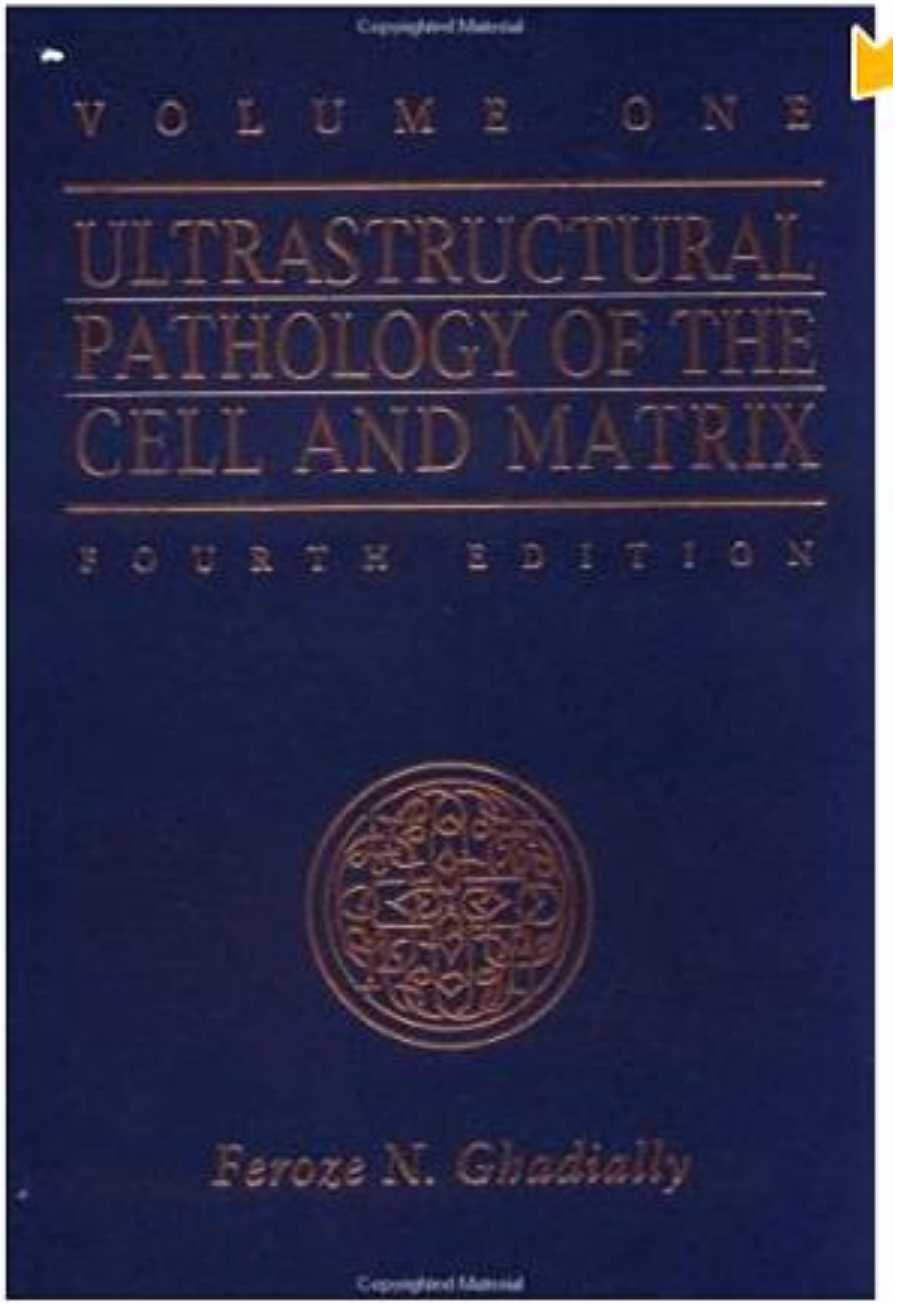

Picture of this cell type
In the chapter on Endoplasmic Reticulum

In the index listed under :
Lymphocyte

Subsection:
Parallel microtubular arrays

Pages 520 - 523

Microtubule group: parallel microtubular arrays

The structures or inclusions described here as *parallel microtubular arrays** are commonly referred to as parallel tubular arrays (*Plates 235 and 236*). Curiously enough, even those who call these structures parallel tubular arrays realize or suspect that these single-membrane-bound structures contain microtubules and not tubules, for when describing the morphology of these structures they speak about "structures resembling microtubules" (White, 1972), "microtubule-like structures comprising the inclusions" (Brunning and Parkin, 1975b), and "typical microtubule-like structure" (Payne and Tennican, 1982).

Parallel microtubular arrays usually present as electron-dense inclusions in the cytoplasm of certain lymphocytes (see below). These round, oval, or elongated, single-membrane-bound inclusions range in size from about 100 to 600 nm, but much larger inclusions (1 to 5 μm) of this type are at times seen. Basically, this inclusion is composed of bundles of parallel, rather thick-walled microtubules (diameter of about 15 to 30 nm or more†) set in a sparse or abundant electron-dense matrix. In some profiles the bundles of microtubules run in one direction only; in others the bundles are oriented in various directions, often at almost 90 degrees to each other. Yet other profiles show that some bundles of parallel microtubules follow a curvilinear course.

These parallel arrays of microtubules set in an electron-dense matrix usually lie in a single-membrane-bound vacuole, but at times they truly or apparently lie free in the cytoplasm. The membrane of the vacuole may be close-fitting, and hence, at times, it is difficult to visualize. On the other hand, at times, complexes of microtubules and dense substance lie in large lucent vacuoles where the limiting membrane is easily visualized.

The nature of parallel microtubular arrays and their mode of genesis are not known. Acid phosphatase has on rare occasions been found in a few of these inclusions (White, 1972; McKenna et al., 1977a), but this is probably because these structures at times fuse with primary or secondary lysosomes. No author has suggested that parallel microtubular arrays are lysosomal in nature. The idea that they develop by the laying down of microtubules within dilated rough endoplasmic reticulum has theoretical appeal (because a variety of microtubular inclusions does develop in the rough endoplasmic reticulum), but there is no clear evidence to support this idea. Another theoretically appealing suggestion would be that these structures develop by the laying down of microtubules in Golgi vacuoles (a precedent for this would be the rod-shaped microtubulated body). There is no firm evidence supporting this proposal, but a cluster of these

*At the moment this structure defies classification because we do not know its mode of genesis. Hence, I do not know which chapter to put it in. I include it in this chapter, not because I believe that it develops within the endoplasmic reticulum (it may or may not do so), but simply to put it in company with other structures, arrays, or aggregates of microtubules— and because it has been confused, and at times is still confused, with the lupus-type microtubuloreticular structure (described on pages 524–536).

†The electron-dense matrix in which the microtubules lie makes it extremely difficult to obtain reliable measurements of their outer diameter. The diameter reported by a majority of authors (White, 1972; Belcher et al., 1975; Brunning and Parkin, 1975; Imamura et al., 1975; Schwendemann, 1976; Dryll et al. 1977; McKenna et al., 1977a, b) lies in the 15-to-30-nm range (which is in keeping with what is seen in *Plate 235 and Plate 236, Figures 1 and 2*). However, a few authors (Hovig et al., 1968; Halie et al., 1975; Payne et al., 1977) have reported outer diameters of up to 40 or 44 nm (which is in keeping with what is seen in *Plate 236, Figure 3*). The inner diameters of these structures (which can be more confidently measured) are rather small (that is, the microtubules are thick-walled) and show smaller variations in size (12 to 17 nm). Therefore, one may conclude that: (1) the marked variations of the outer diameter reflect principally the amount of dense material deposited on the walls of these microtubules; and (2) the structures are basically less than 30 nm in diameter and hence qualify as microtubules.

Plate 235

Circulating lymphocyte in blood vessel in a lymph node from a case of AIDS. Several single membrane-bound bodies or inclusions that we call parallel microtubular arrays are seen around the cell center wherein lie the centriole (C) and Golgi complex (G). Such bodies were not present in the rest of the cell cytoplasm. Profiles of longitudinally cut parallel microtubules (arrowheads) and transversely cut microtubules (arrows) are seen in these inclusions. The microtubule indicated by the long arrow has an outer diameter of about 30 nm and an inner diameter of about 15 nm. × 75,000

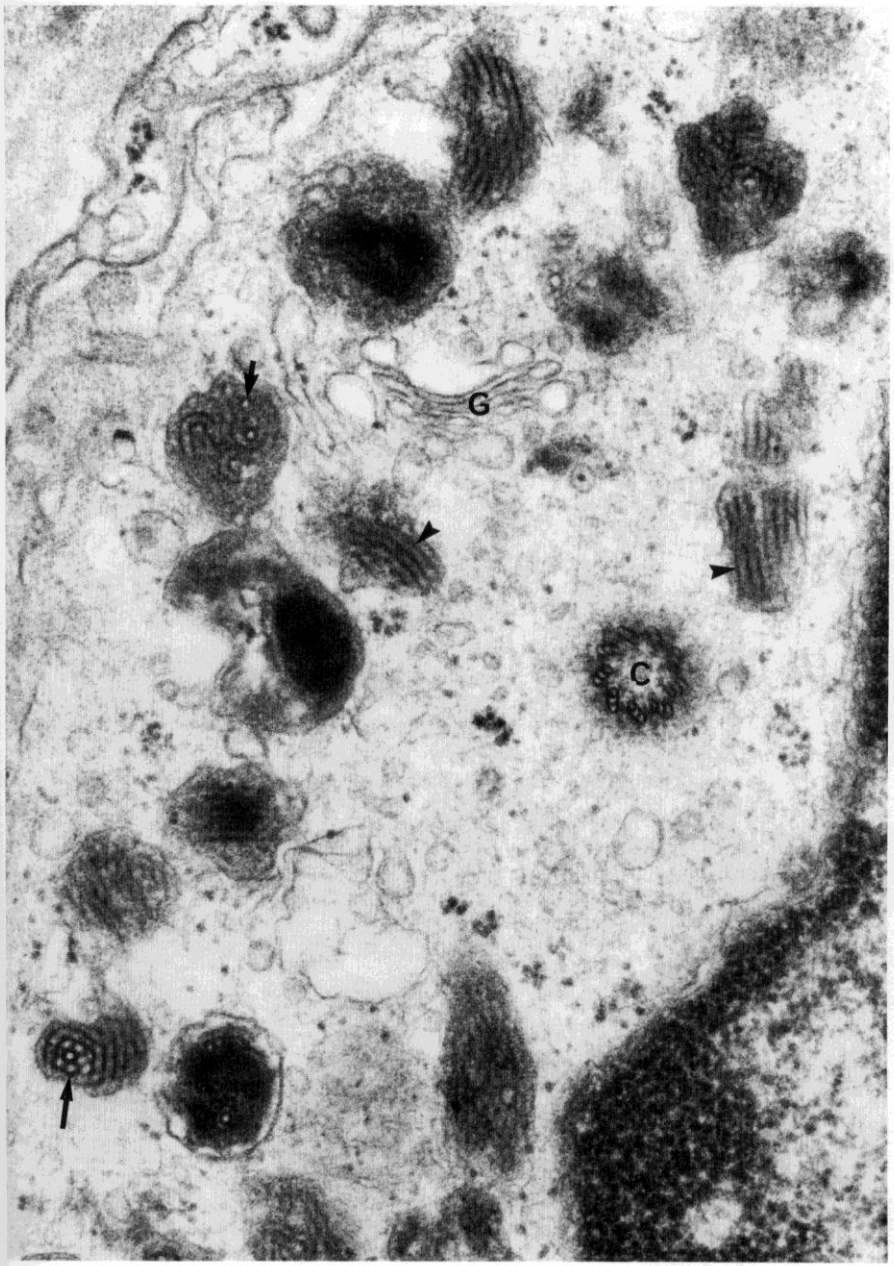

inclusions is, at times, seen in the Golgi region. Yet another possibility is that the microtubules of this structure develop from the ends of the centriolar microtubules (the analogy here is microtubules of cilia), and indeed a fairly, but not totally, convincing illustration depicting this has been published (see Figure 3 in Brunning and Parkin, 1975b). The idea here is that microtubules are first assembled in the cytoplasm and then become enveloped by a membrane, but no suggestions as to how this happens or where the membrane comes from are forthcoming.

Parallel microtubular arrays have been found* in lymphocytes from: (1) cases of rheumatoid arthritis (Hovig et al., 1968; Dryll et al., 1977); (2) late-onset amaurotic idiocy and Tay-Sachs disease (Witzleben, 1972; Noonan et al., 1976); (3) juvenile types of generalized ceroid lipofuscinosis (Schwendemann, 1976); (4) Chediak-Higashi syndrome (White, 1972); (5) systemic and discoid lupus erythematosus (Goodman et al., 1973; Imamura et al., 1975); (6) Hodgkin's disease (Halie et al., 1975; Dryll et al.,1977); (7) sarcoidosis (Belcher et al., 1975); (8) chronic lymphocytic leukemia (Brunning and Parkin, 1975b; McKenna et al., 1977b); (9) severe combined immunodeficiency disease (Payne et al., 1977); (10) infectious mononucleosis (Brunning and Parkin, 1975b; McKenna et al., 1977b; Payne and Tennican, 1982); and (11) many normal or apparently normal individuals (Huhn, 1968; Imamura et al., 1975; Dryll et al. 1977; McKenna et al., 1977a; Payne et al., 1977, 1983; Payne and Glasser, 1978, 1981; Payne and Nagel, 1980; Payne and Tennican, 1982).

As noted above (item 11), lymphocytes containing parallel microtubular arrays have frequently been reported to occur in normal individuals, and it is now widely accepted that this is the normal state. It would appear that in certain pathological states there is an increase in the number of lymphocytes bearing parallel microtubular arrays.

Payne and Glasser (1981) have shown that parallel microtubular array-containing cells constitute the major portion of the third population of lymphoid cells (non-T, non-B). These cells include K cells and NK cells. In a later study, Payne et al. (1983) state that "It is probable that NK cells, K cells, and Ty cells all belong to a distinct third mononuclear cell population which has properties of both T-lymphocytes and monocytes and are characterized morphologically at the light microscopic level as large granular lymphocytes (LGL), and at the ultrastructural level by the presence of parallel tubular arrays (PTA)."

The function of parallel microtubular arrays is not known, but Payne et al. (1983) have hypothesized that these structures "may represent accumulations of some metabolite necessary for the killing process." This is in keeping with the studies of Henkart and Henkart (1982), who have shown that parallel microtubular arrays are released from killer cells in a cytotoxic assay system and that the size of the holes produced in cell membranes by effectors of antibody-dependent, cell-mediated cytotoxicity is similar to the size of the parallel microtubular arrays.

*Single-membrane-bound bodies (about 1 to 3 μm in diameter) containing crystals (hexagonal arrangement) of thick-walled microtubules (inner diameter 10 to 13 nm, wall thickness 8 to 9 nm) have been seen in immature neutrophils in a case of chronic myeloid leukemia (Takemori et al., 1994). In passing, one may note that the crystals in Auer bodies are composed of microtubules that have a diameter of about 16.5 nm. Both structures described in this footnote are myeloperoxidase positive.

Plate 236

From circulating lymphocytes in normal peripheral blood donated by a technician in our department.

Figures 1, 2, and 3. Examples of parallel microtubular arrays where the complexes of microtubules embedded in dense substance lie in large lucent vacuoles. Circular profiles of the rather thick-walled microtubules (arrows) are evident. The microtubules indicated by arrows in *Figures 1 and 2* have an inner diameter of about 12 nm and an outer diameter of about 29 nm, while that indicated by an arrow in *Figure 3* has an inner diameter of about 16.6 nm and an outer diameter of about 40 nm. The cells were well preserved, and there was no evidence of mitochondrial swelling. Therefore the lucent vacuole is unlikely to be a swelling artifact. × 90,000, × 90,000, × 150,000

Figure 4. This parallel microtubular array comprises a complex of microtubules and dense substance bounded by a loose fitting membrane. The microtubules are not too well visualized, hence reliable measurements are not possible. × 145,000

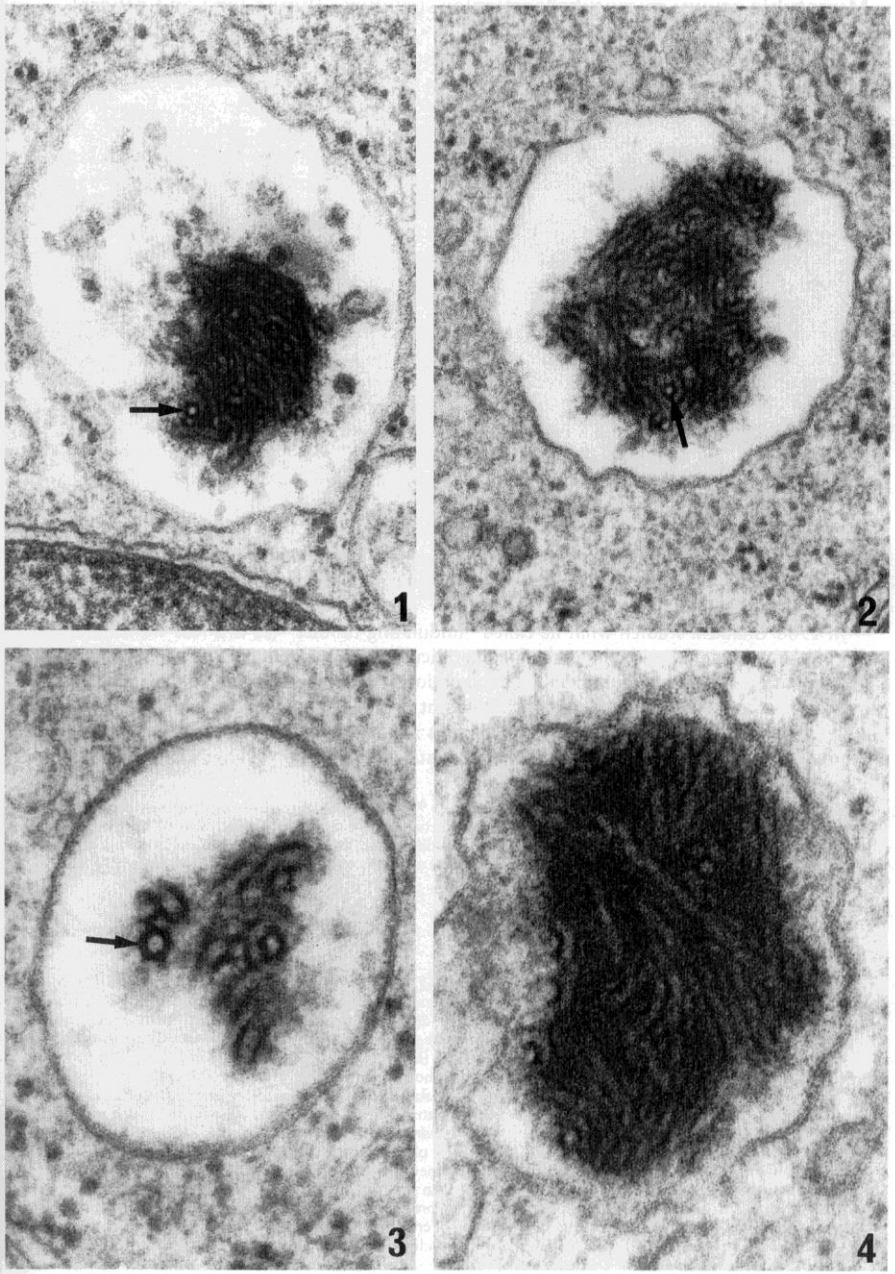

The lymphocytes with granules with tubular substructure are

normal Large Granular Lymphocytes (LGL) or Natural Killer (NK) cells.

And **not** evidence of a lysosomal storage disorder

Other pseudo lysosomal storage phenomenon often found in blood lymphocytes

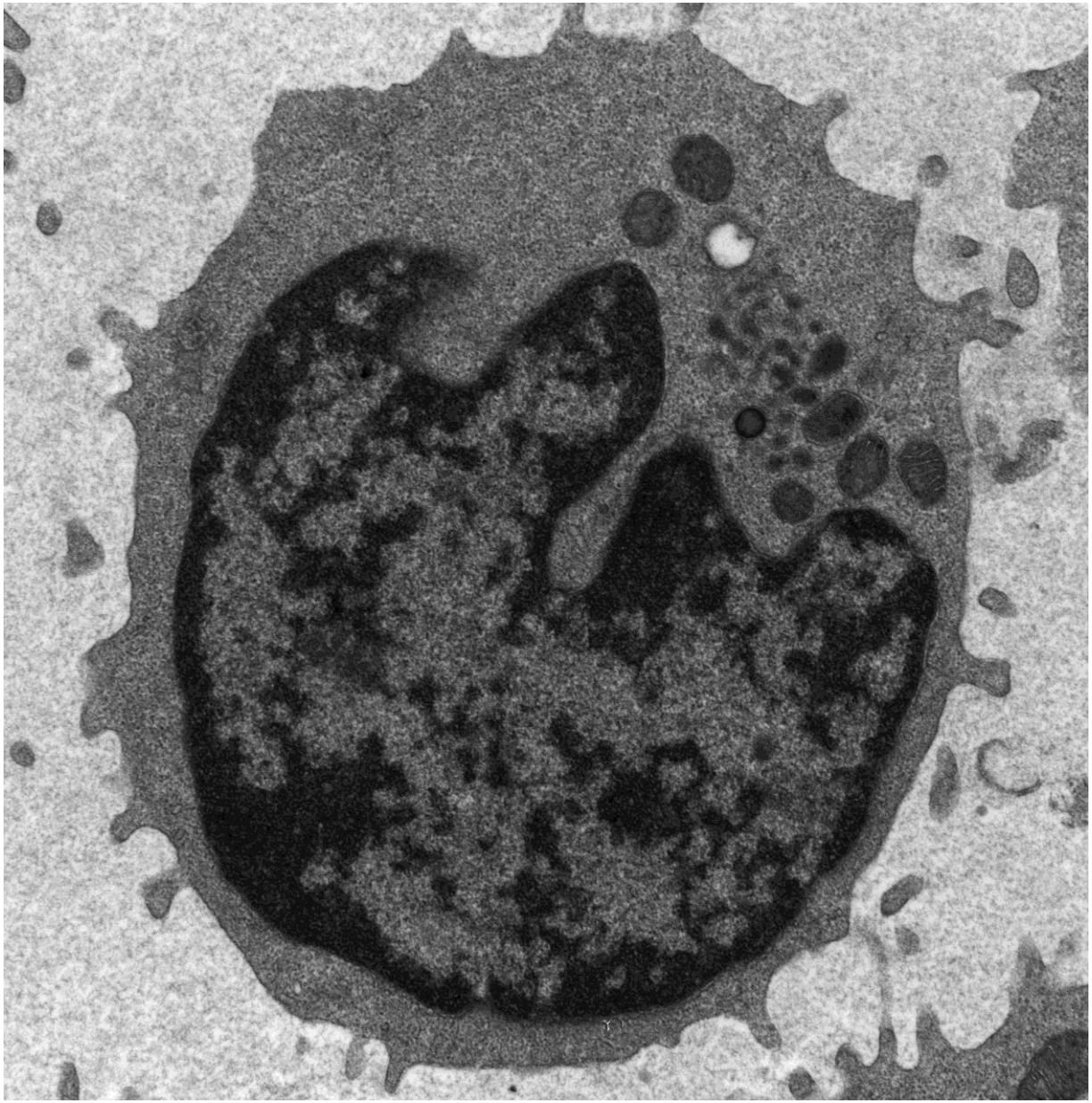

Blood sample from a 2 month old infant with central hypotonia (2013)

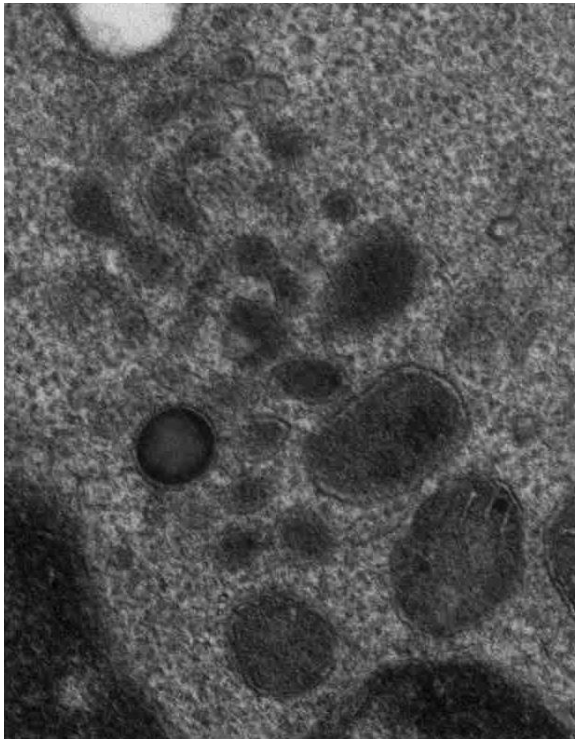

Normal lymphocyte lysosomes

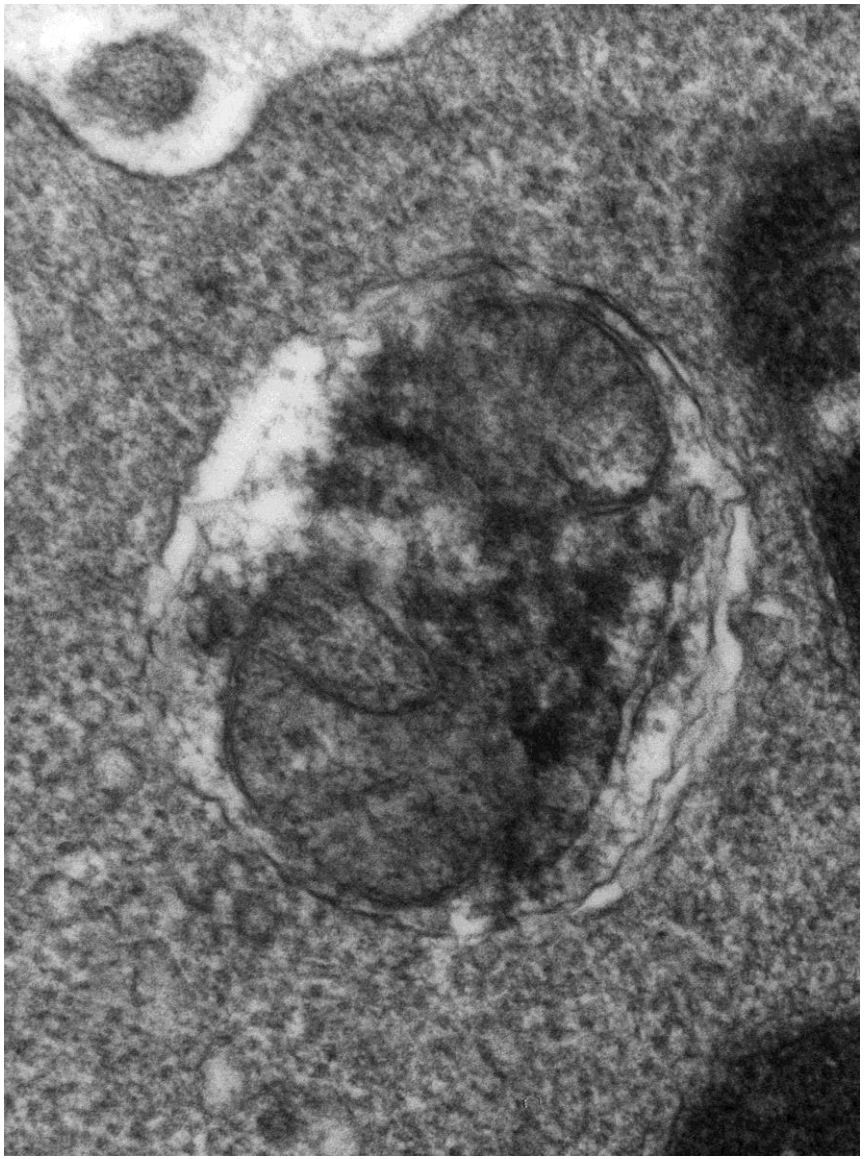

Blood sample from a 2 month old infant with central hypotonia (2013)

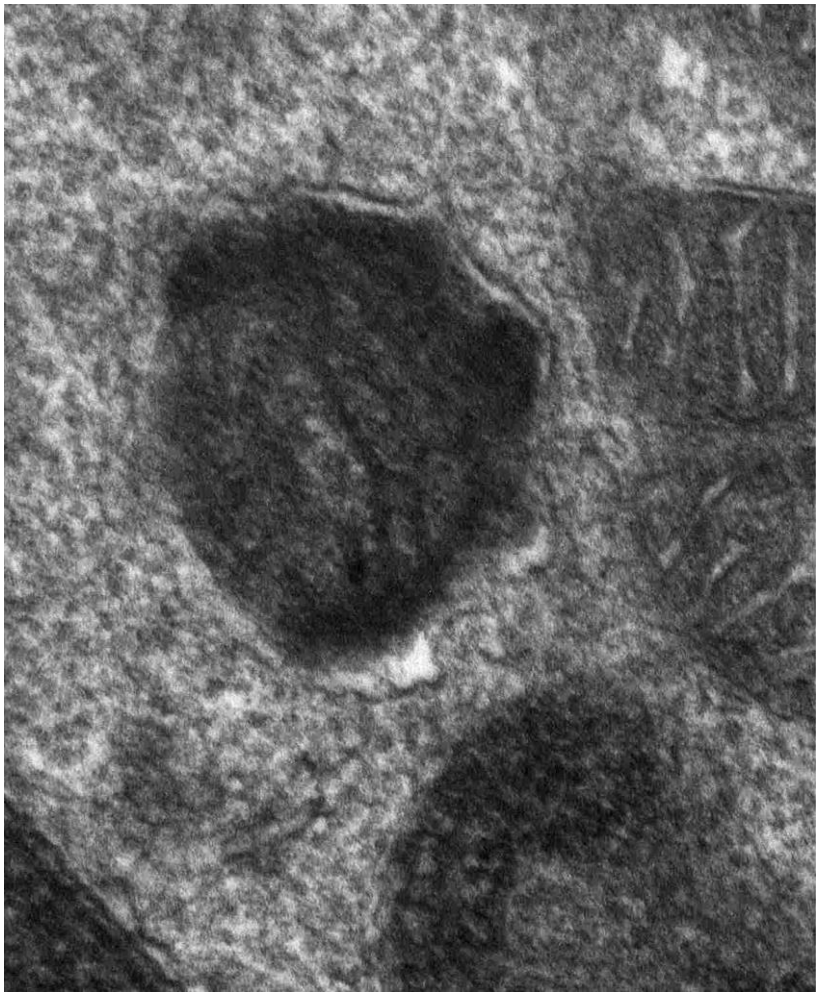

Degenerate mitochondria in autophagocytoplasmic vacuole in lymphocyte

Blood sample from a 2 month old infant with central hypotonia (2013)

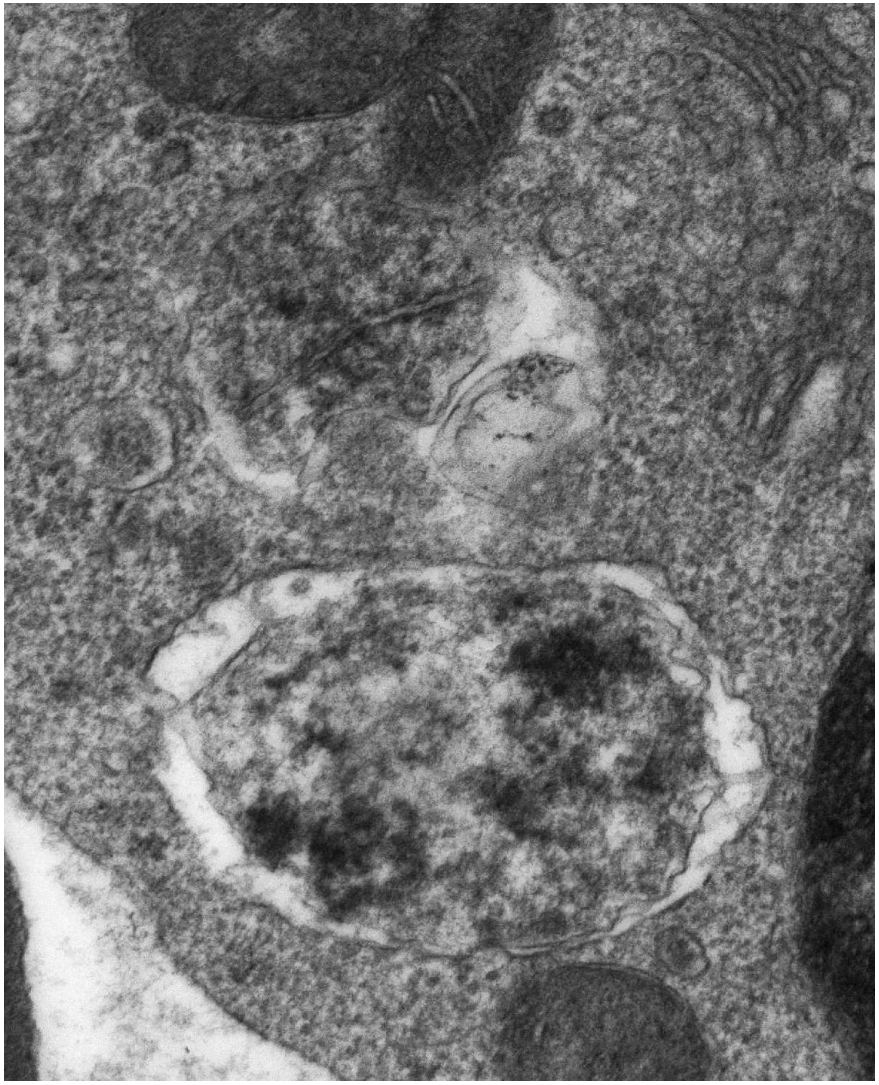

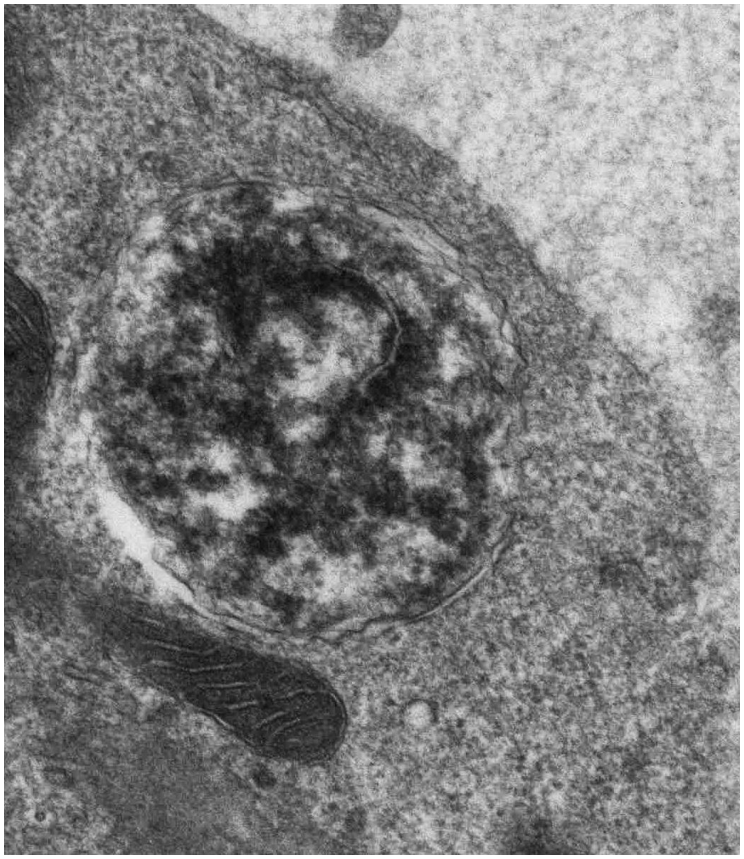

Autophagolysosome in lymphocyte

Blood sample from a 2 month old infant with central hypotonia (2013)

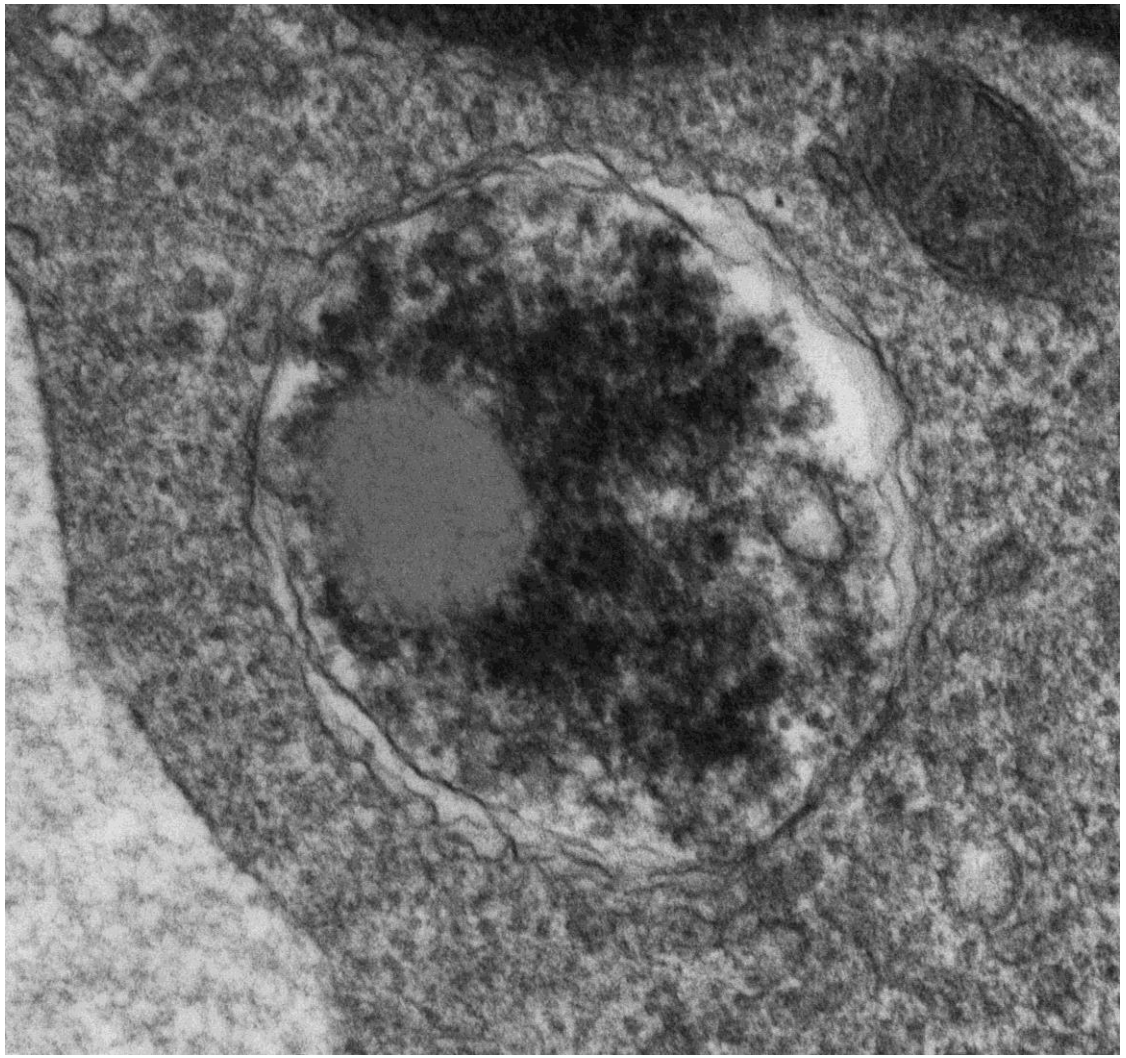

Autophagolysosome in lymphocyte,
which may be confused for a lysosomal storage disorder.
In particular, infantile Batten.

Venous blood lymphocyte

Case of Infantile Batten courtesy of Glenn Anderson, Great Ormond Street Hospital, London

Higher magnification of previous slide
Infantile Batten

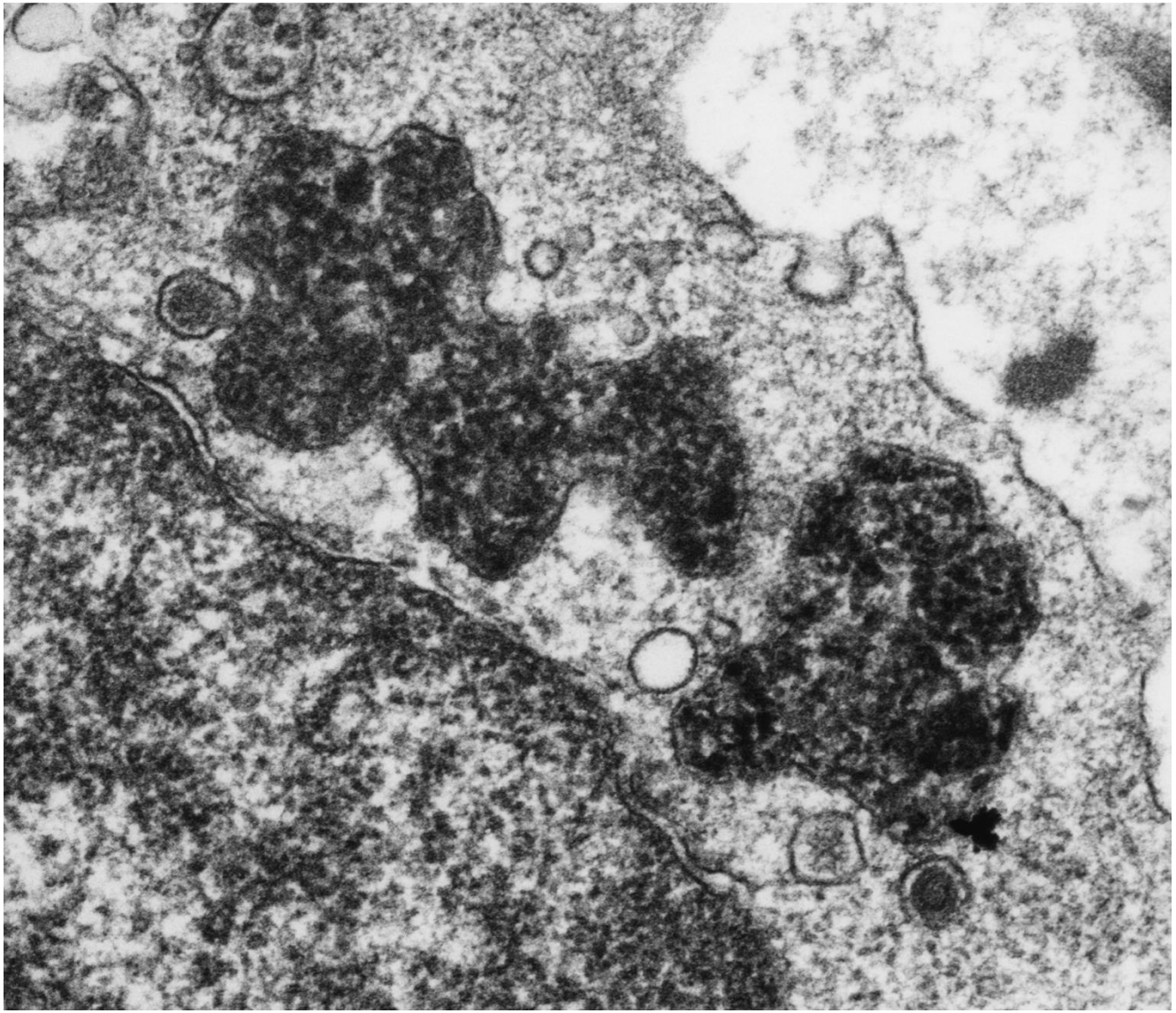

Lysosomes with irregular outline and granular osmiophilic deposits (GROD)

Other normal cells which can be confused for a lysosomal storage disorder

Renal biopsy with intracapillary circulating immature mast cell

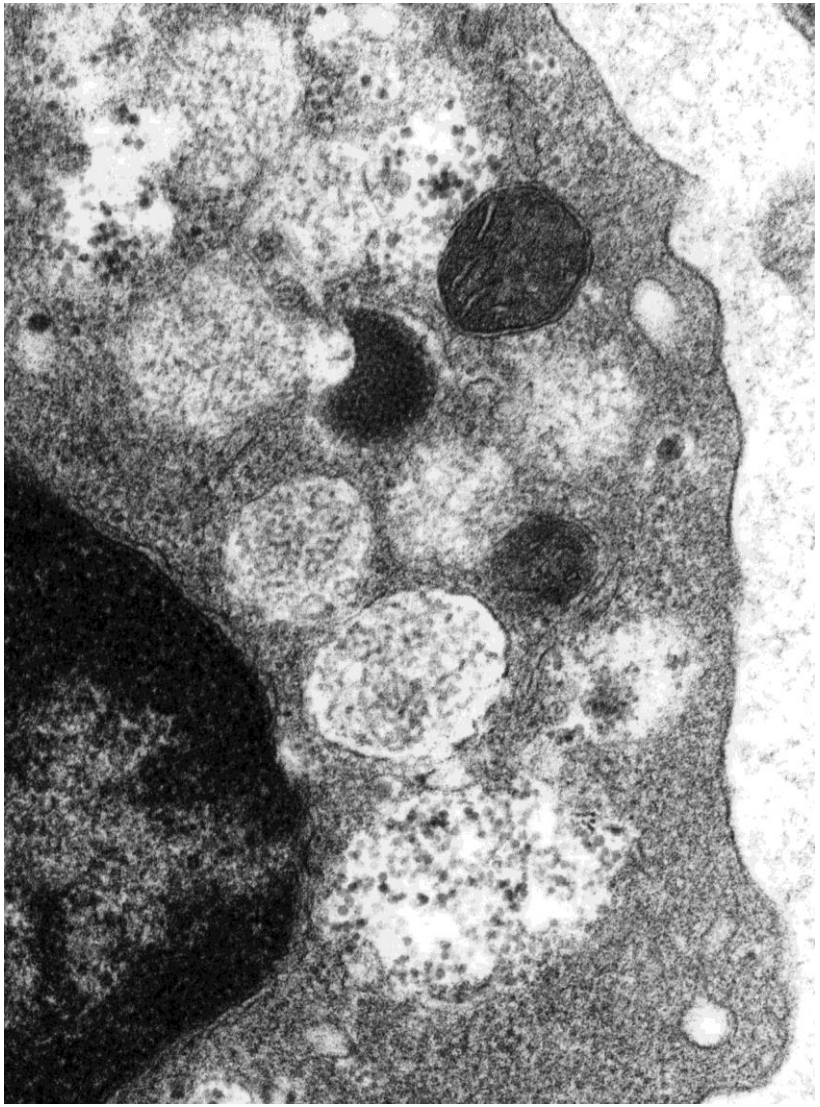

Not evidence of a lysosomal storage disease

Renal biopsy with intracapillary circulating basophil

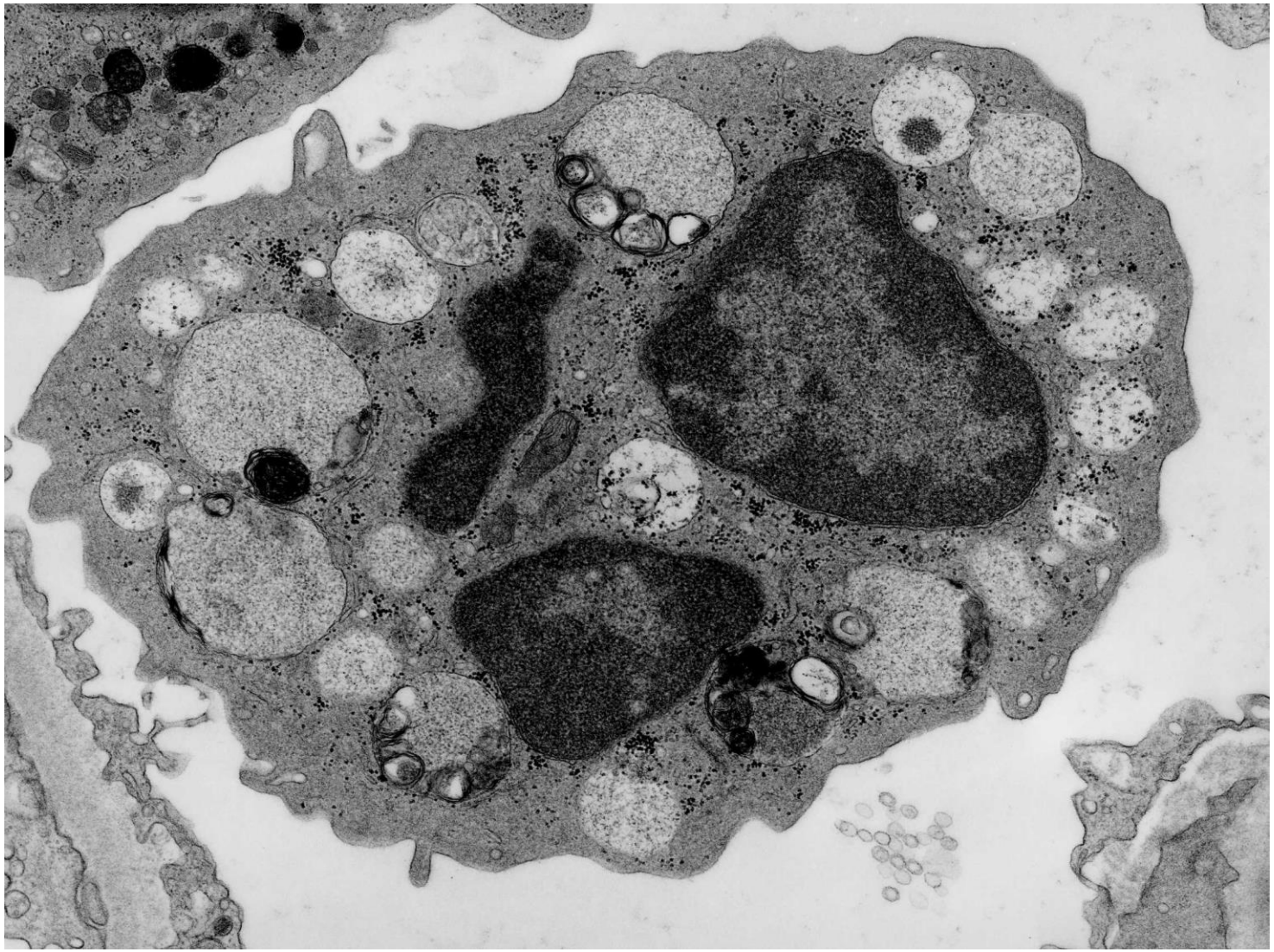

Not evidence of a lysosomal storage disease

Yet another caveat

- When I look at venous blood samples sent for EM from children with neurological symptoms
- In addition to checking lymphocyte lysosomes
- Look at neutrophils for evidence of Jordan's anomaly,
- Platelets for reduced or abnormal alpha granules
- Platelet open canalicular system lipid for hyperlipidaemia
- Monocytes and lymphocytes for tubuloreticular complexes

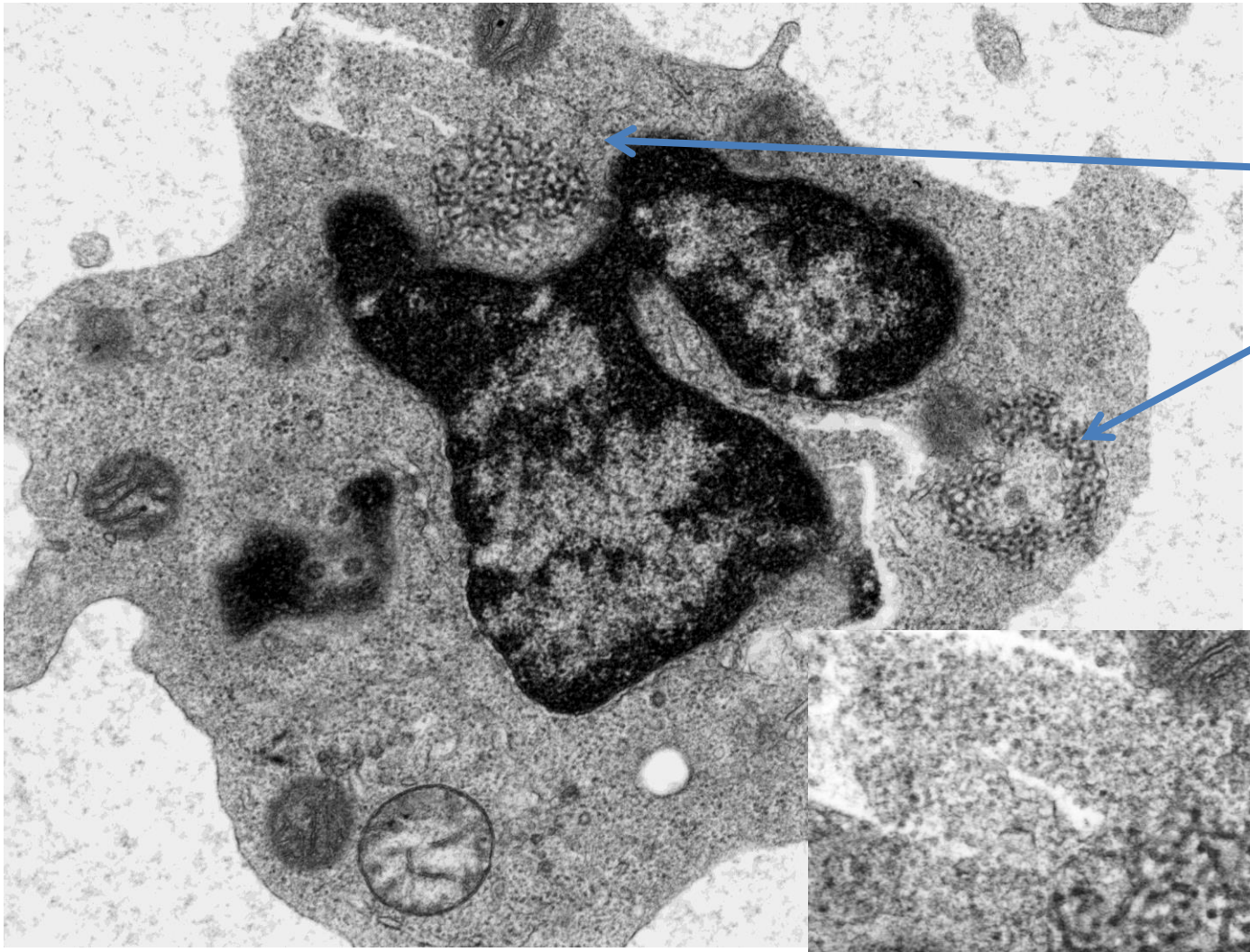

Lymphocyte with large tubuloreticular complexes. Lysosomes all normal

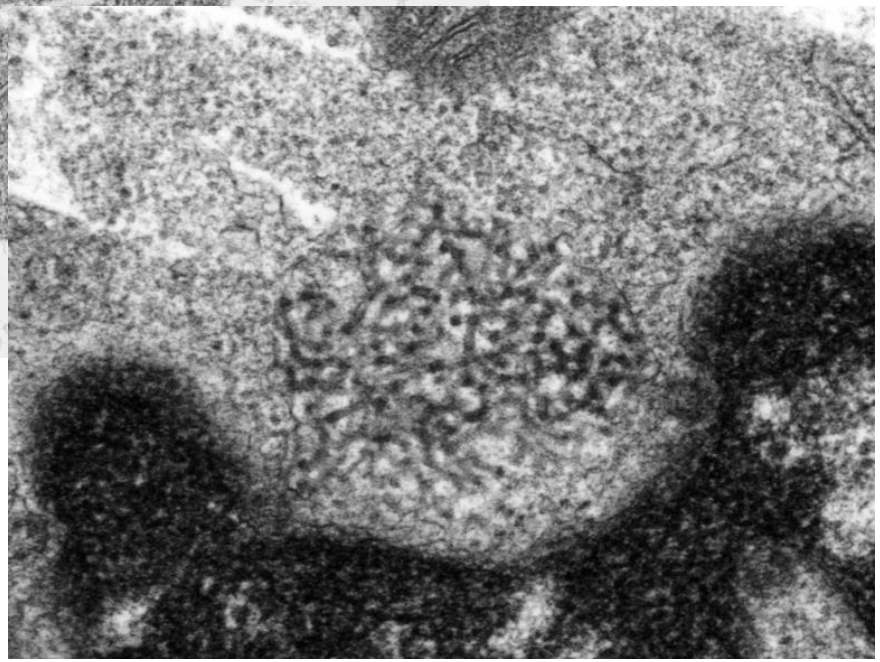

4 month old girl with developmental delay/regression and focal seizures

Aicardi-Goutieres syndrome

Jordans' anomaly (excessive number and size of lipid droplets in granulocytes).

N.B. Normal to have some lipid in granulocytes

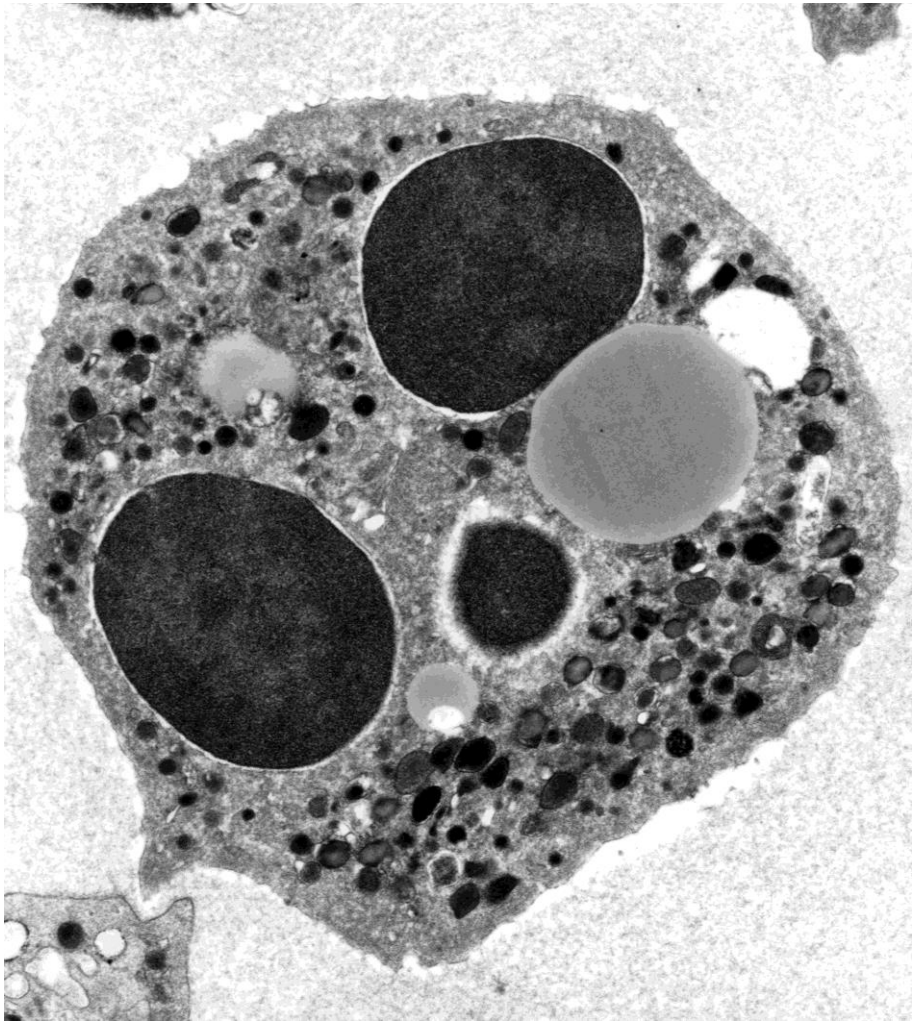

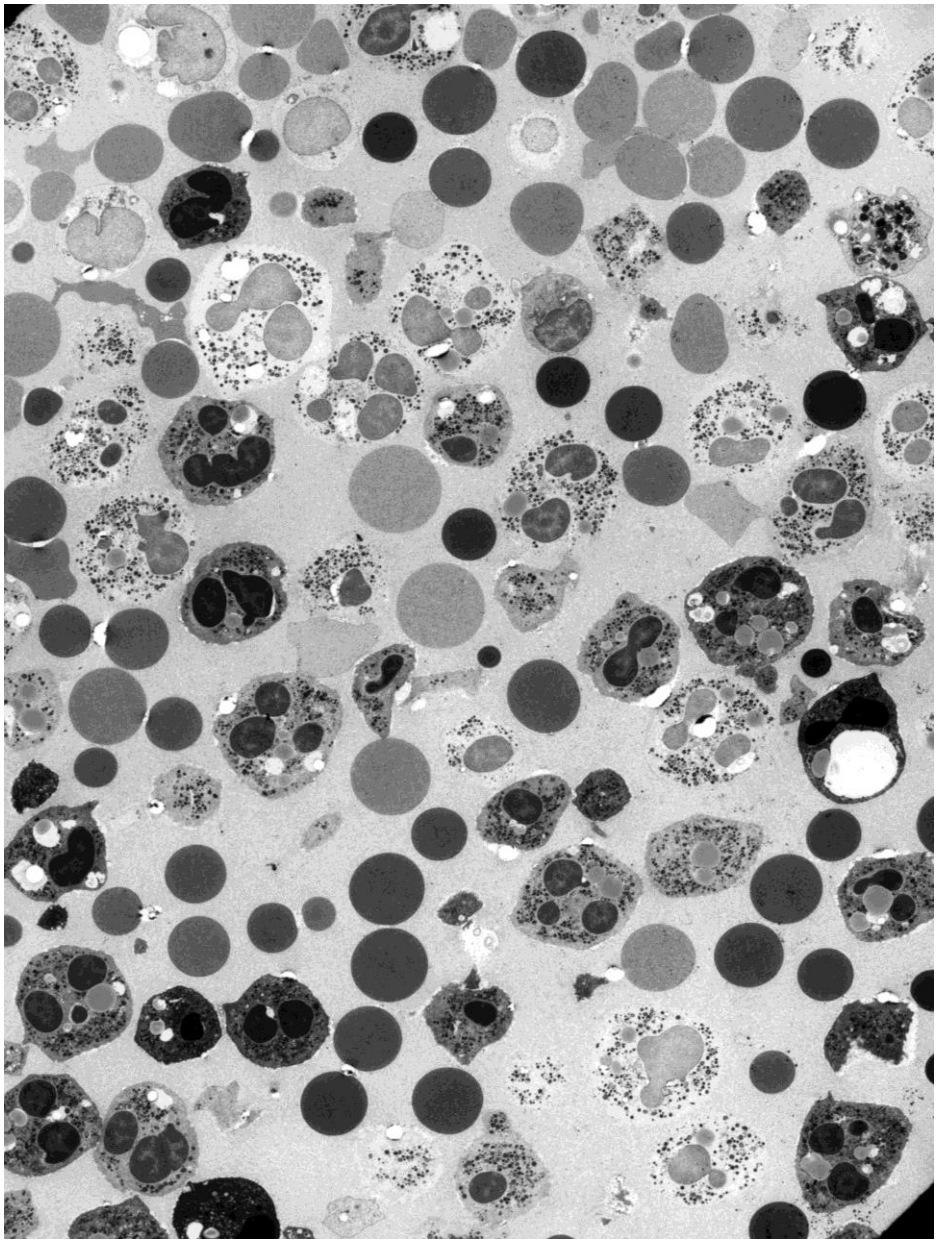

Suspected Chanarin-Dorfman syndrome case

Diabetic ketoacidosis (DKA)

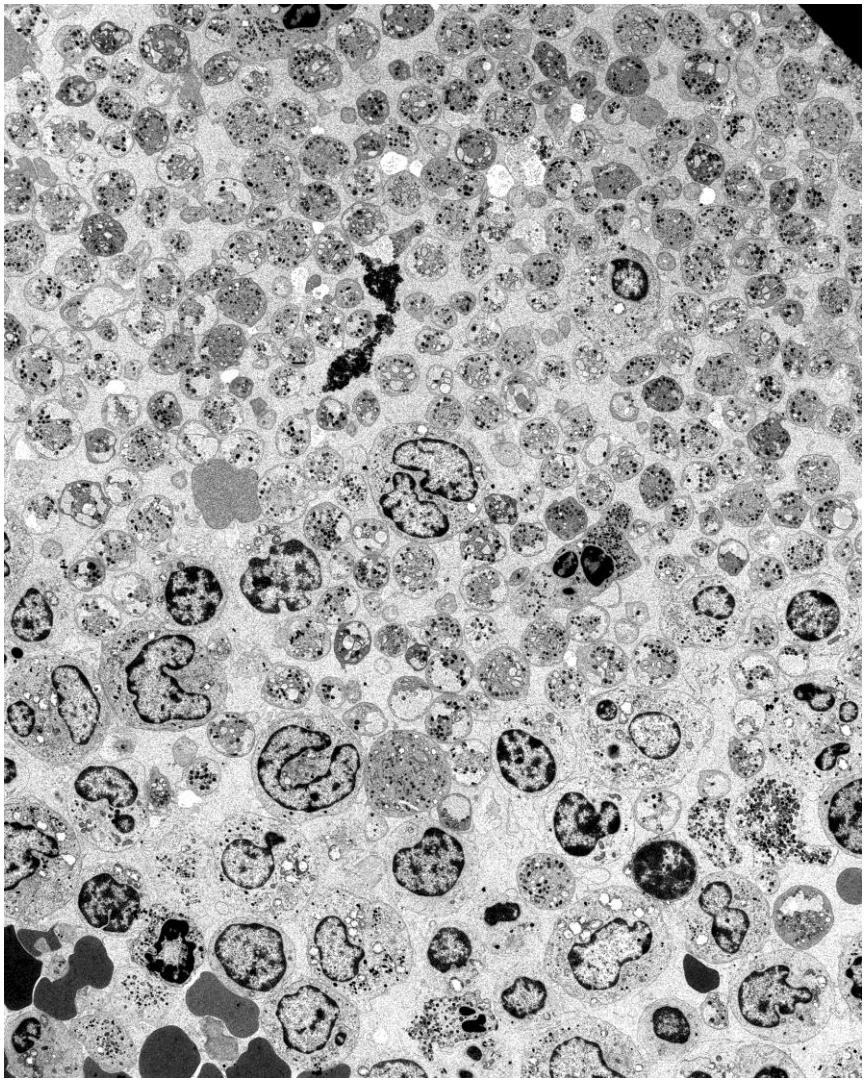

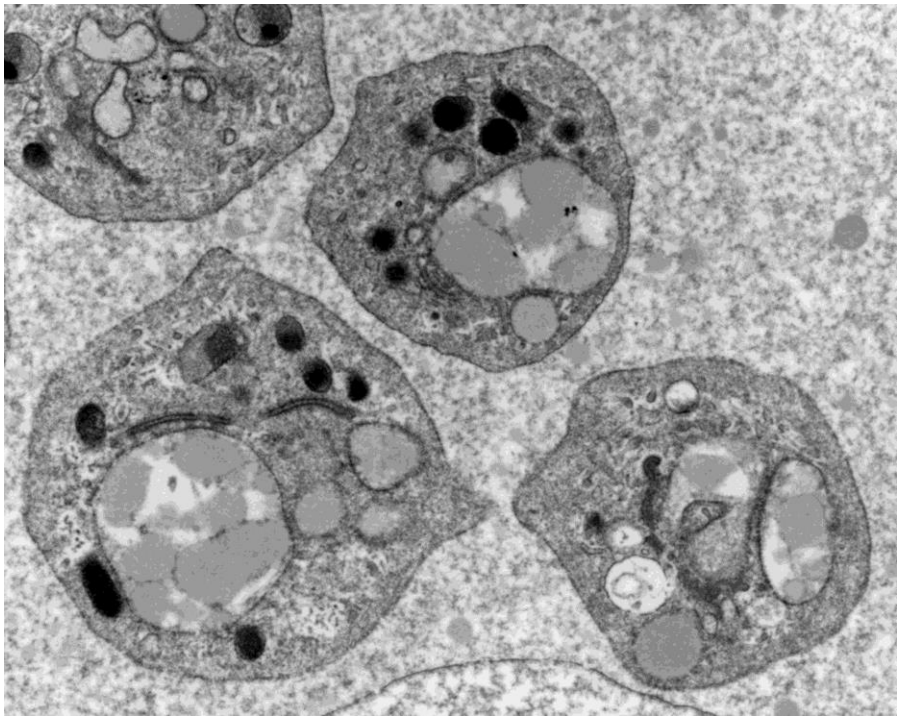

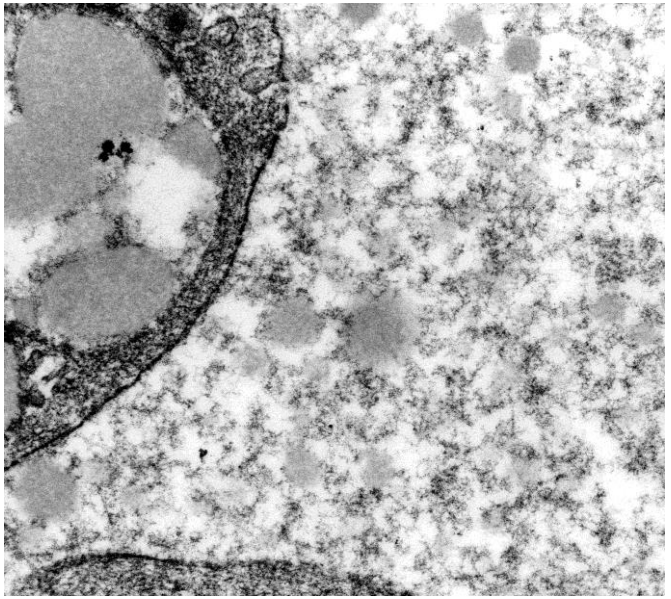

Hyperlipidaemic sample

Lipid in plasma and in platelet open canalicular system (OCS)

Lipid is sequestrated in OCS

Any questions?

5 minute break

Next case

Skin biopsy (2009)

- 16 month old boy
- Ichthyosis
- ?clinical subtype please

Skin biopsy 16 month old boy.

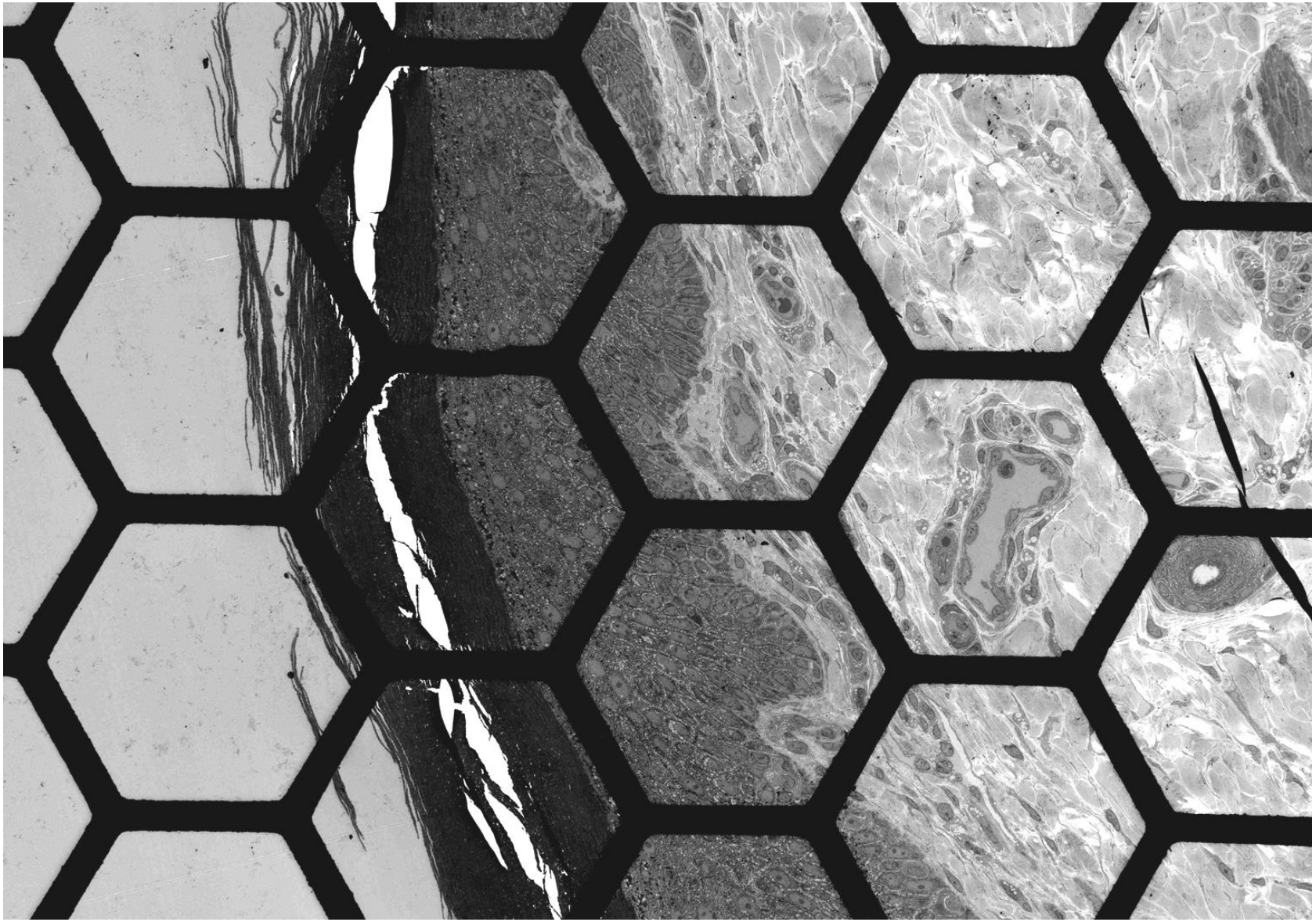

Acanthotic hyperkeratotic epidermis

Ichthyosis 16 month old boy.

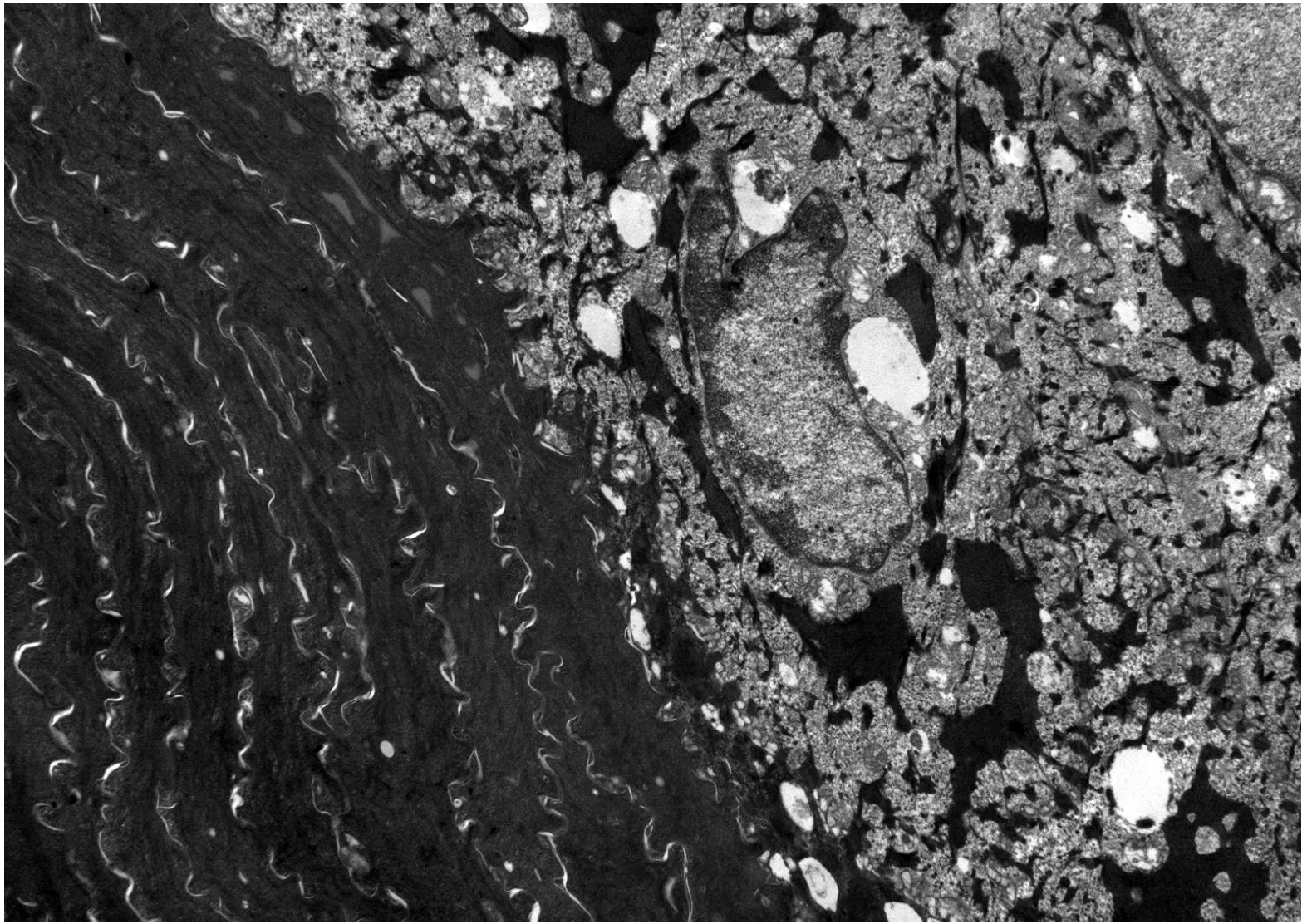

Hyperkeratotic epidermis
Vacuoles in granular layer keratinocytes

Ichthyosis 16 month old boy

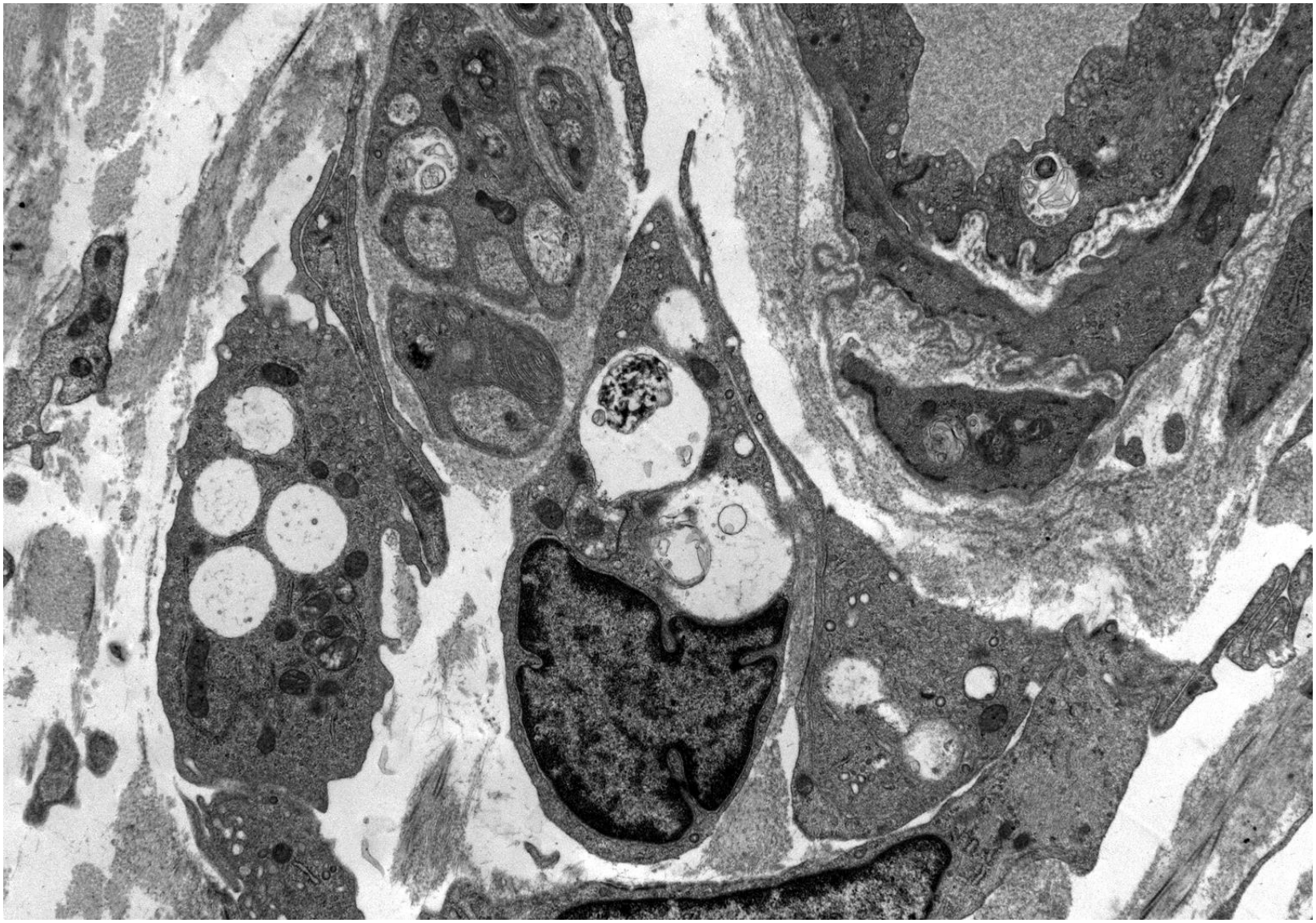

Vacuolated lymphocytes in papillary dermis

Ichthyosis 16 month old boy

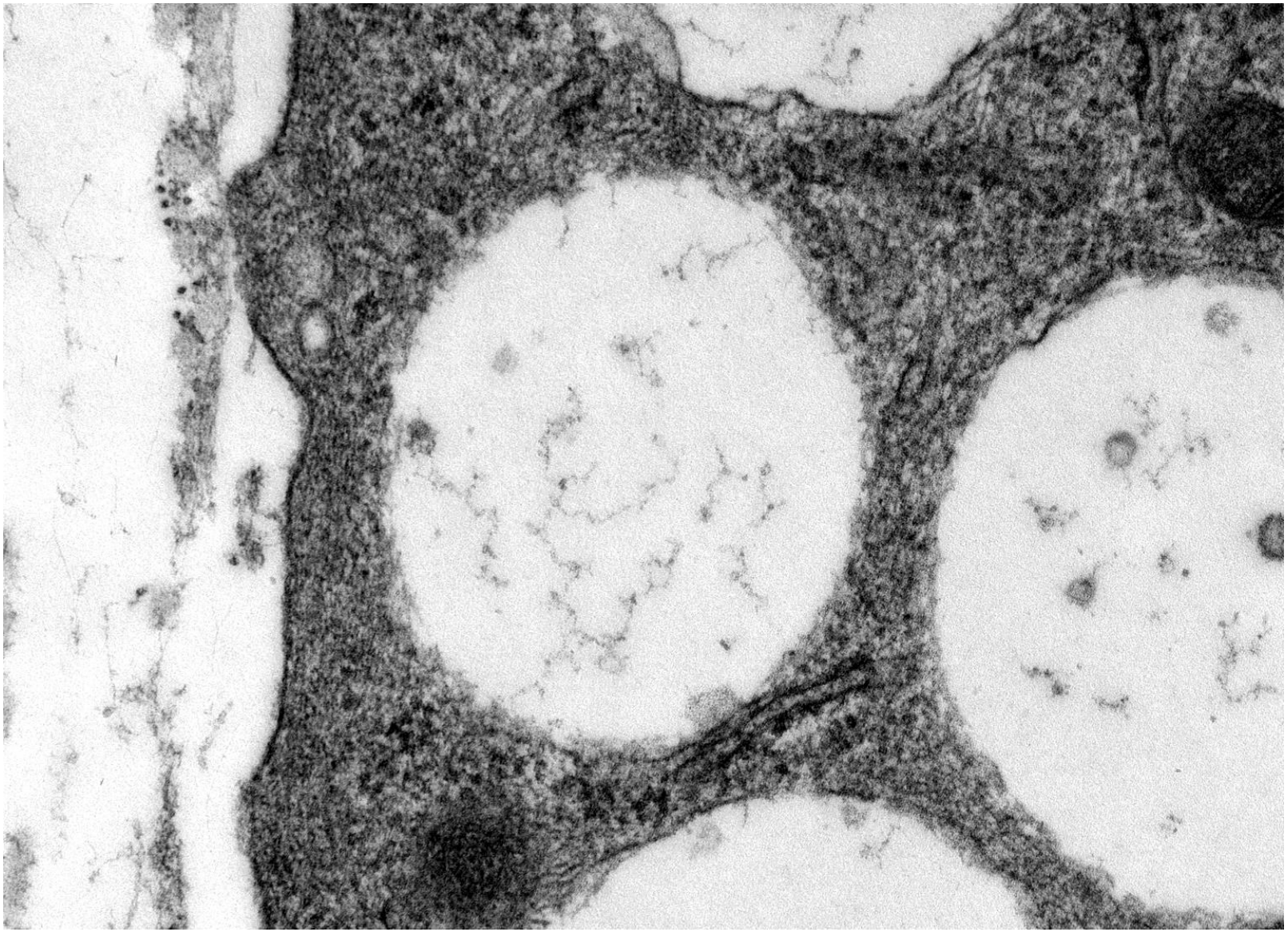

Vacuoles in lymphocyte

Literature search for

- Lysosomal storage disorder
- Ichthyosis

Literature search for

- Lysosomal storage disorder
- Ichthyosis

- **Result**
- Gaucher
- Multiple sulphatase deficiency

Blood sample sent to Biochemistry Department at Manchester Children's Hospital

- A selected number of enzymes associated with lysosomal storage disorders checked

- <<We have already run our lysosomal enzyme screen and urine mucopolysaccharide and oligosaccharide screen on this patient. All results were normal, I will review the results today just to check. I am somewhat at a loss as what to suggest.>>

- EM of blood also done (by me) – all cells normal.

EM images emailed to a few EM colleagues in different parts of the world.

- None of them had come across any condition like it.

EM images emailed to a few EM colleagues in different parts of the world.

- None of them had come across any condition like it.
- Later sent email to Society of Cutaneous Ultrastructure Research (SCUR) members (via secretary, Dr Christine Betts)
- Dr Wolfgang Muss in Salzburg sent me a pdf of an article on Lysosomal Storage Disorder in skin

Ultrastruct Pathol. 2006 Nov-Dec;30(6):489-503.

Skin biopsy: a useful tool in the diagnosis of lysosomal storage diseases.

Alroy J, Ucci AA.

Source

Department of Pathology, Tufts University School of Medicine and Tufts-New England Medical Center, Boston, Massachusetts 02111, USA. joseph.alroy@tufts.edu

Abstract

In this report, the authors summarize their 19-year experience with over 200 biochemically proven cases of lysosomal storage diseases using electron microscopic screening of more than 950 skin biopsies. They found that electron microscopy (EM) is a highly sensitive, efficient, cost-effective, and rapid diagnostic screening tool for evaluation of lysosomal storage diseases in skin biopsies. Although EM is more expensive than a single enzyme assay, it can exclude more than 90% of cases in which lysosomal storage disease is being considered. EM is critical for diagnosis of neuronal ceroid lipofuscinosis and mucolipidosis IV and is the most cost-effective screening tool in patients with previously unrecognized storage diseases.

On page 502:
In some skin biopsies there is storage of lipids that is similar to, but needs to be **distinguished from classical inherited lysosomal storage diseases**. These include diseases such as lipid proteinosis [38], neutral lipid storage [39], and drug-induced lysosomal storage. Drug-induced storage includes numerous systemic cationic amphophilic drugs [40] as well as some **locally administrated creams [41].** Therefore, it is essential that skin biopsies to evaluate storage diseases require **a detailed history including the drugs that the patient is or was treated with**.

41.
J Inherit Metab Dis. 2004;27(4):507-11.
Pseudo-lysosomal storage disease caused by EMLA cream.
Vallance H, Chaba T, Clarke L, Taylor G.

I rang the author Dr Alroy, who confirmed my now suspicion that I had been **barking up the wrong tree**

Correct interpretation
in the other tree

99% sure
100% wrong

Dr Wolfgang Muss kindly sent me the pdf of the paper in reference 41 and thanked me for the educational opportunity acquired in reading the paper.

J Inherit Metab Dis. 2004;27(4):507-11.

Pseudo-lysosomal storage disease caused by EMLA cream.

Vallance H, Chaba T, Clarke L, Taylor G.

Source

Department of Pathology, Children's and Women's Health Centre of British Columbia, 4500 Oak Street, Room 2F22, Vancouver, British Columbia V6H 3N1, Canada. hvallance@cw.bc.ca

Abstract

Prilocaine-lidocaine emulsion (EMLA cream) is a topical anaesthetic commonly used prior to diagnostic and therapeutic procedures. While undergoing clinical investigation for the suspicion of a metabolic disorder, a series of children underwent skin biopsy with EMLA cream pretreatment. In each case, the pathologist identified ultrastructural features consistent with a lysosomal storage disorder, yet the clinical features were not consistent with the pathological findings. Ultrastructural artefact was suspected, resulting from the use of the EMLA cream. All patients underwent repeat skin biopsy without EMLA cream. Biopsies were reviewed by two pathologists blinded to the previous biopsy findings. Electron microscopy repeated without the use of EMLA cream was normal. It is concluded that the use of EMLA cream causes ultrastructural artefact and should be avoided prior to skin biopsy for electron microscopy.

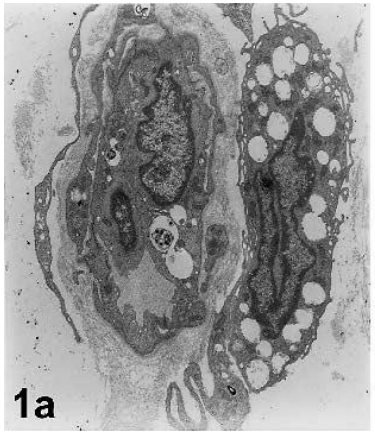

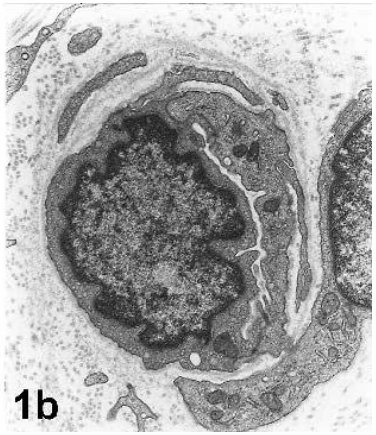

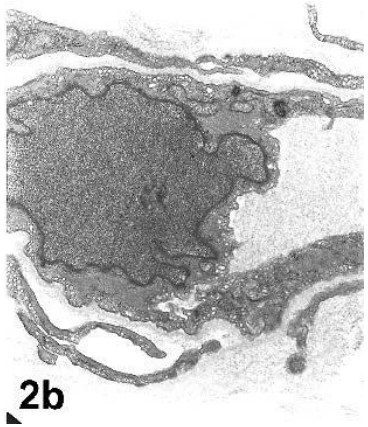

I then recalled that one of the dermatologists I had met at a previous SCUR meeting had commented that lysosome membrane pumps can be iatrogenically made dysfunctional, resulting in lysosomal swelling.

Swollen lysosomes can be found in renal transplant biopsies

Renal biopsy 2 months post-transplant.
Early FSGS and Calcineurin Inhibitor (CNI) toxicity

Interstitial cell with swollen lysosomes

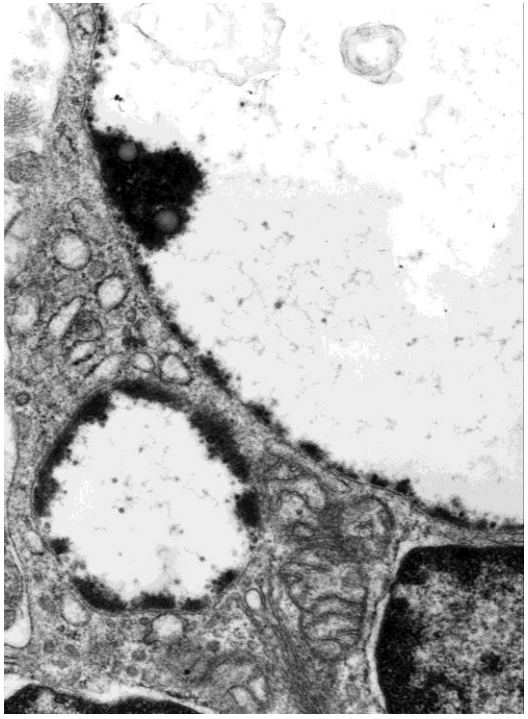

Higher magnification of previous

Swollen lysosomes in proximal convoluted tubule

Am J Kidney Dis. 2008 Mar;51(3):491-503. doi: 10.1053/j.ajkd.2007.10.044.

Osmotic nephrosis: acute kidney injury with accumulation of proximal tubular lysosomes due to administration of exogenous solutes.

Dickenmann M, Oettl T, Mihatsch MJ.

Source

Clinic for Transplantation Immunology and Nephrology, University Hospital, Basel, Switzerland.

Abstract

Osmotic nephrosis describes a morphological pattern with vacuolization and swelling of the renal proximal tubular cells. The term refers to a nonspecific histopathologic finding rather than defining a specific entity. Osmotic nephrosis can be induced by many different compounds, such as sucrose, hydroxyethyl starch, dextrans, and contrast media. It has a broad clinical spectrum that includes acute kidney injury and chronic kidney failure in rare cases. This article discusses the pathological characteristics, pathogenesis, and various clinical entities of osmotic nephrosis.

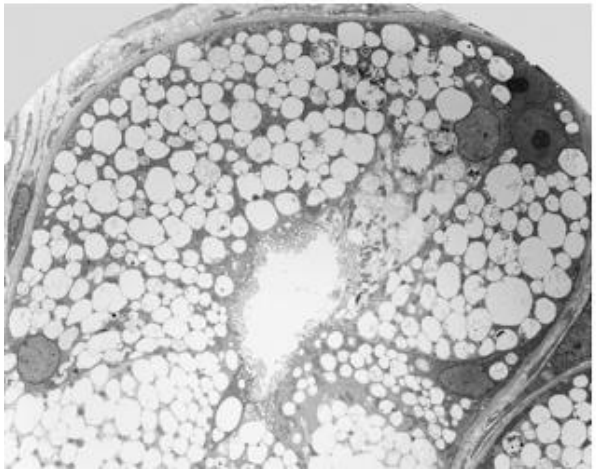

Any questions?

Next topic

Heart Biopsy from St elsewhere (2009)

- Images emailed to me from a paediatric pathologist I had previously helped
- Patient is a 3 month old girl with heart problems
- 2 healthy siblings
- Parents are cousins

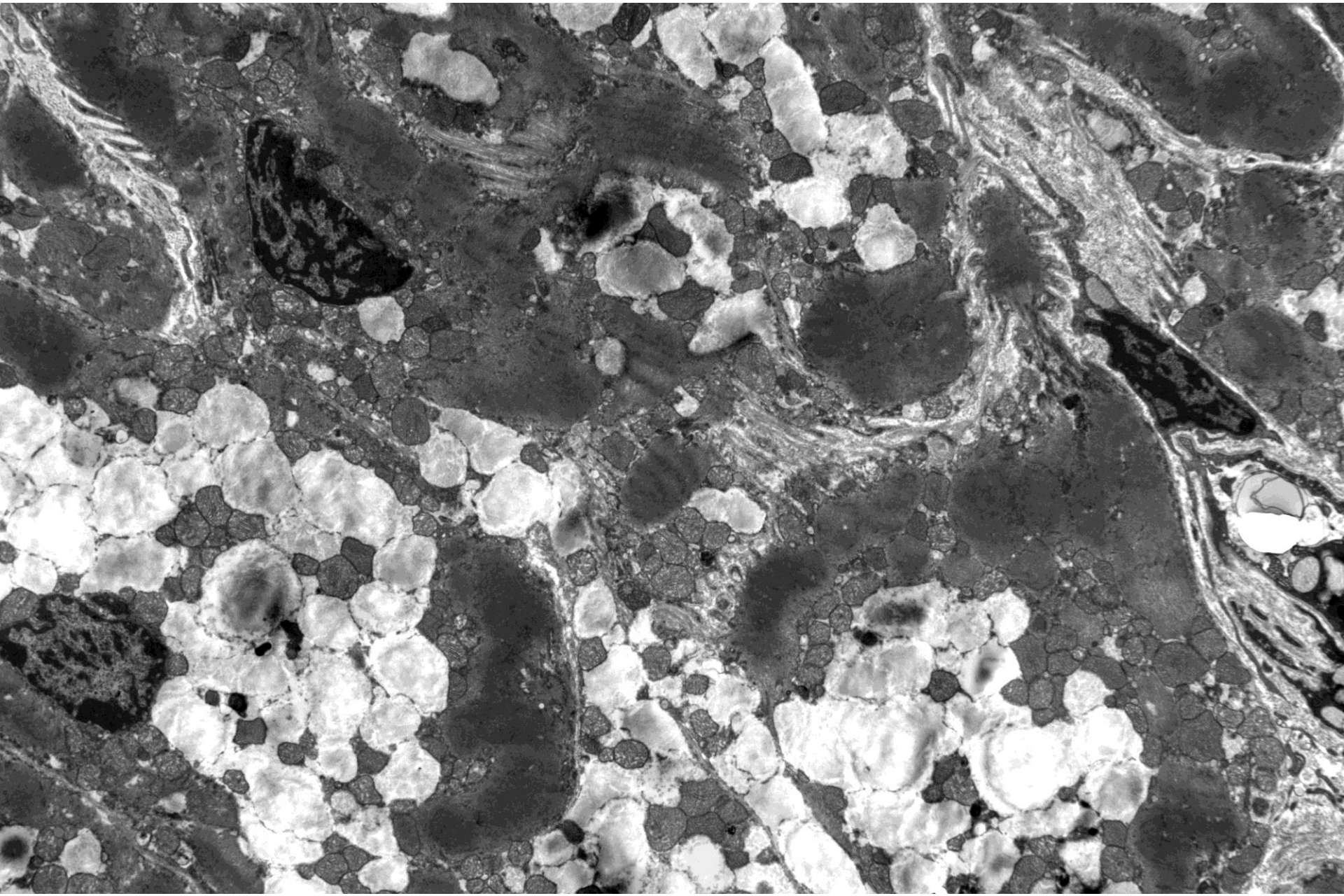

EM images of heart biopsy from St Elsewhere

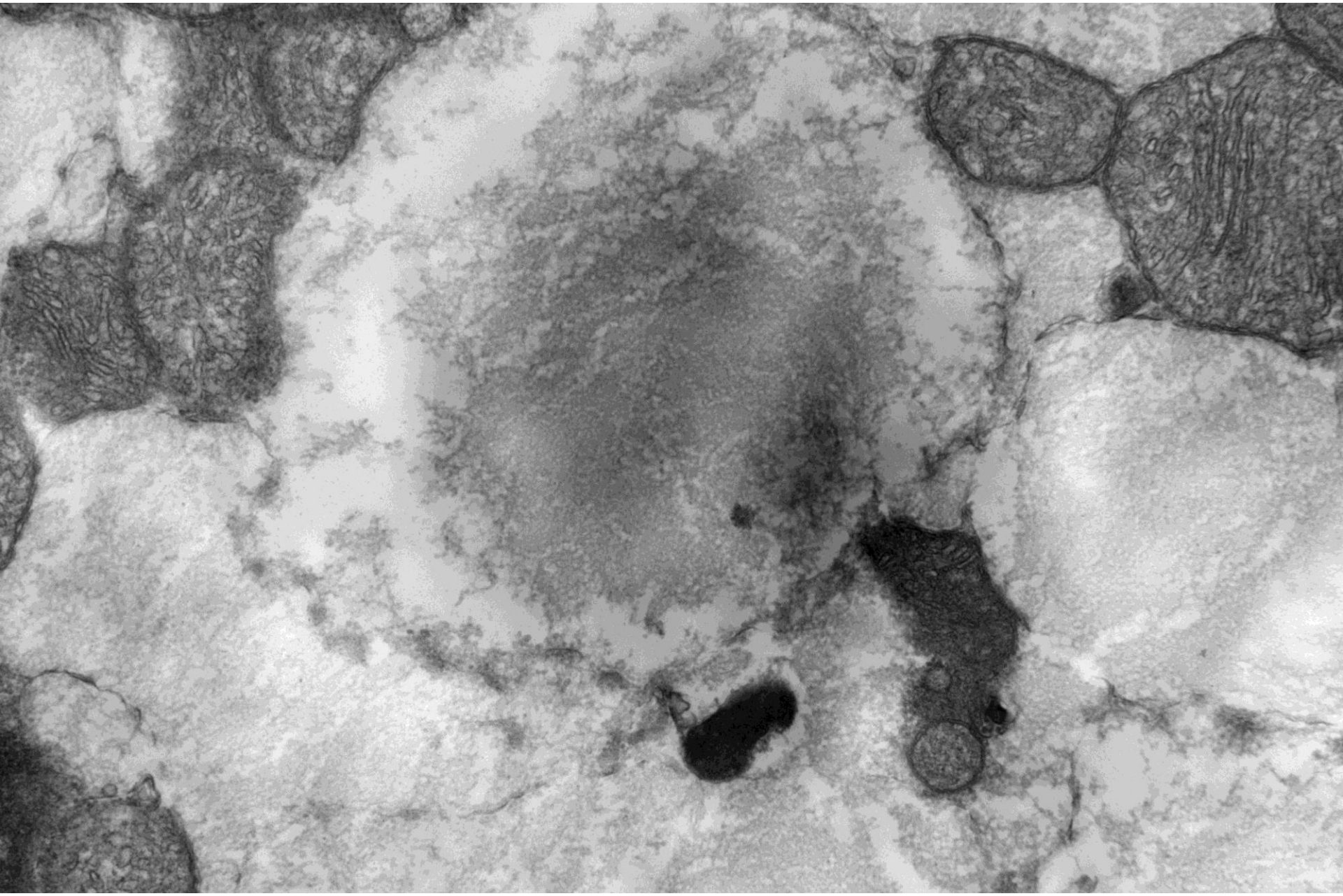

Higher magnification of previous EM image

<<Bart,

Thanks for showing the case. I did show it myself to other paediatric pathologists and three of them thought that the material was not intralysosomal, but bounded by ER. None of them had a definitive idea what it was, somebody ventured ‘some sort of fat’.>>

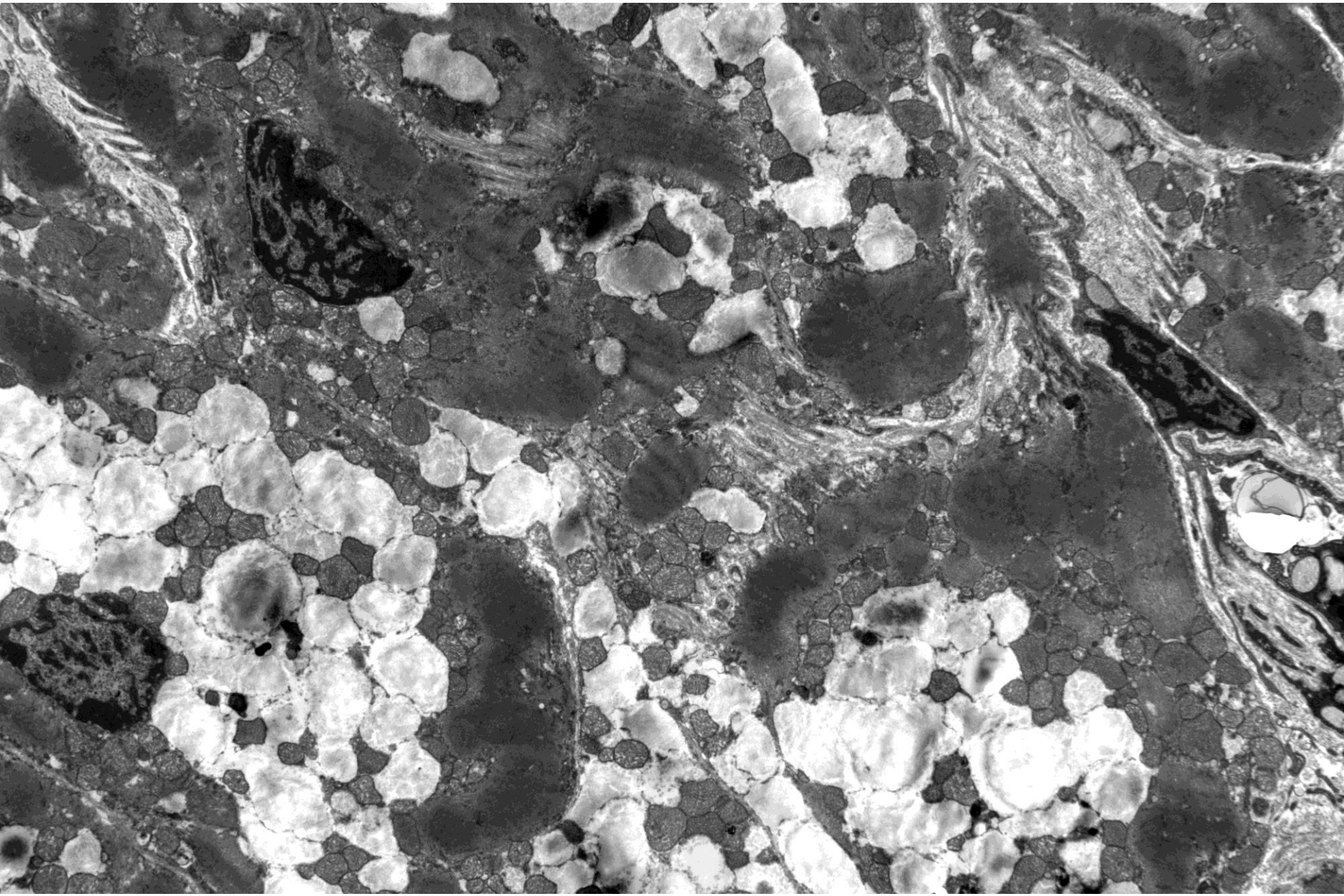

Looks a little like lipid droplets

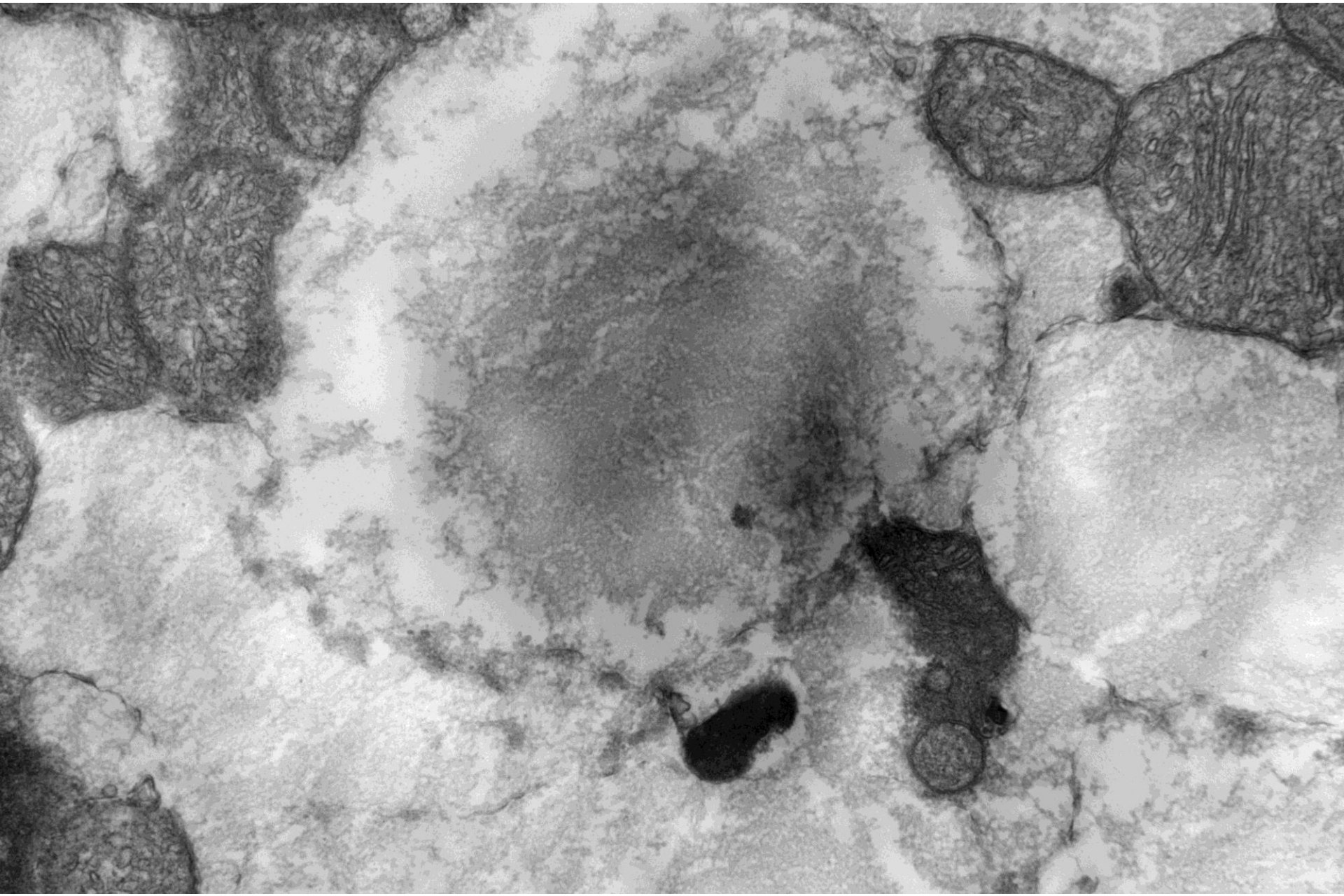

A hint of granularity

Zoomed in view of previous slide

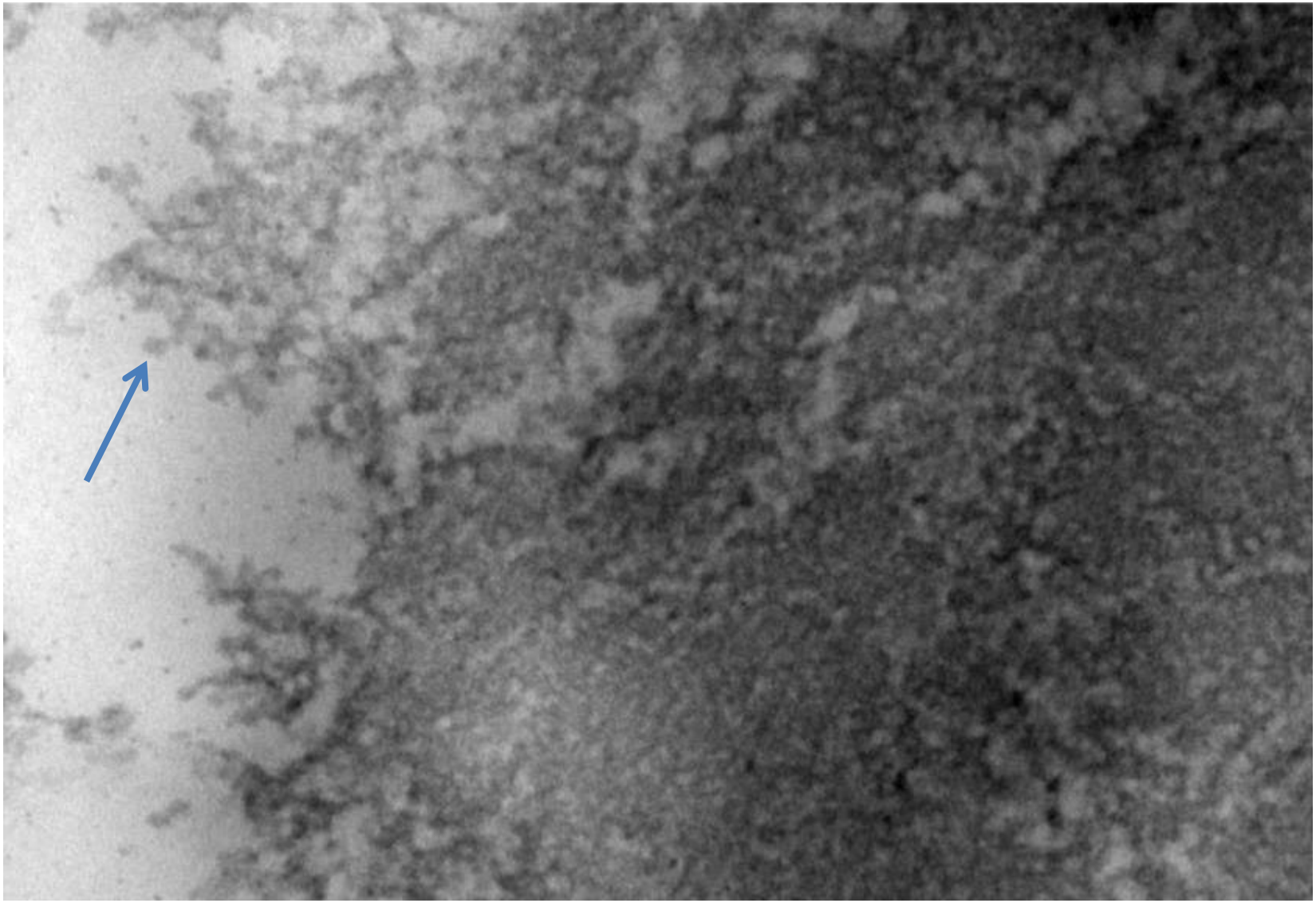

A hint of granularity at higher magnification

Resin block sent over to Sheffield the next day

- Section prepared and images emailed

Cardiac myocyte with abundant glycogen

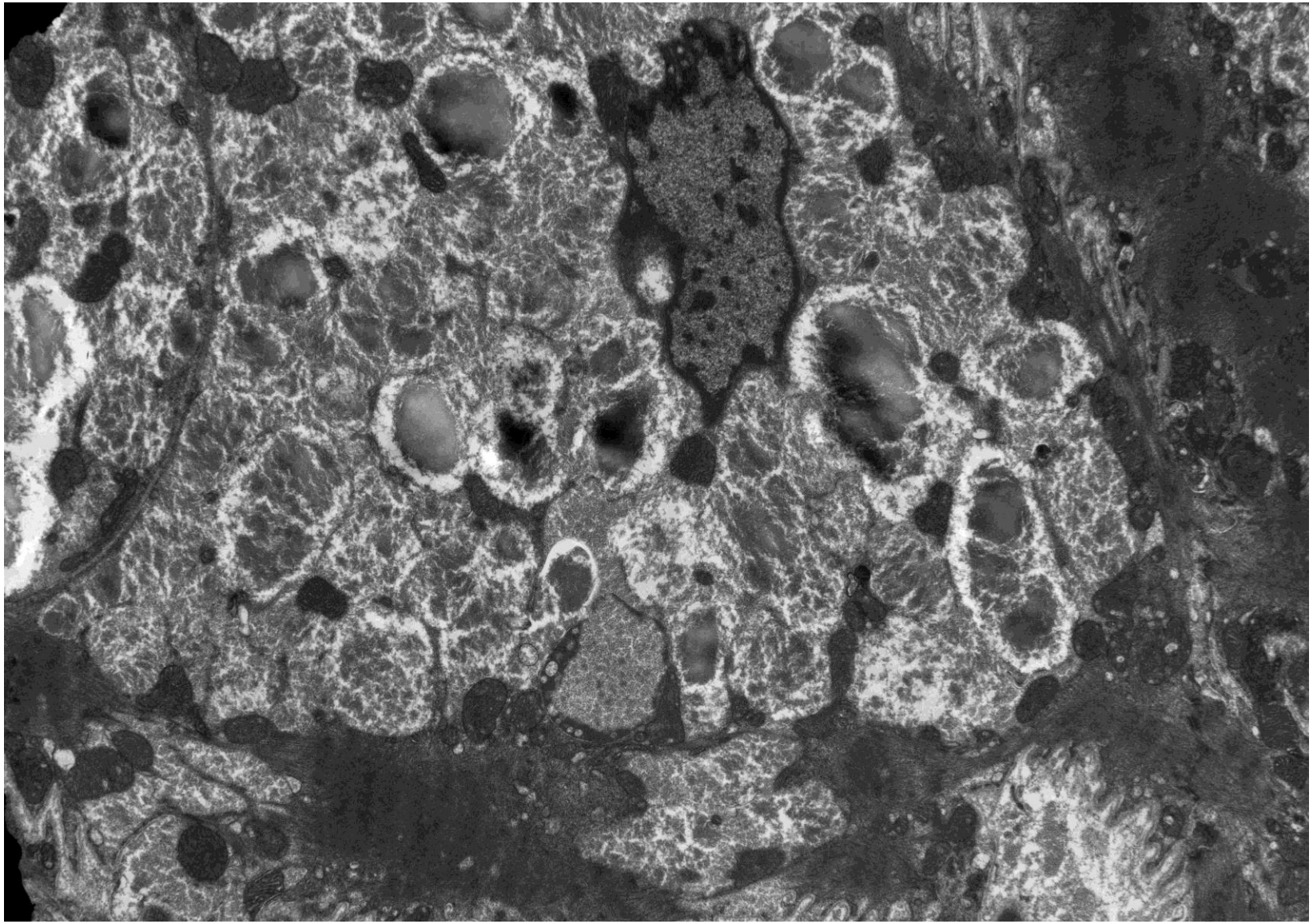

Abundant glycogen, intra-lysosomal and cytosolic

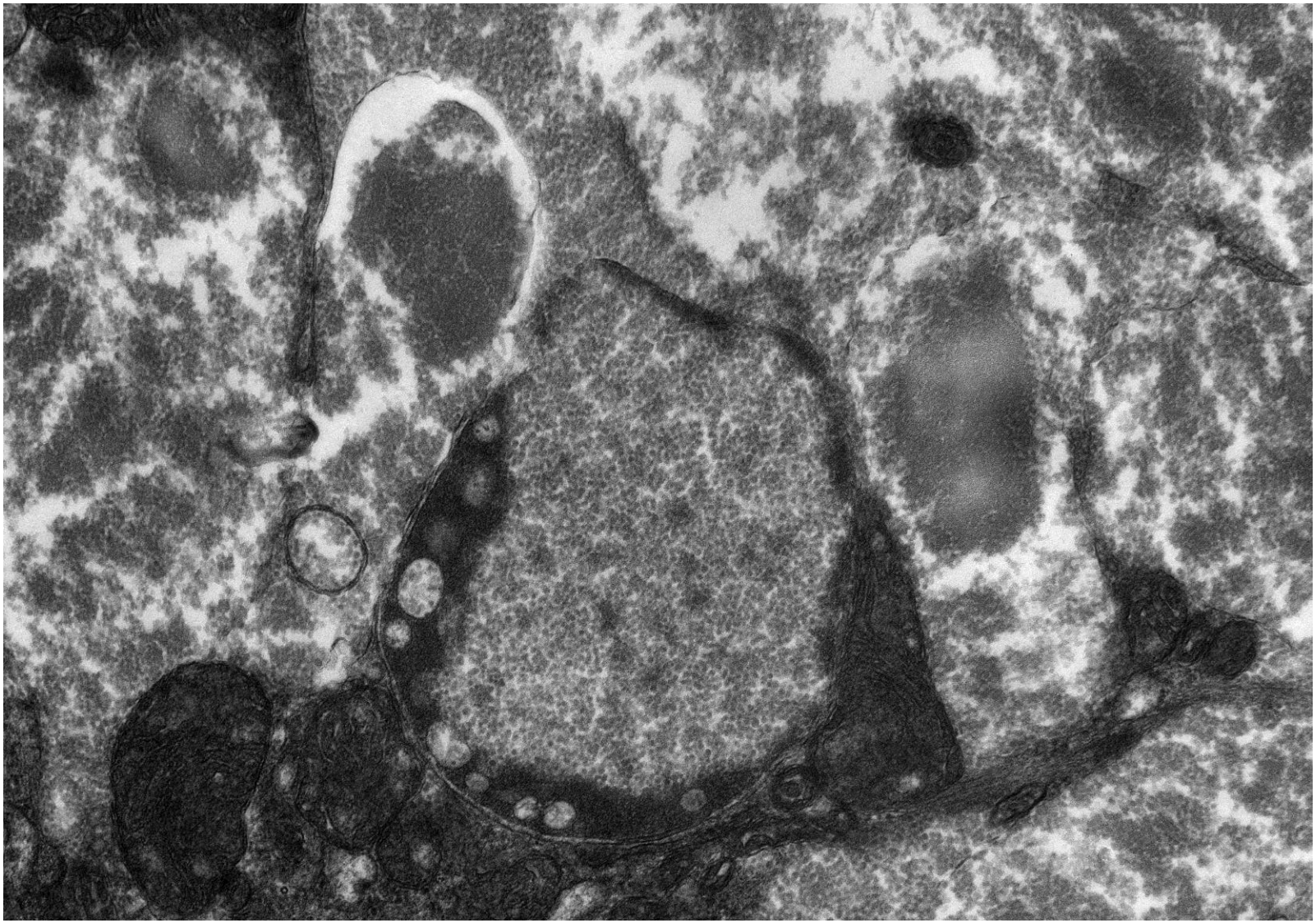

Higher magnification of previous slide

Mono-particulate intra-lysosomal glycogen 22nm in diameter

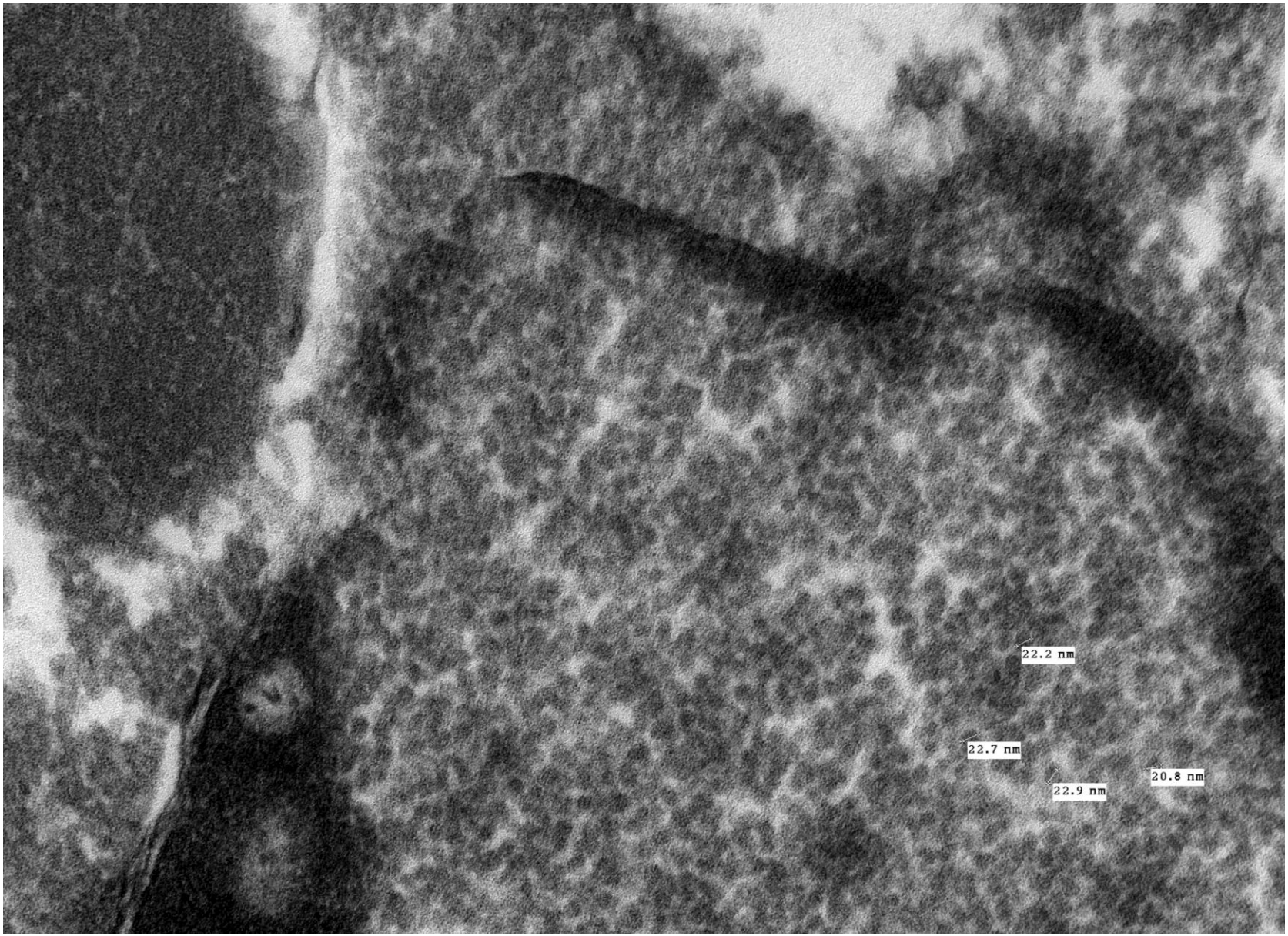

Higher magnification of previous slide

Glycogen filled lysosomes in endothelial cells

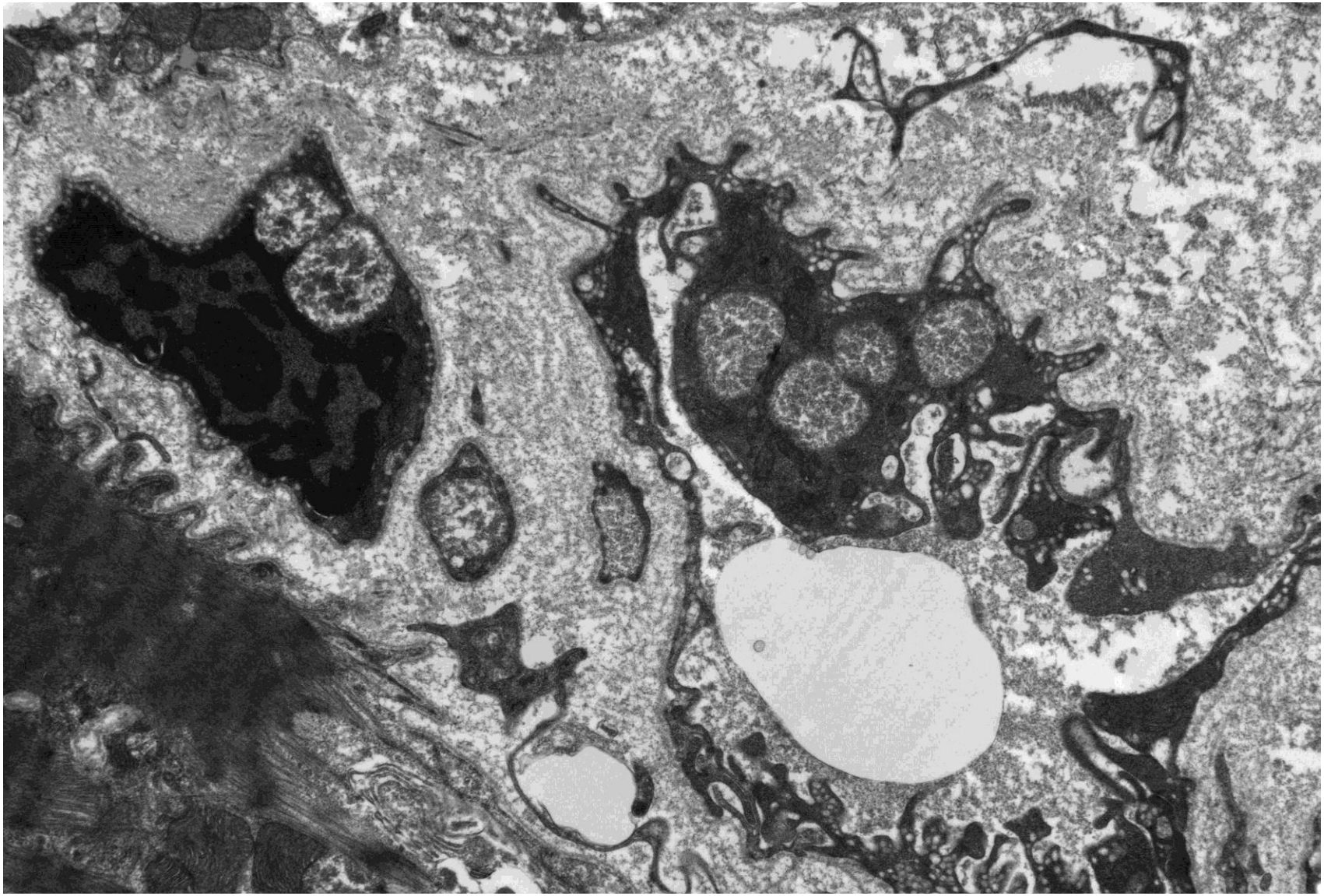

Blood sample sent to biochemistry department confirming diagnosis of Pompe's disease

Glycogen storage disorder type IIa

Heart biopsy learning points

- Worth emailing different people until you get an answer.
- Mild tissue drying (pre-fixation desiccation) present.
- Did this cause the PAS stain on the histology sample to appear to be negative?
- Was the original EM section over-washed causing the glycogen staining to be reduced?

Any questions?

Received a request to talk about platelet EM

Blood samples for inherited platelet disorders

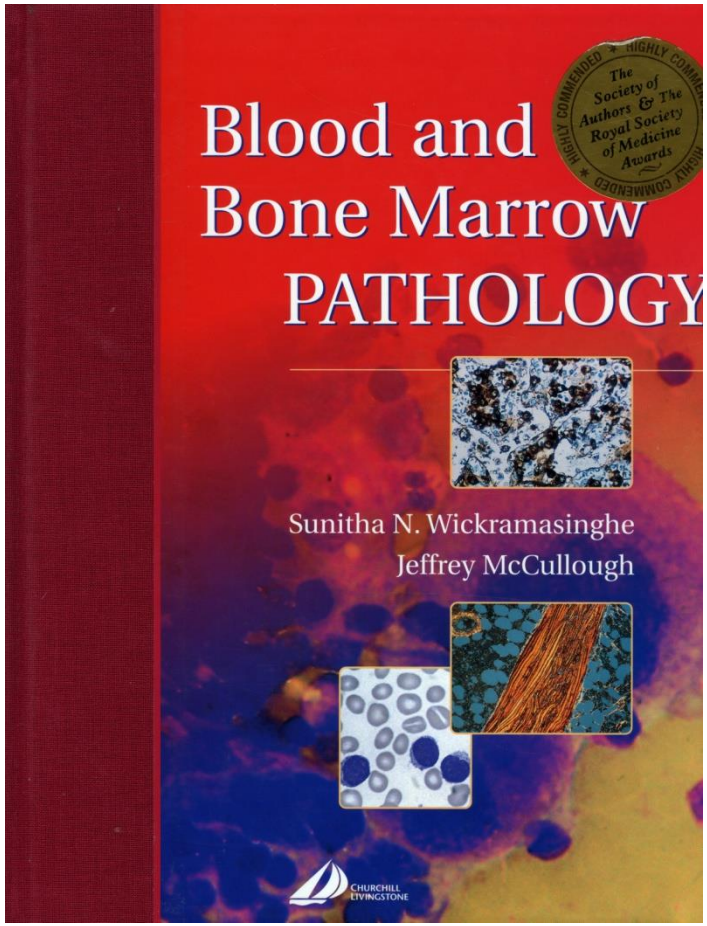

2003

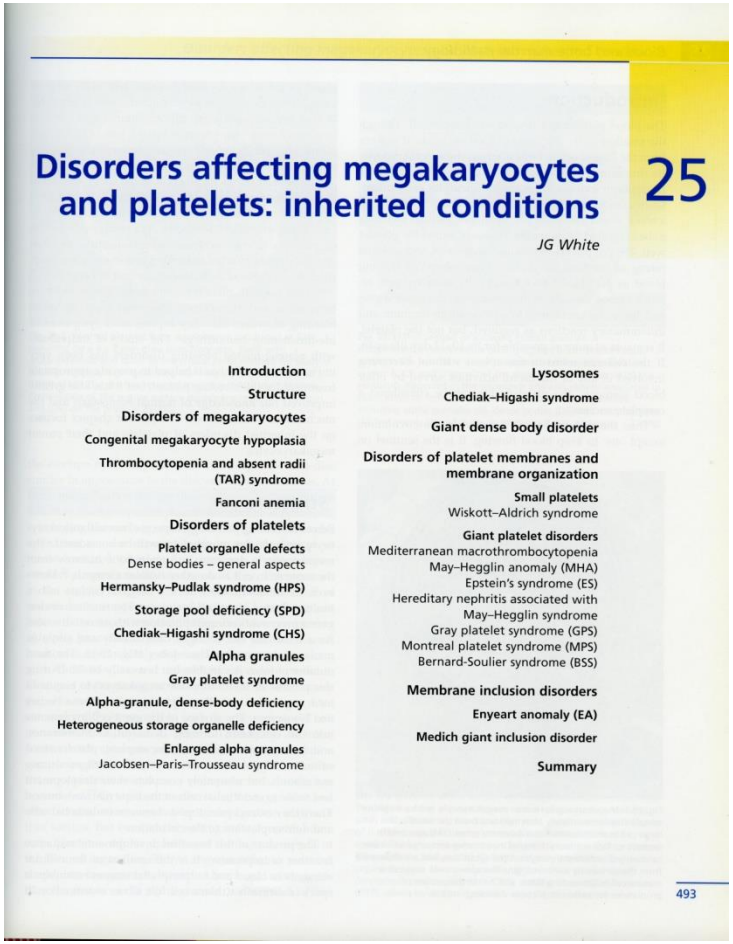

Disorders affecting megakaryocytes and platelets: inherited conditions 25

JG White

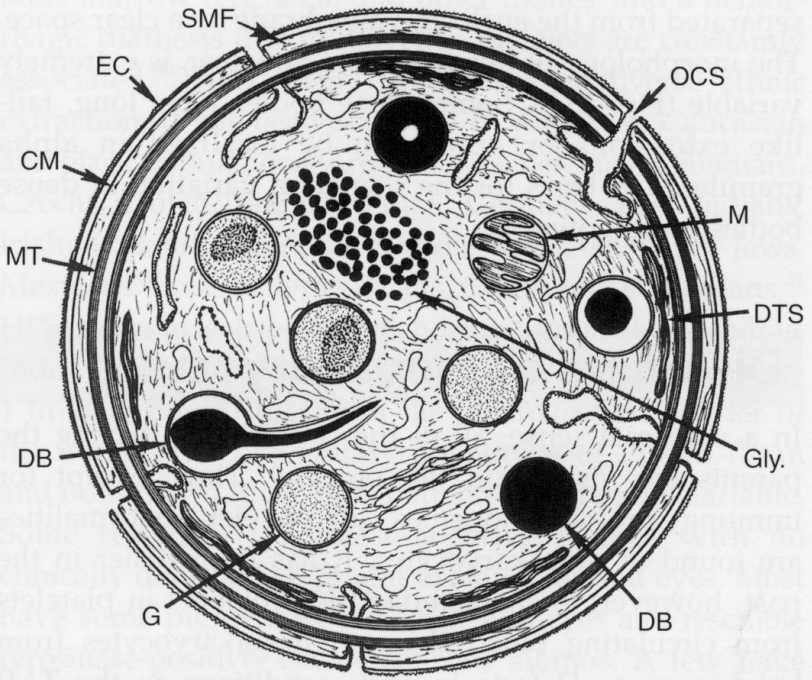

Fig. 25.4 The diagram summarizes ultrastructural features observed in thin sections of discoid platelets cut in the equatorial plane. Components of the peripheral zone include the exterior coat (EC), trilaminar unit membrane (CM) and submembrane area containing specialized filaments (SMF) which form the wall of the platelet and line channels of the surface-connected canalicular system (CS). The matrix of the platelet interior is the sol-gel zone containing actin microfilaments, structural filaments, the circumferential band of microtubules (MT) and glycogen (Gly). Formed elements embedded in the sol-gel zone include mitochondria (M), granules (G) and dense bodies (DB). Collectively, they constitute the organelle zone. The membrane systems include the surface-connected canalicular system (OCS) and the dense tubular system (DTS), which serve as the platelet sarcoplasmic reticulum.

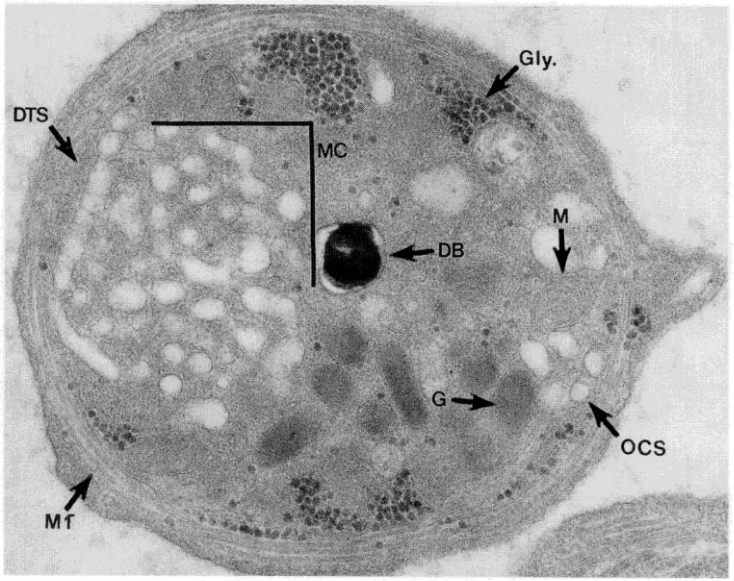

Fig. 25.3 Thin section of a discoid human platelet. A circumferential microtubule (MT) lying just under the cell wall supports the lentiform shape. Elements of the open canalicular system (OCS) and channels of the dense tubular system (DTS) are randomly dispersed in the cytoplasm and also closely associated in some areas to form membrane complexes (MC). Organelles, including alpha granules (G), dense bodies (DB) and mitochondria (M) are evenly spread throughout the cell. Gly, glycogen. × 37 000.

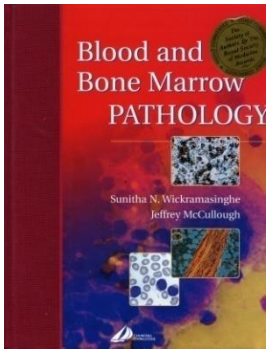

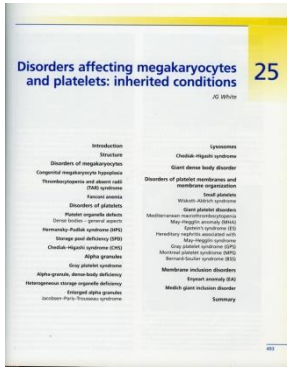

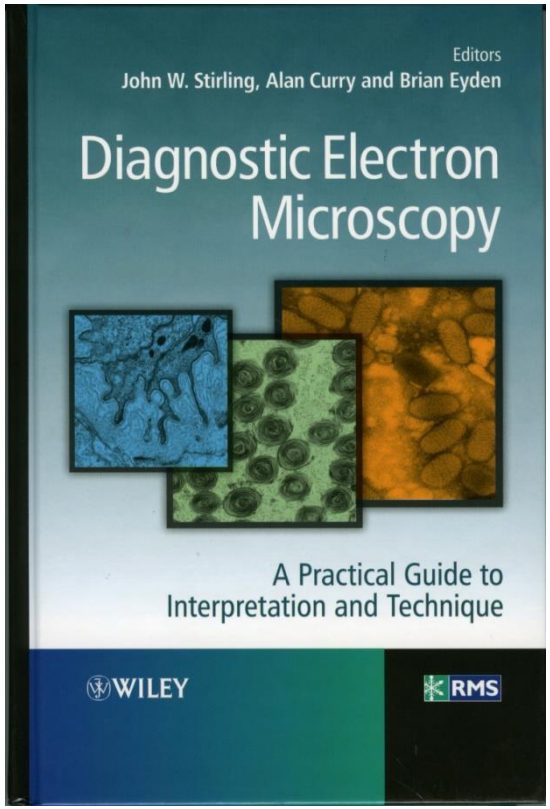

2013

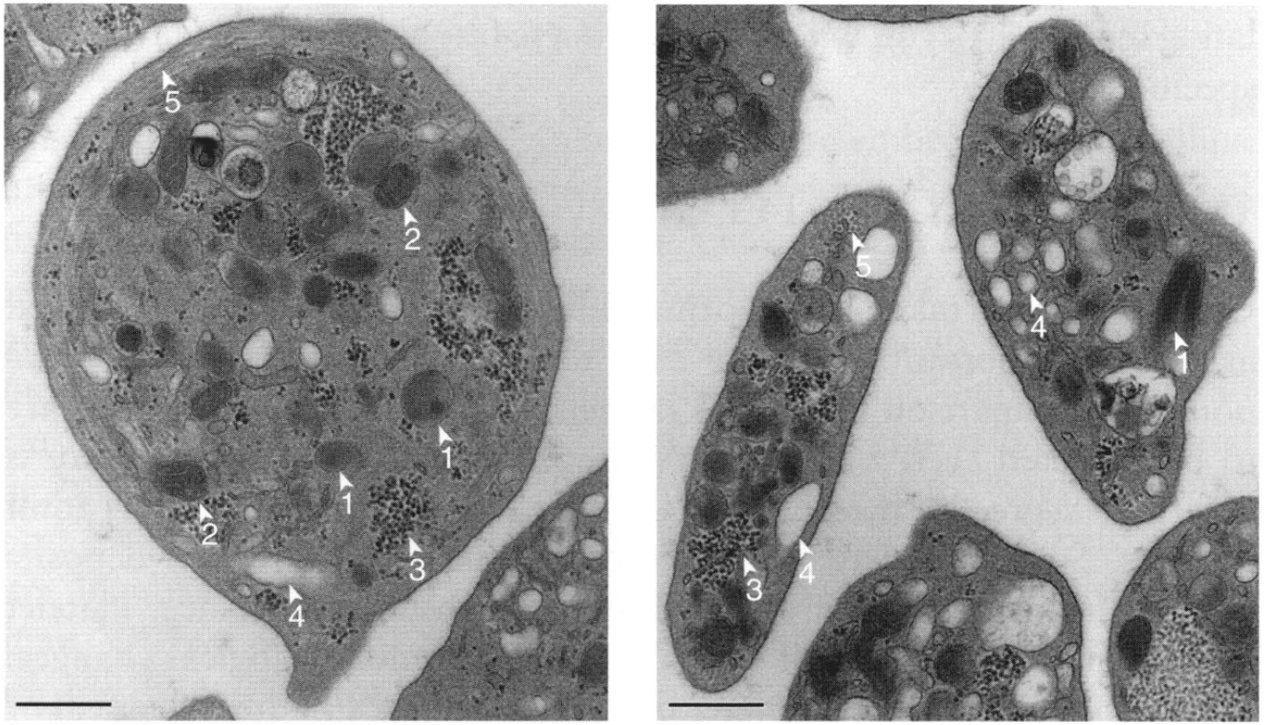

Figure 10.1 Normal platelets. Thin sections are shown for cells cut through the equatorial plane (a) and perpendicular plane (b). Magnification is 30 000×. The black bar represents 500 nm. Platelet structures are indicated by white arrows: (1) α-granules, (2) mitochondria, (3) glycogen stores, (4) open canalicular system and (5) microtubule coil.

Blood. 2010 Aug 19;116(7):1147-56. doi: 10.1182/blood-2010-02-268680. Epub 2010 May 3.

The platelet interior revisited: electron tomography reveals tubular alpha-granule subtypes.

van Nispen tot Pannerden H, de Haas F, Geerts W, Posthuma G, van Dijk S, Heijnen HF.

Source
Cell Microscopy Center and Department of Cell Biology, University Medical Center Utrecht, Utrecht, The Netherlands.

Abstract
We have used (cryo) electron tomography to provide a 3-dimensional (3D) map of the intracellular membrane organization of human platelets at high spatial resolution. Our study shows that the open canalicular system and dense tubular system are highly intertwined and form close associations in specialized membrane regions. 3D reconstructions of individual alpha-granules revealed large heterogeneity in their membrane organization. On the basis of their divergent morphology, we categorized alpha-granules into the following subtypes: spherical granules with electron-dense and electron-lucent zone containing 12-nm von Willebrand factor tubules, subtypes containing a multitude of luminal vesicles, 50-nm-wide tubular organelles, and a population with 18.4-nm crystalline cross-striations. Low-dose (cryo) electron tomography and 3D reconstruction of whole vitrified platelets confirmed the existence of long tubular granules with a remarkably curved architecture. Immunoelectron microscopy confirmed that these extended structures represent alpha-granule subtypes. Tubular alpha-granules represent approximately 16% of the total alpha-granule population and are detected in approximately half of the platelet population. They express membrane-bound proteins GLUT3 and alphaIIb-beta3 integrin and contain abundant fibrinogen and albumin but low levels of beta-thromboglobulin and no von Willebrand factor. Our 3D study demonstrates that, besides the existence of morphologically different alpha-granule subtypes, high spatial segregation of cargo exists within individual alpha-granules.

Figure 1. EM tomography of the intracellular membrane organization in nonstimulated platelet. (A-C) Tomographic slices of directly fixed platelet. Dual axis tilt series were generated from chemically fixed platelets as described in "Tomography and data analysis." The membranes and other structures of interest were manually traced to generate a 3D representation of the structure. Dark blue represents OCS; light blue, platelet secretory-granule; and red, dense granule. (D) Microtubules are located at the platelet periphery. The OCS membranes are continuous with the cell surface at multiple sites (panel E and arrowheads in panel I), and span the platelet cell surface from one side to the other, revealing numerous branching areas. (An animated model of the OCS is included as supplemental Video 1.) (F-H) Manual tracking of the peripheral microtubular coil (yellow dots at the cell periphery) reveal a microtubule ending at an OCS invagination (supplemental Video 2). indicates -granule; , dense granule; mt, microtubules; and dts, dense tubular system. (A) Bars represent 200 nm.
(B-G) Bars represent 100nm.

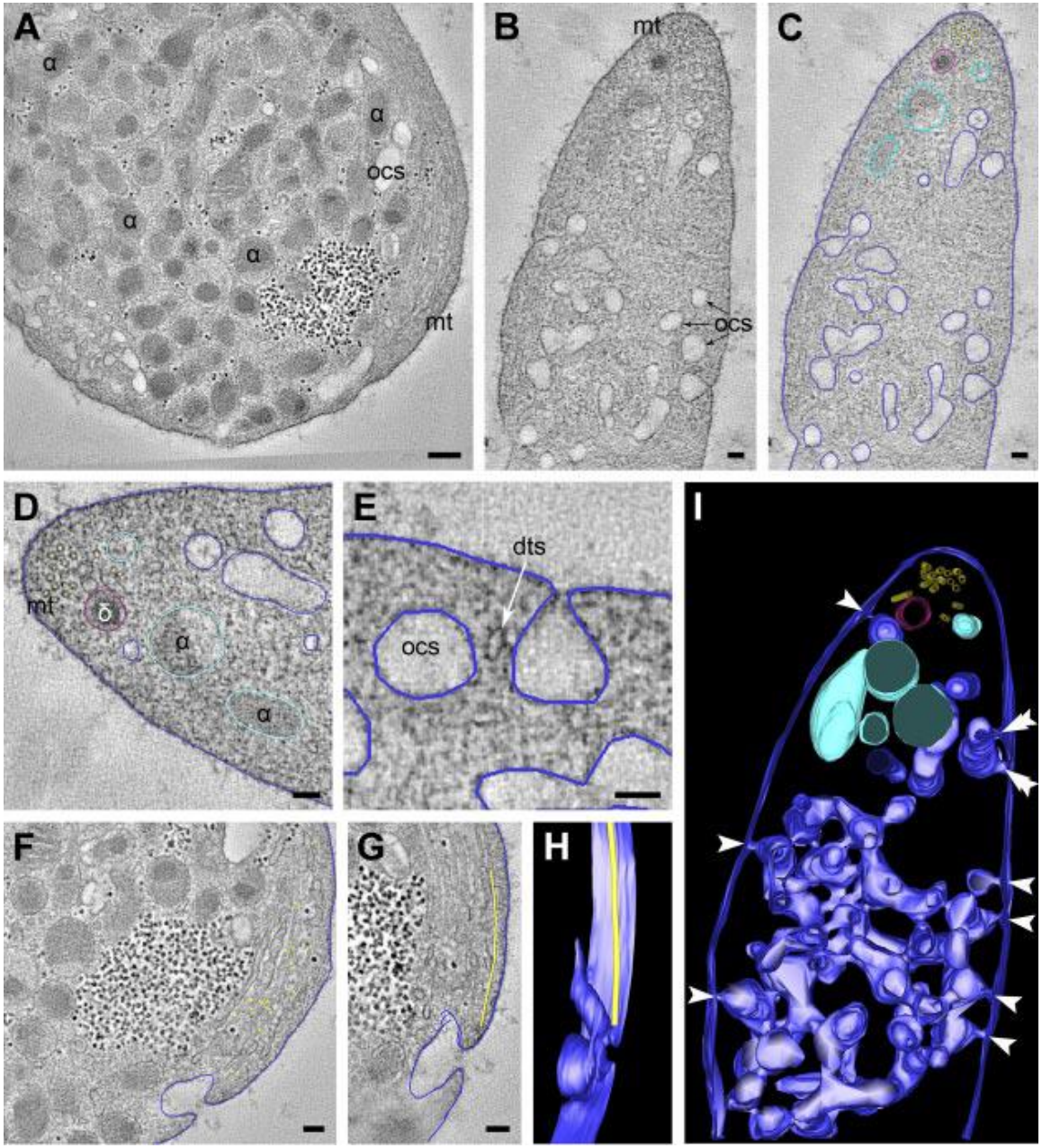

For on-line videos follow

http://bloodjournal.hematologylibrary.org/content/116/7/1147/suppl/DC1

Renal biopsy

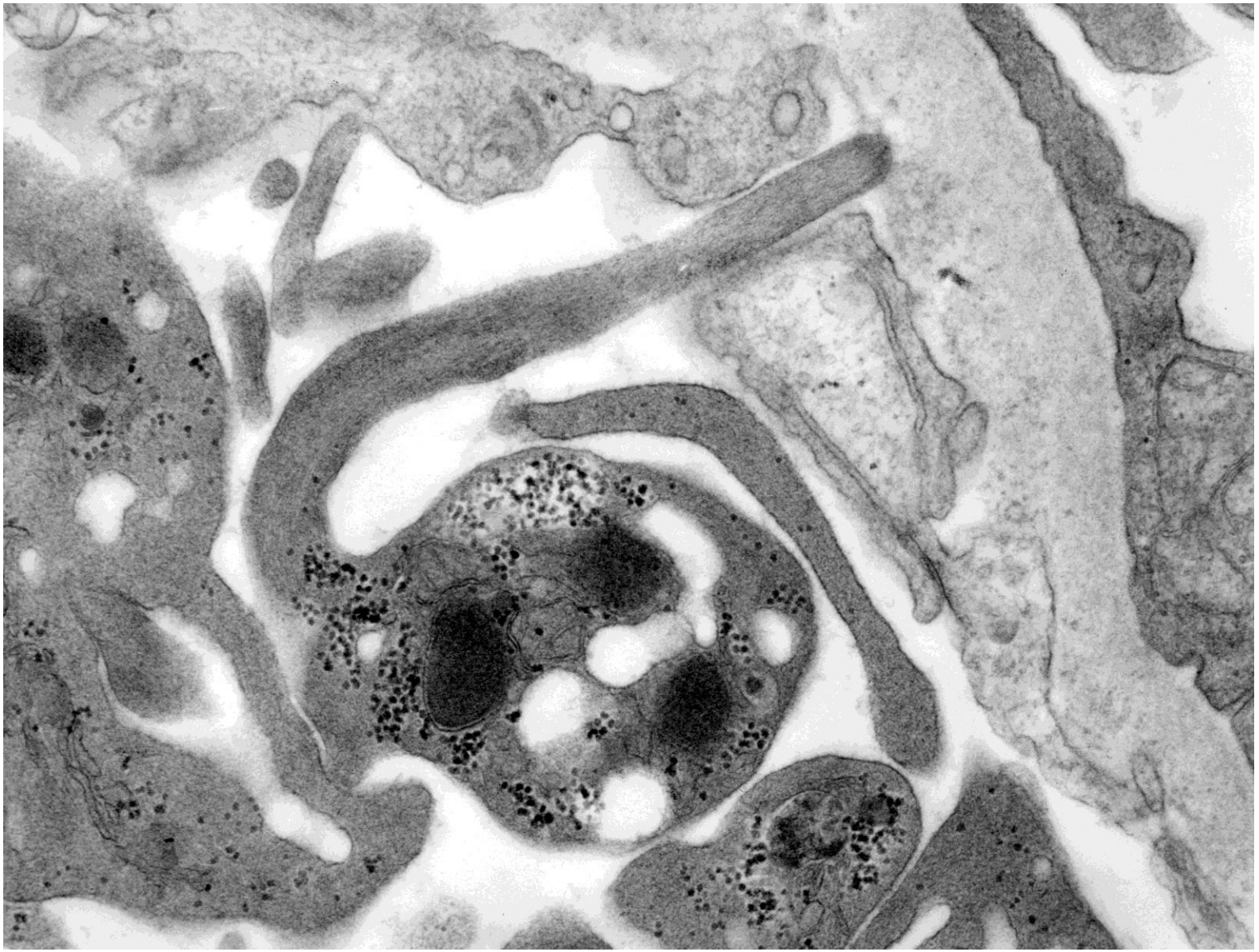

Normal activated platelet with long pseudopdia adherent to GBM at point of gap in endothelium

Renal biopsy

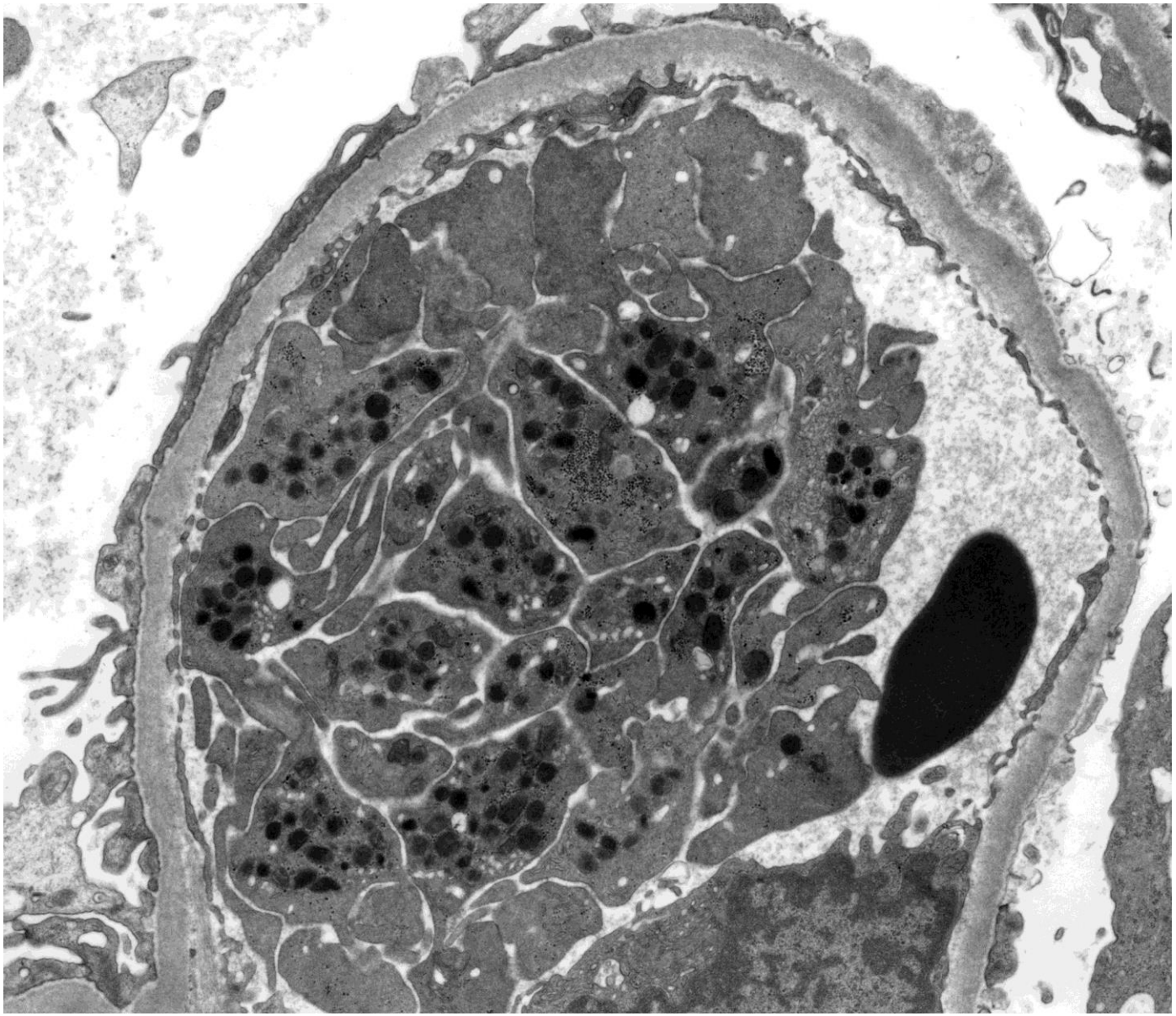

Platelet thrombus with pseudopodial activation and degranulation

Pediatr Blood Cancer. 2011 Jun;56(6):975-83. doi: 10.1002/pbc.22988. Epub 2011 Feb 3.

Platelet disorders in children: A diagnostic approach.

Israels SJ, Kahr WH, Blanchette VS, Luban NL, Rivard GE, Rand ML.

Source

Department of Pediatrics and Child Health, University of Manitoba, Winnipeg, Manitoba, Canada. israels@cc.umanitoba.ca

Abstract

The investigation of children with suspected inherited platelet disorders is challenging. The causes of mucocutaneous bleeding are many, and specialized testing for platelet disorders can be difficult to access or interpret. An algorithm developed for the investigation of suspected platelet disorders provides a sequential approach to evaluating both platelet function abnormalities and thrombocytopenia. Investigation begins with a clinical evaluation and laboratory testing that is generally available, including platelet counting, peripheral blood cell morphology, and aggregometry. Based on results of initial investigations, the algorithm recommends specialized testing for specific diagnoses, including flow cytometry, immunofluorescence microscopy, **electron microscopy**, and mutational analysis.

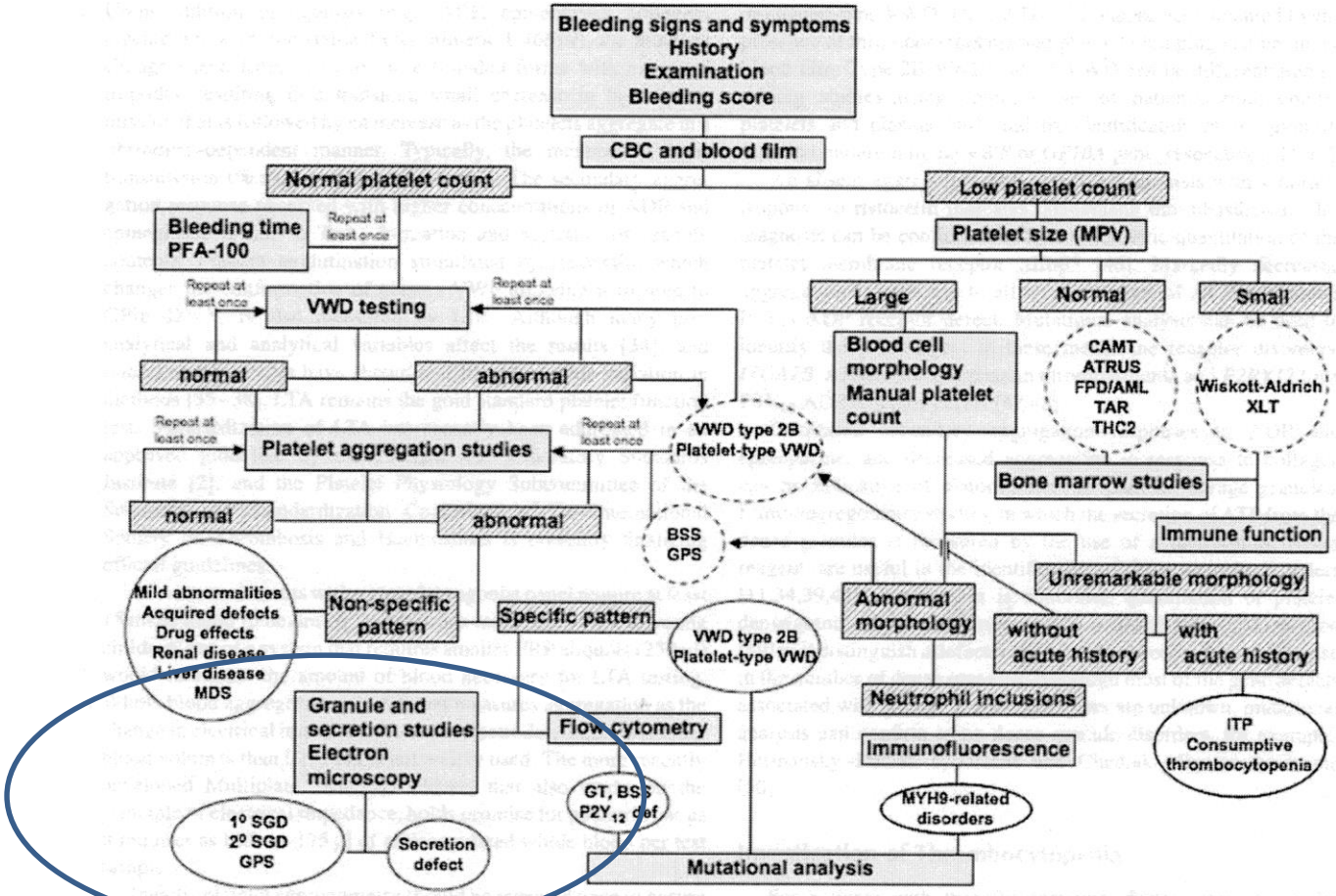

Fig. 2. Algorithm for evaluation of children with suspected platelet disorders. Suggested investigations are in gray boxes and potential results in hatched boxes. The circles and dotted circles contain diagnoses and suspected diagnoses, respectively. BSS, Bernard–Soulier syndrome; CAMT, congenital amegakaryocytic thrombocytopenia; ATRUS, amegakaryocytic thrombocytopenia with radio-ulnar synostosis; FPD/AML, familial platelet disorder and predisposition to acute myelogenous leukemia; GT, Glanzmann thrombasthenia; GPS, gray platelet syndrome; SGD, storage granule disorder; TAR, thrombocytopenia with absent radii; THC2, autosomal dominant thrombocytopenia; XLT, X-linked thrombocytopenia. Rare disorders not included in the algorithm: (i) Quebec platelet disorder—delayed-onset bleeding symptoms, absent aggregation with epinephrine, diagnosis by presence of platelet urokinase by immunoblotting or ELISA; (ii) Scott syndrome—mucocutaneous bleeding, normal aggregation with all agonists, diagnosis by absence of annexin A5 binding to activated platelets by flow cytometry; (iii) thromboxane A_2 receptor defect—mucocutaneous bleeding, decreased/absent aggregation with arachidonic acid and U46619, diagnosis by mutational analysis of *TBXA2R* gene.

Platelet disorders in which EM used as part of investigation

- **Dense core granule disorders**
- Hermansky-Pudlak Syndrome (reduced dense core granules with oculocutaneous albinism)
- Storage pool deficiency (reduced dense core granules without albinism)
- Chediak-Higashi syndrome (reduced dense core granules, pseudoalbinism and susceptibility to infection)

Platelet disorders in which EM used as part of investigation

- **Alpha granule abnormality**
- Gray platelet syndrome
- Arthrogryposis Renal dysfunction Cholestasis (ARC) syndrome
- Quebec platelet disorder
- Jacobsen Paris Trousseau syndrome

Dense core granule quantitation Method:

- Citrate anticoagulated venous blood
- Platelet rich plasma (PRP)
- Drop of PRP on one side of Formvar coated grid for 15 secs
- Wash off with 3 drops of distilled water
- Blot edges of grid
- View directly in TEM

- If too many platelets, repeat and reduce time. (and visa versa)
- If too much plasma, repeat and increase number of drops of water.

Formvar coated grid with platelet rich plasma

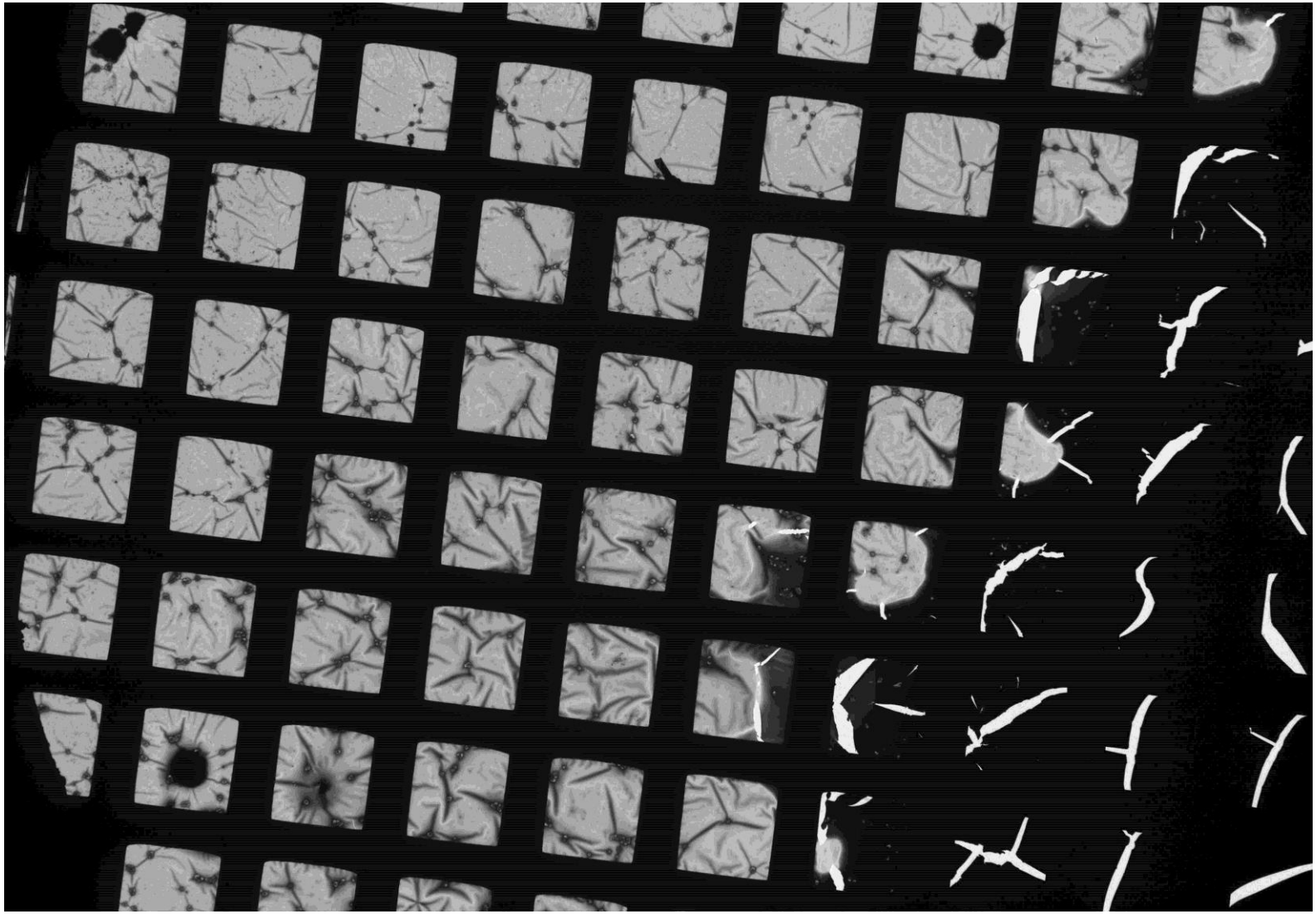

Too much plasma left
at this end of the grid

Formvar coated grid with whole unfixed, unstained platelets

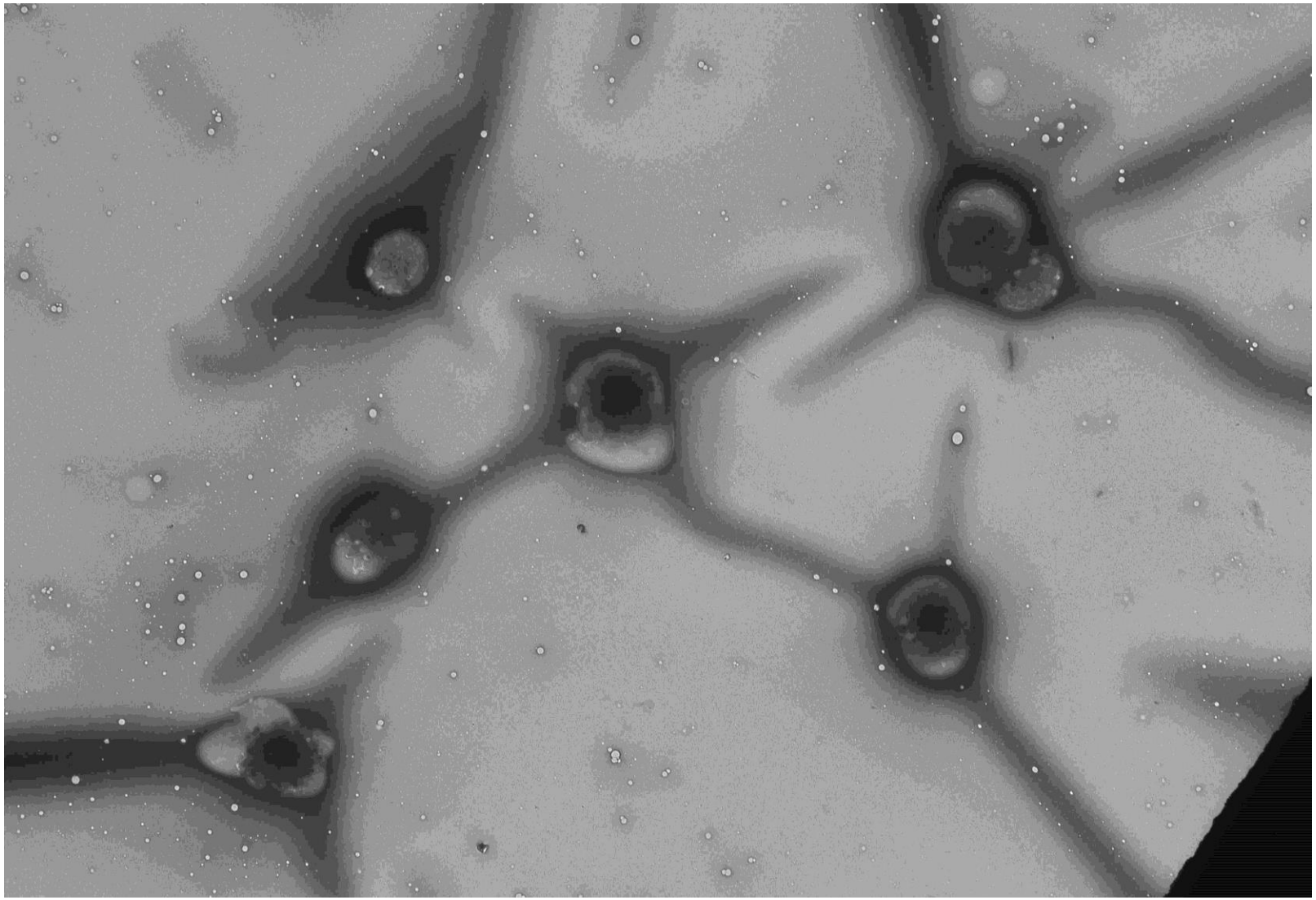

Best if platelets are separate;

achieved by keeping settling and sticking time to a minimum

Two whole platelets

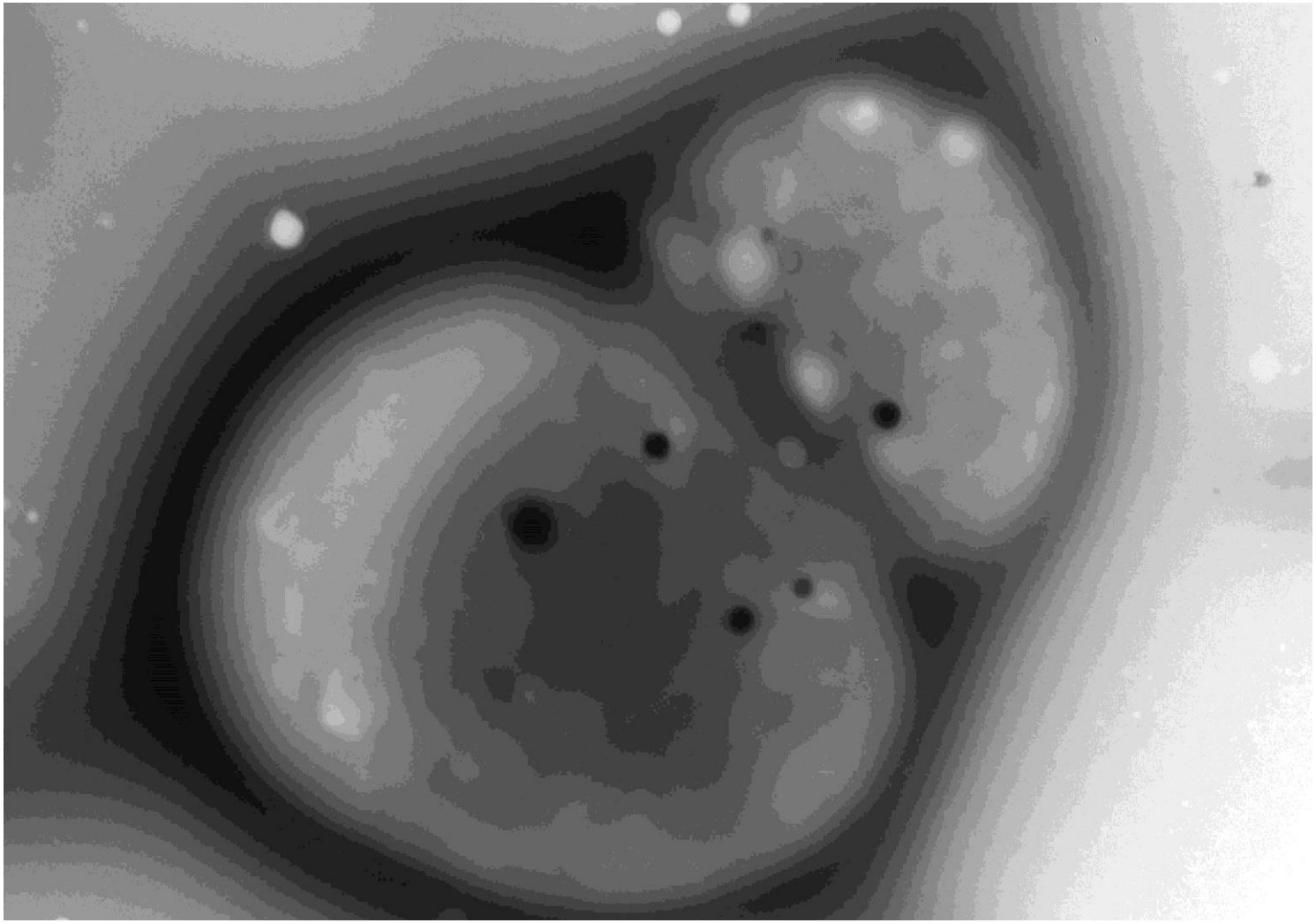

4 and 3 dense core granules

Normal mean dense core granule count is 5.3/whole platelet

Hematology
1997, Vol 2
pp161-167

Normal platelet – one of mine

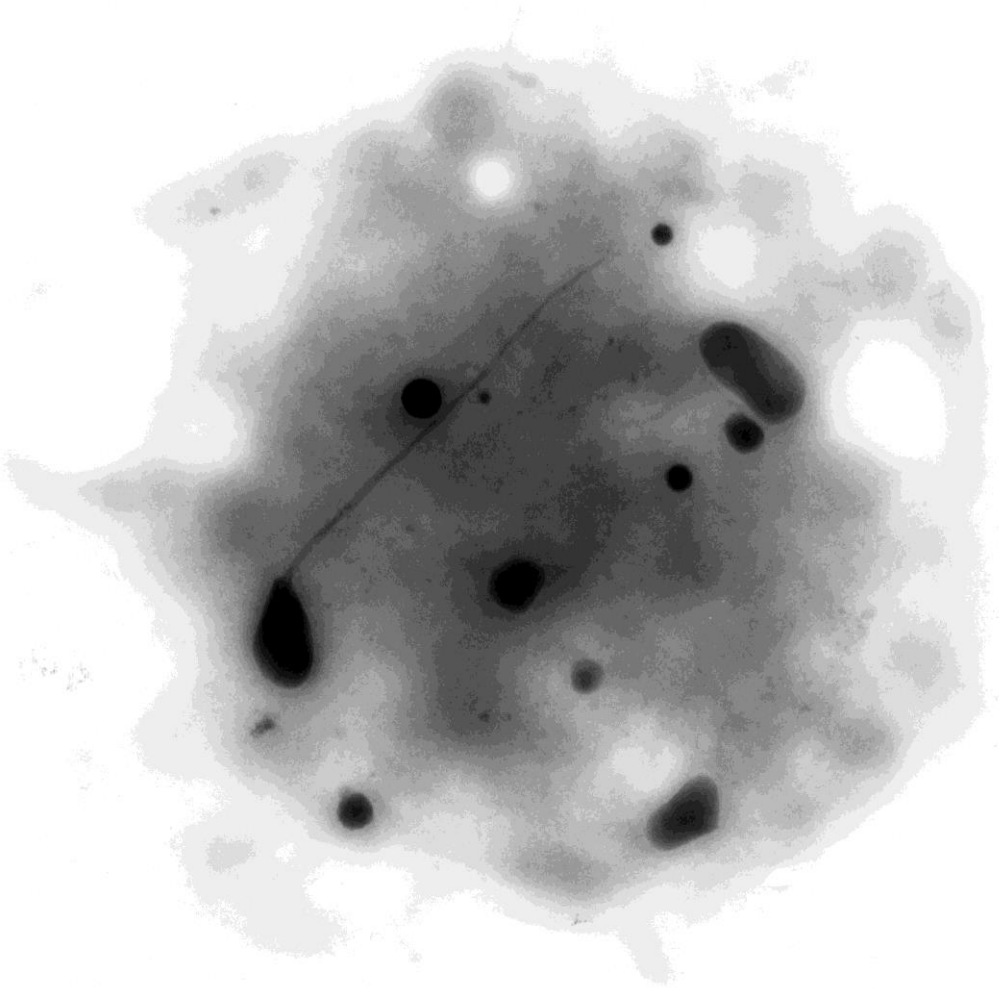

Dense core granules – 11 of them

Normal mean dense core granule count is 5.3 + - 2SD/whole platelet

Hematology 1997, Vol 2 pp161-167

Platelets from patient with Hermansky-Pudlak Syndrome

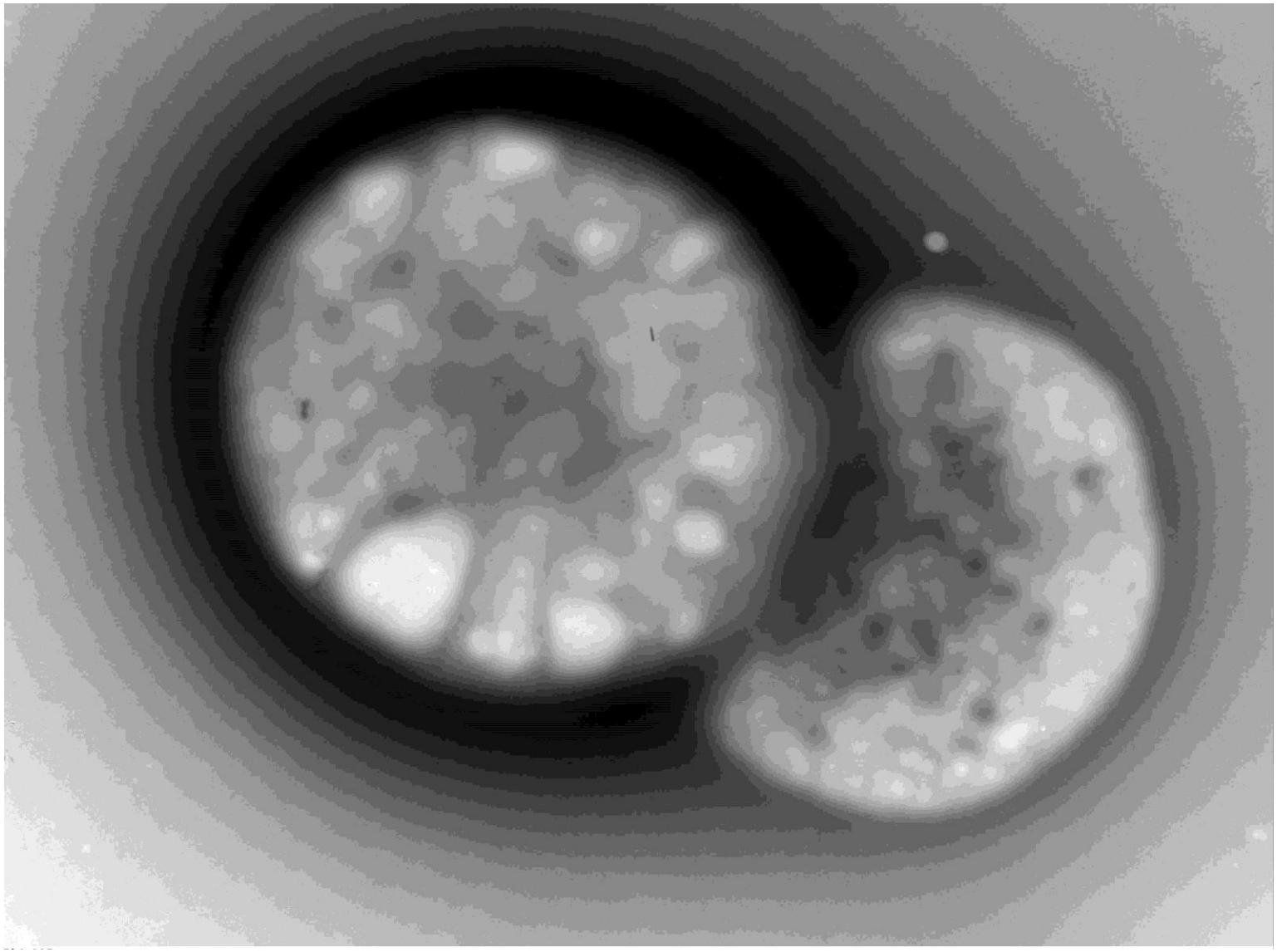

No dense core granules

Hermansky-Pudlak syndrome

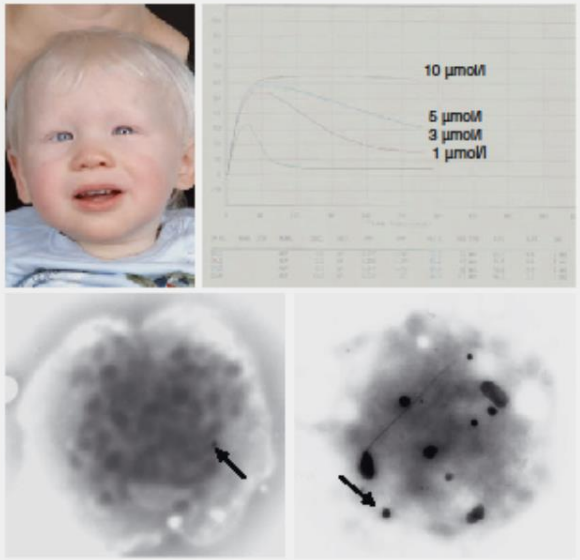

An 8-month-old boy with ocular cutaneous albinism (top left), the only child of Caucasian parents, underwent investigations for easy bruising and epistaxis. Platelet aggregometry demonstrated reduced aggregation with collagen, ristocetin and arachidonic acid, and disaggregation after primary aggregation on exposure to adenosine diphosphate (ADP; top right). The latter was shown to be due to reduced ADP stores in the nucleotide release assay. Transmission electron microscopy of whole unfixed platelets confirmed that the patient's storage pool deficiency was due to dense body deficiency (arrows, bottom left – patient, bottom right – control). The clinical and laboratory features were consistent with Hermansky-Pudlak syndrome (HPS) which is a rare autosomal recessive disorder of proteins involved in vesicle formation and trafficking whose manifestations include oculo-cutaneous albinism, delta platelet storage pool deficiency and ceroid deposition in bone marrow, intestinal macrophages and lung, the latter leading to pulmonary fibrosis. Certain mutations are also associated with inflammatory bowel disease in adult life. To date, mutations have been described in eight human genes *HPS1*, *AP3B1* (also known as *HPS2*), *HPS3*, *HPS4*, *HPS5*, *HPS6*, *DTNBP1* (also known as *HPS7* or *DYSBINDIN*) and *BLOC1S3* (also known as *HPS8*). Most patients with HPS have mutations in *HPS1* or *HPS4*; the former predominates in Puerto Rico, where HPS is the most common genetic disorder with a prevalence of 1:800.

Mark Walker[1]
Jeanette Payne[1]
Bart Wagner[2]
Ajay Vora[1]
[1]*Department of Paediatric Haematology, Sheffield Children's Hospital, Sheffield, and* [2]*Department of Histopathology, Northern General Hospital, Sheffield, UK.*
E-mail: ajay.vora@sch.nhs.uk

First published online 17 July 2007
doi:10.1111/j.1365-2141.2007.06713.x

Comparison of platelets with and without dense core granules

Storage pool disorder

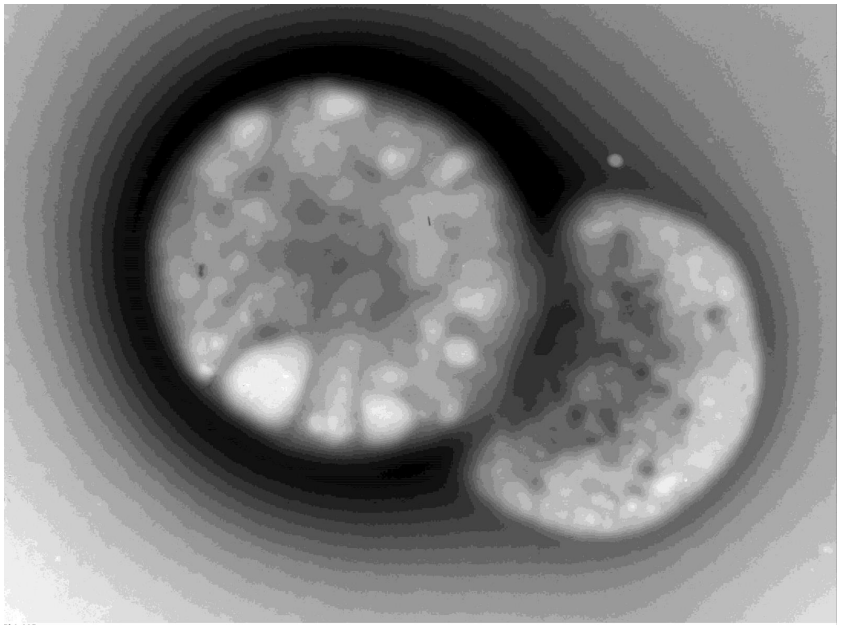

Platelets from patients with Hermansky – Pudlak syndrome tend to have no dense core granules, whilst storage pool disorder have a mean dense core granule count below 3.5

20 – 40 platelets assessed

Normal

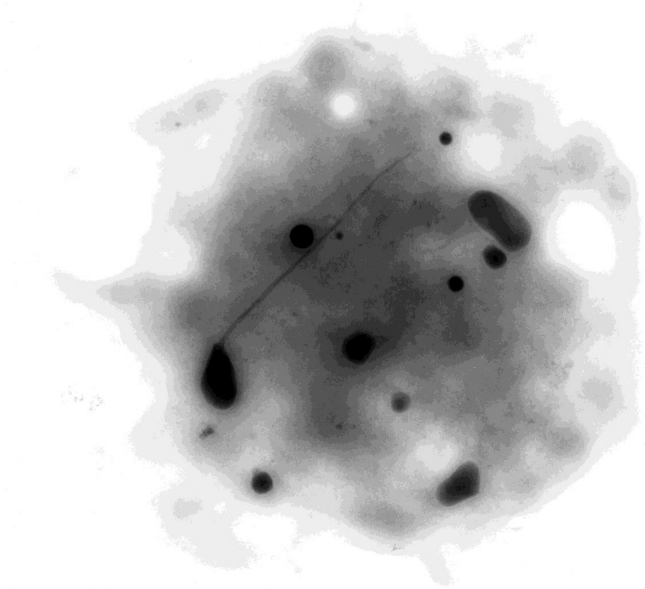

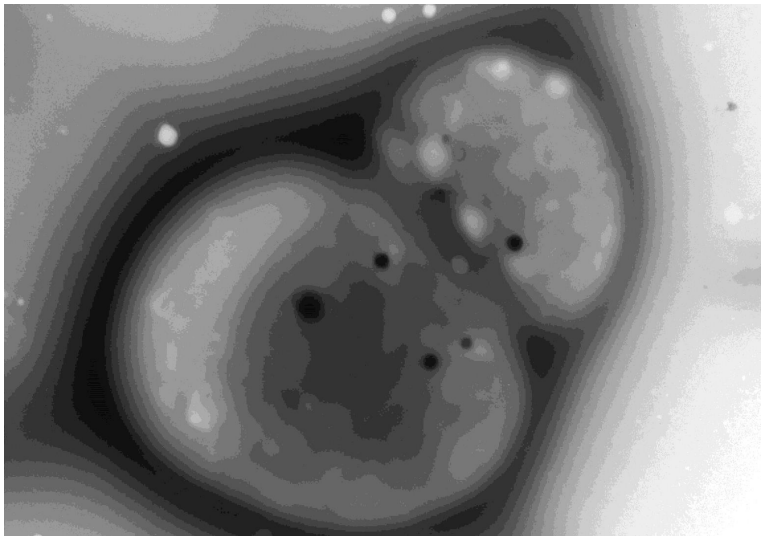

Normal is 5.3 + - 2 SD

Thin section (normal) platelet EM.

Calcium added to fixative. Unstained section

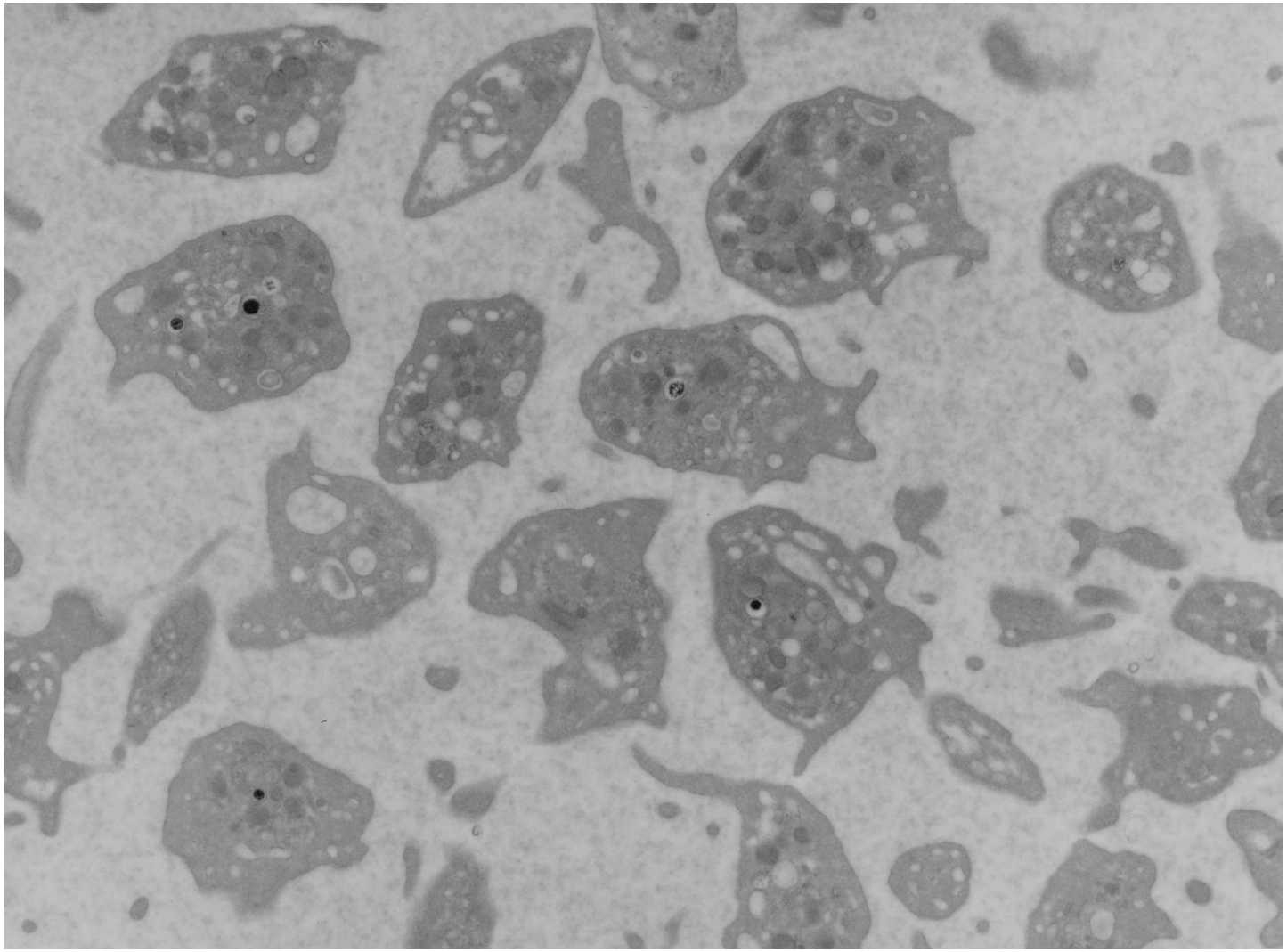

Not suitable for dense core granule quantitation

Alpha granule disorders

- Thin section TEM essential

Alpha granule disorders

- Thin section TEM essential
- Jacobsen Paris Trousseau syndrome

Jacobsen Paris Trousseau syndrome

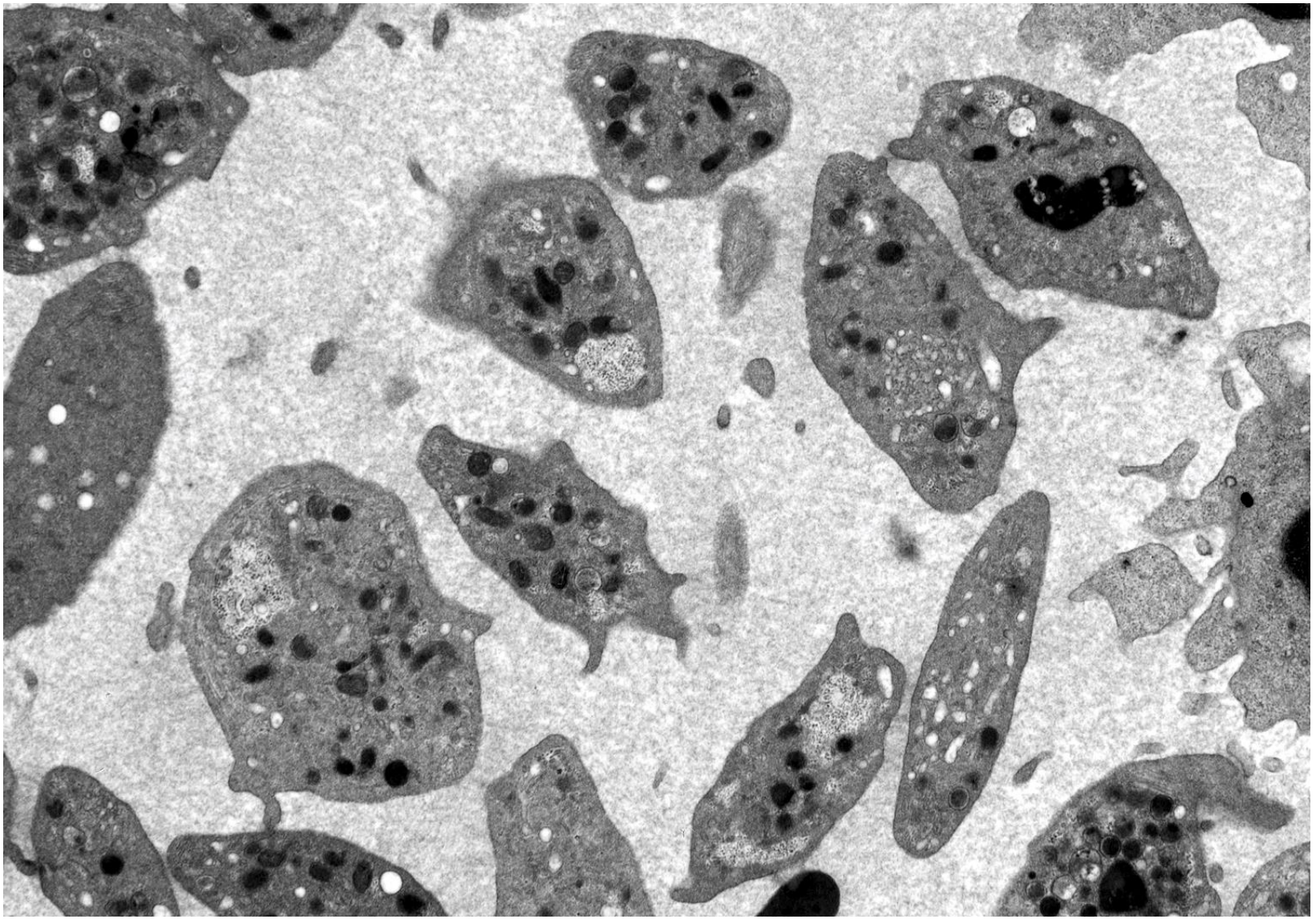

Giant, as well as normal, alpha granules

Low dense core granule counts

Jacobsen Paris Trousseau syndrome

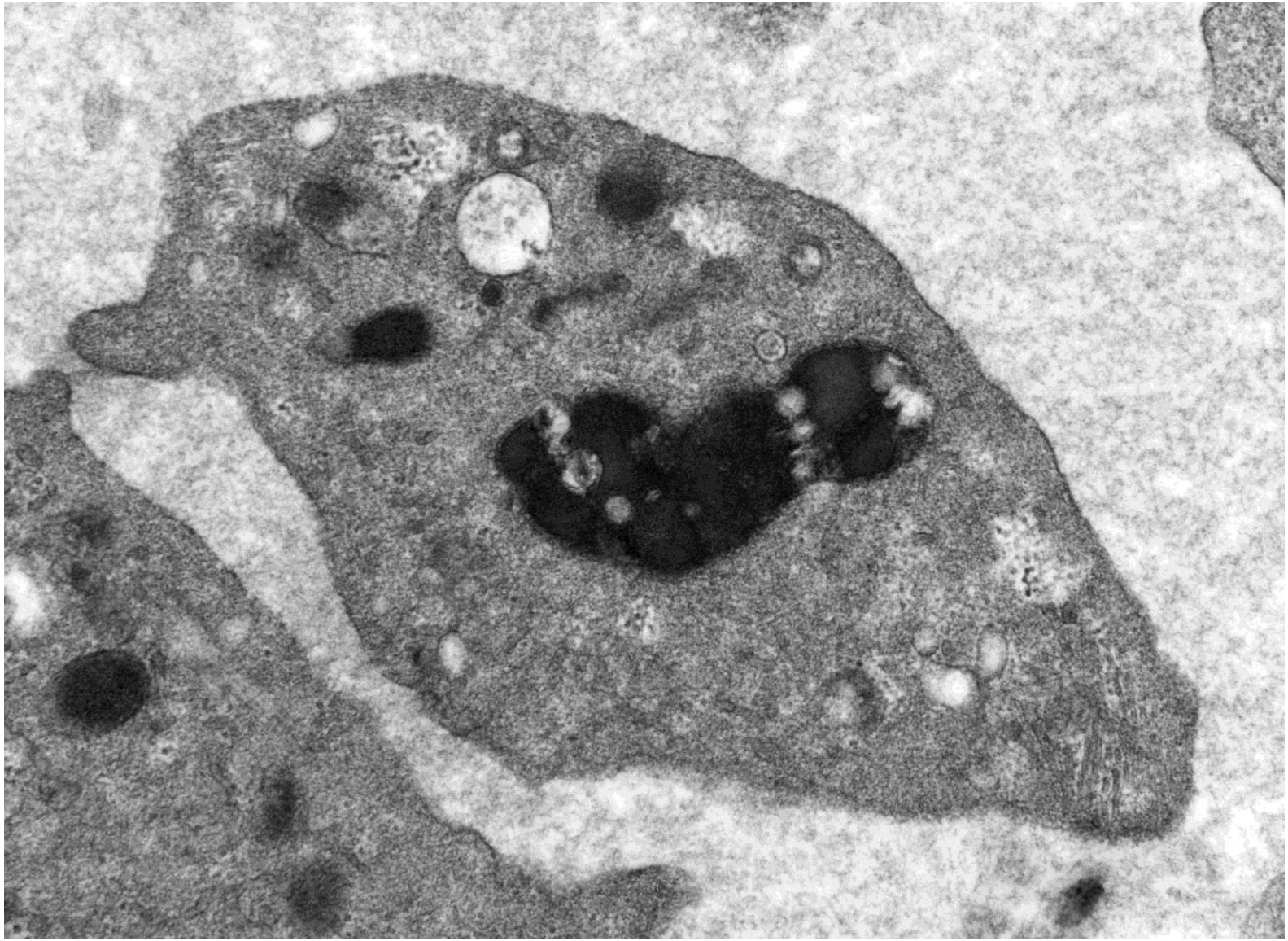

Giant alpha granules

Alpha granule disorders

- Thin section TEM essential
- Gray platelet syndrome

Gray platelet syndrome

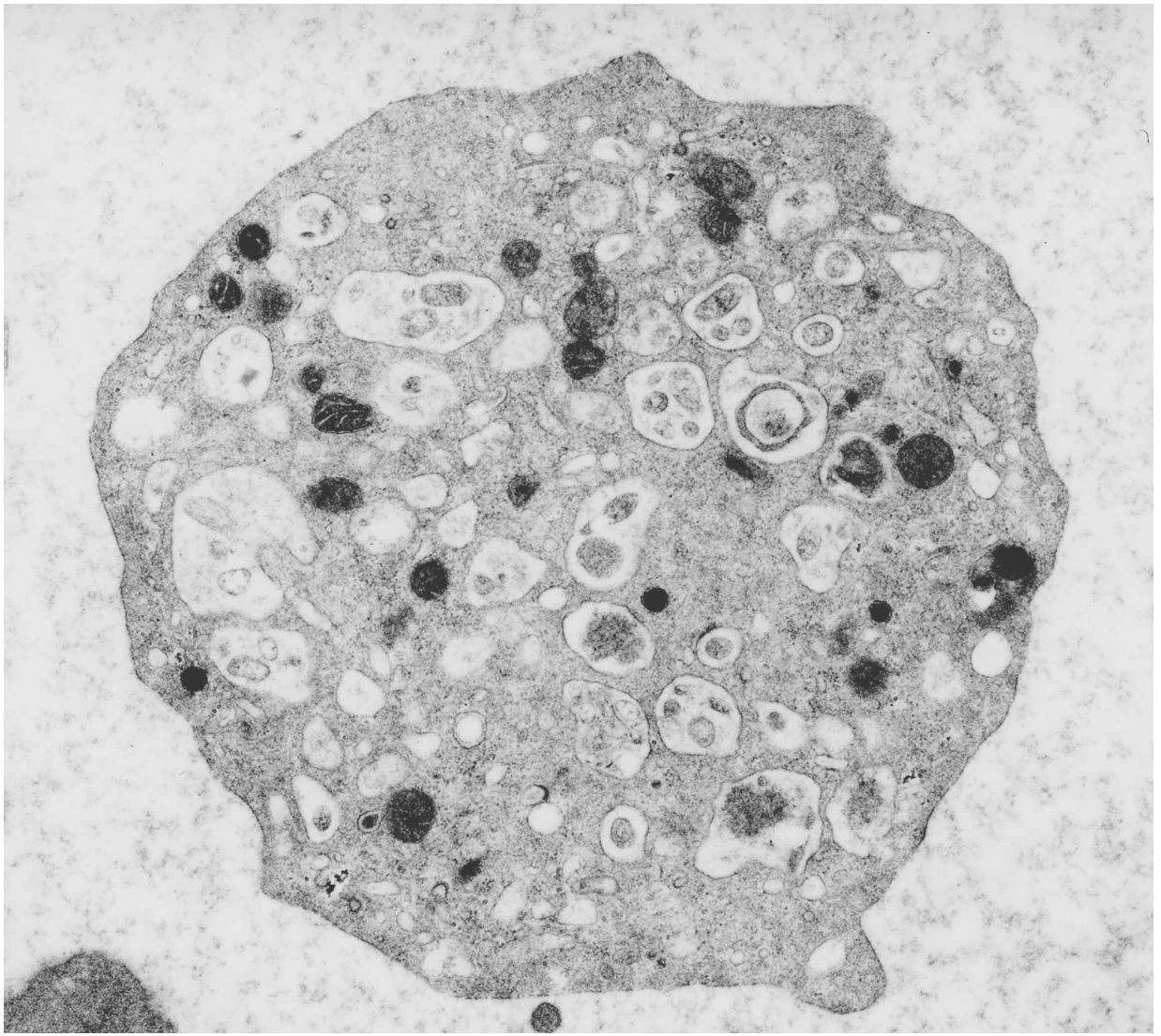

Alpha granules are swollen and contents loose

Platelets are enlarged

Gray platelet syndrome

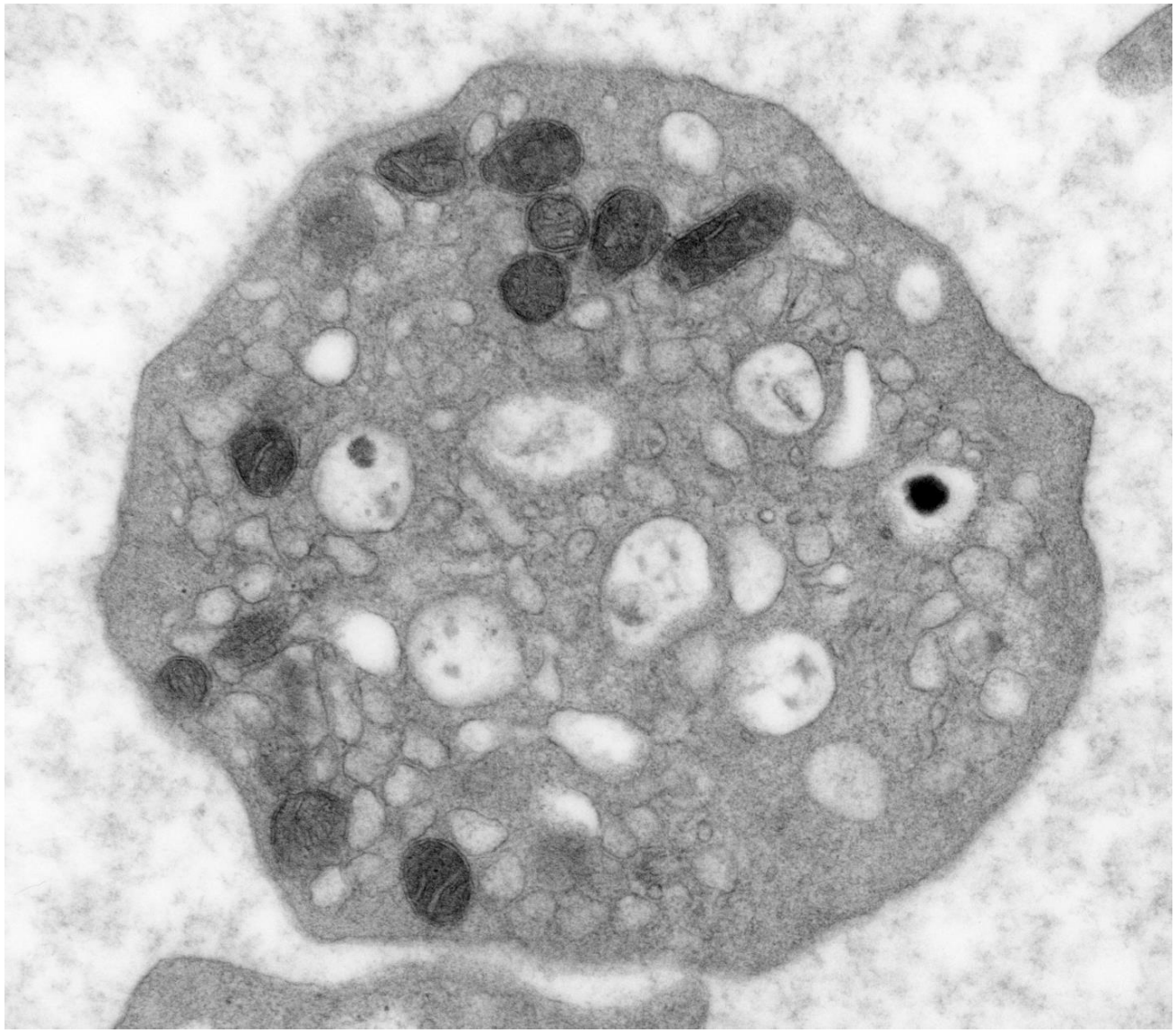

Alpha granules swollen and contents loose

Dense core granule count normal

Alpha granule disorders

- Thin section TEM essential
- Arthrogryposis–renal dysfunction–cholestasis (ARC) syndrome

Arthrogryposis–renal dysfunction–cholestasis (ARC) syndrome

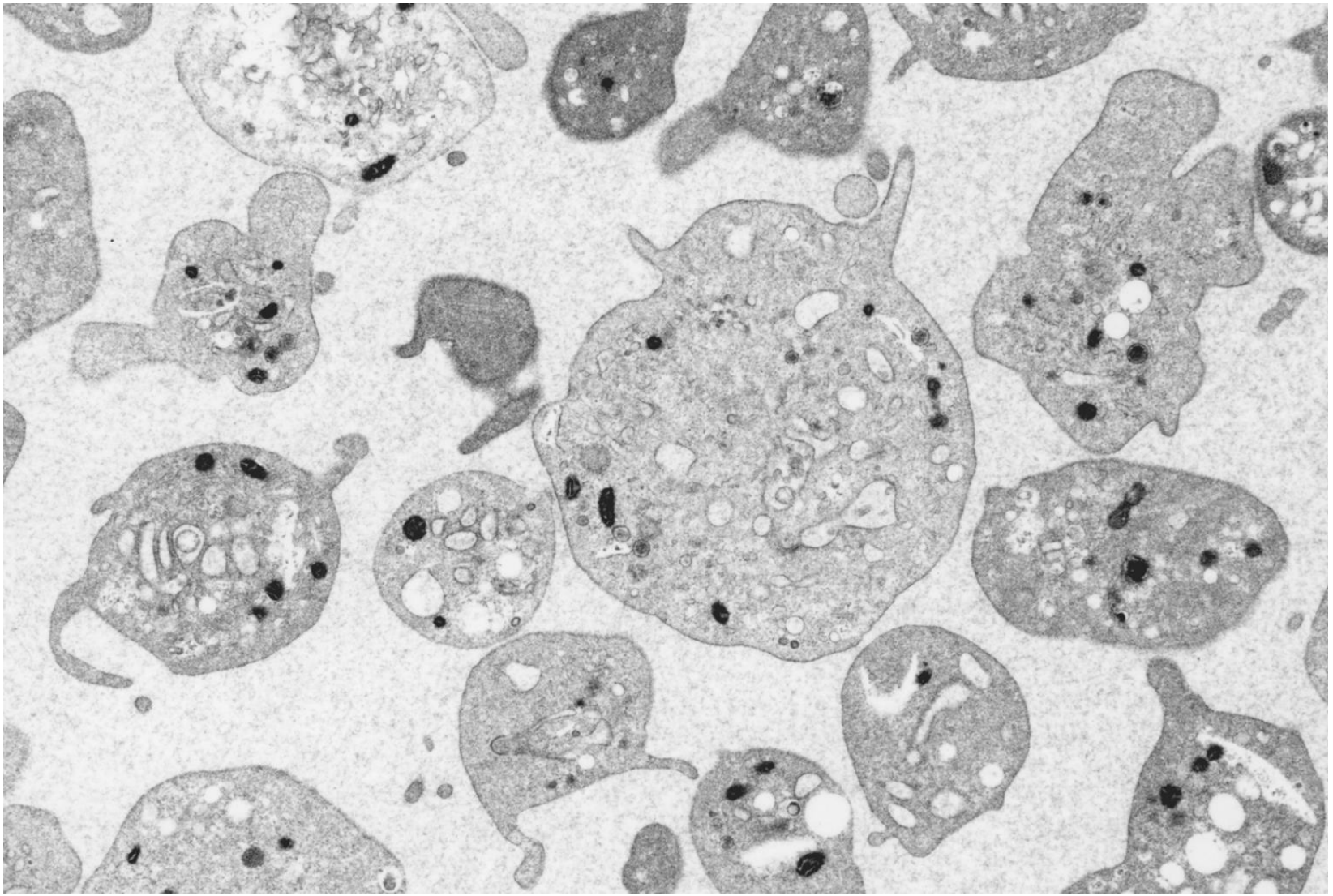

Alpha granules absent

Arthrogryposis–renal dysfunction–cholestasis (ARC) syndrome

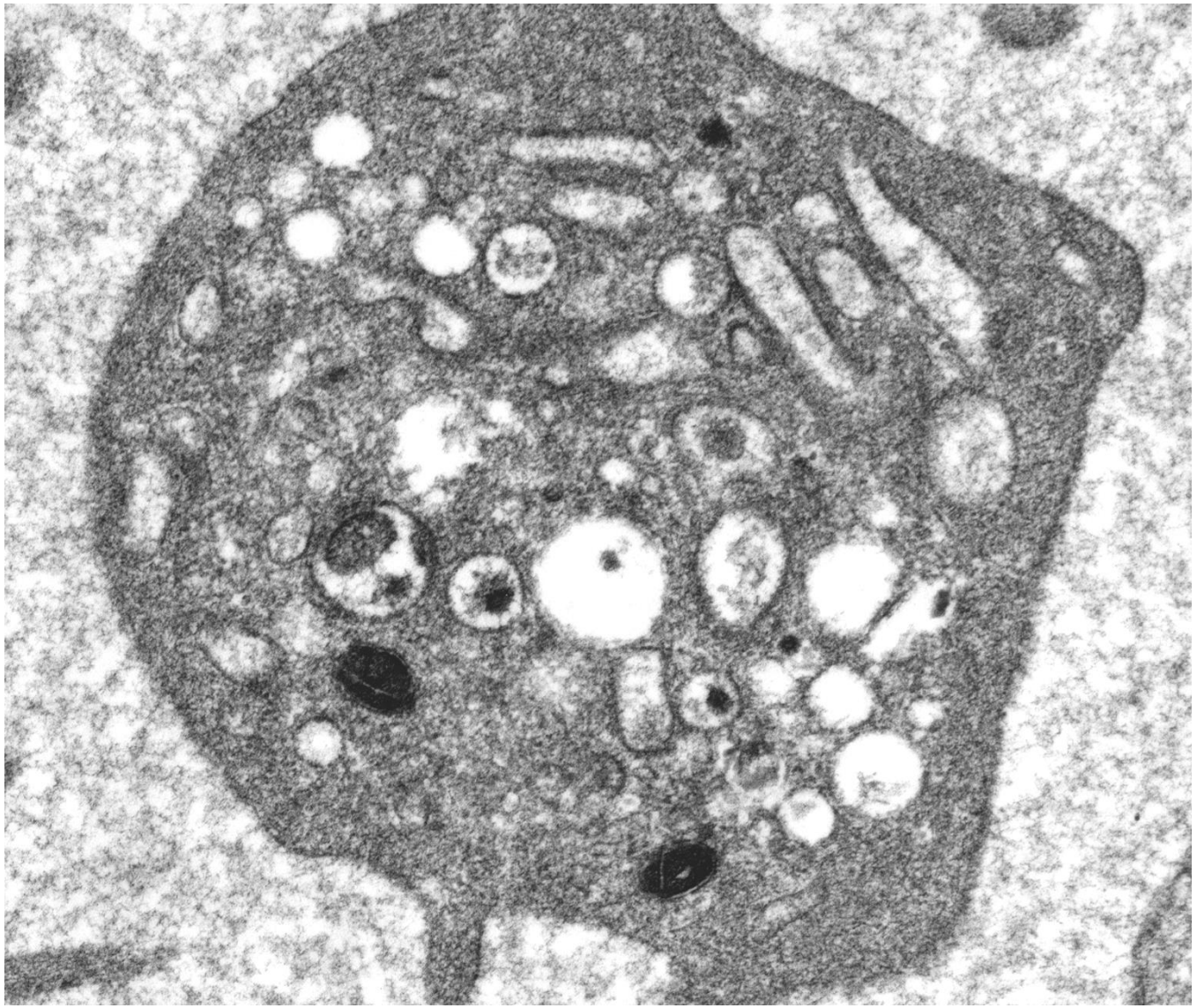

Poorly formed alpha granules,

Numerous dense core granules

Alpha granule disorders

- Thin section TEM essential
- Chediak-Higashi syndrome

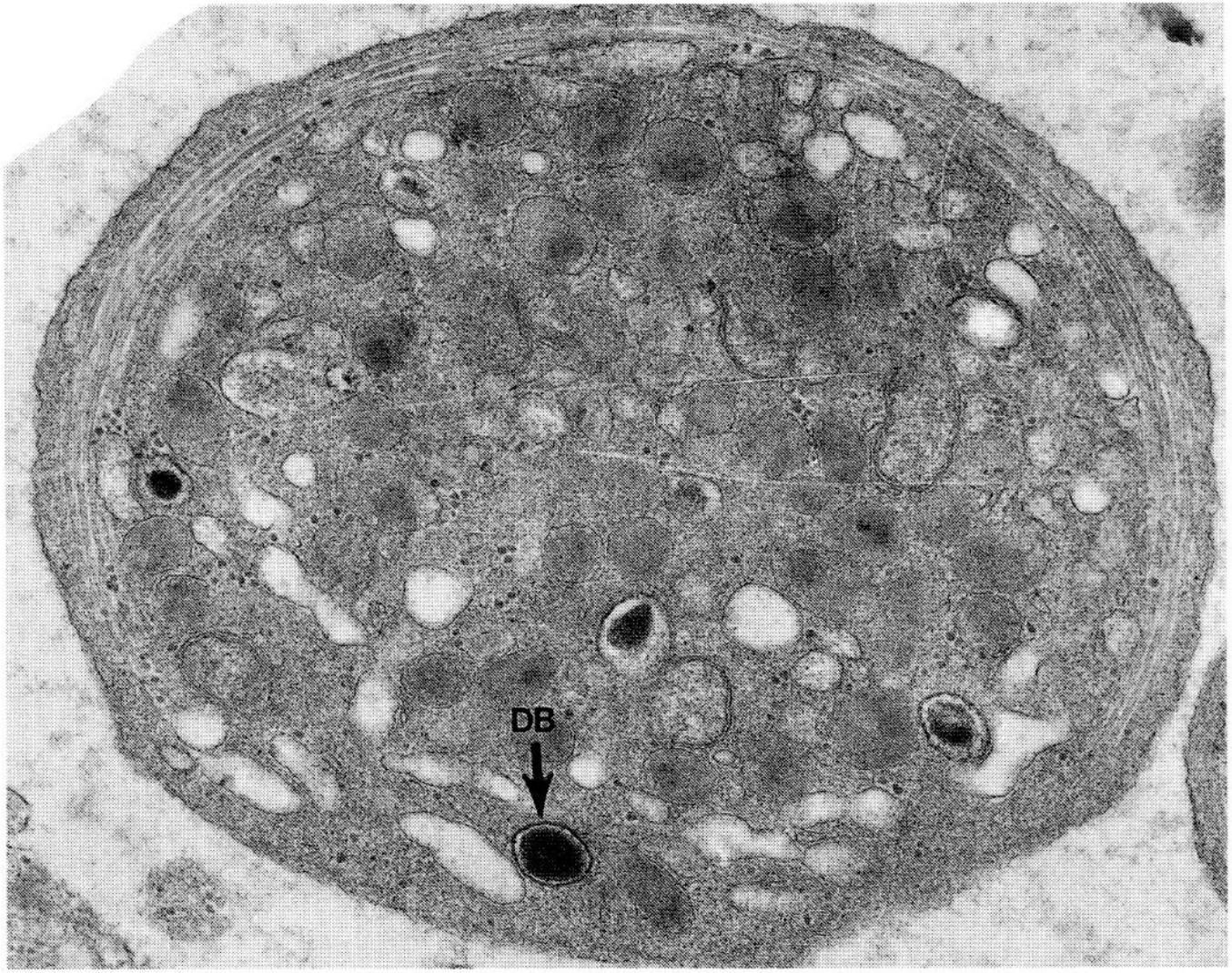

Fig. 25.10 Chediak–Higashi syndrome (CHS). Platelets from most patients with CHS are storage-pool deficient. However, some patients are only mildly abnormal. The cell in this illustration is from a patient with all of the features of CHS. However, his platelets contain about half the normal number of dense bodies (DB). × 30 000.

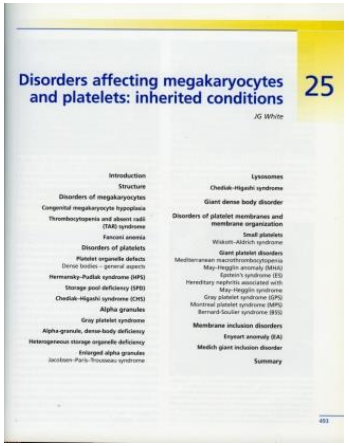

Disorders affecting megakaryocytes and platelets: inherited conditions 25

JG White

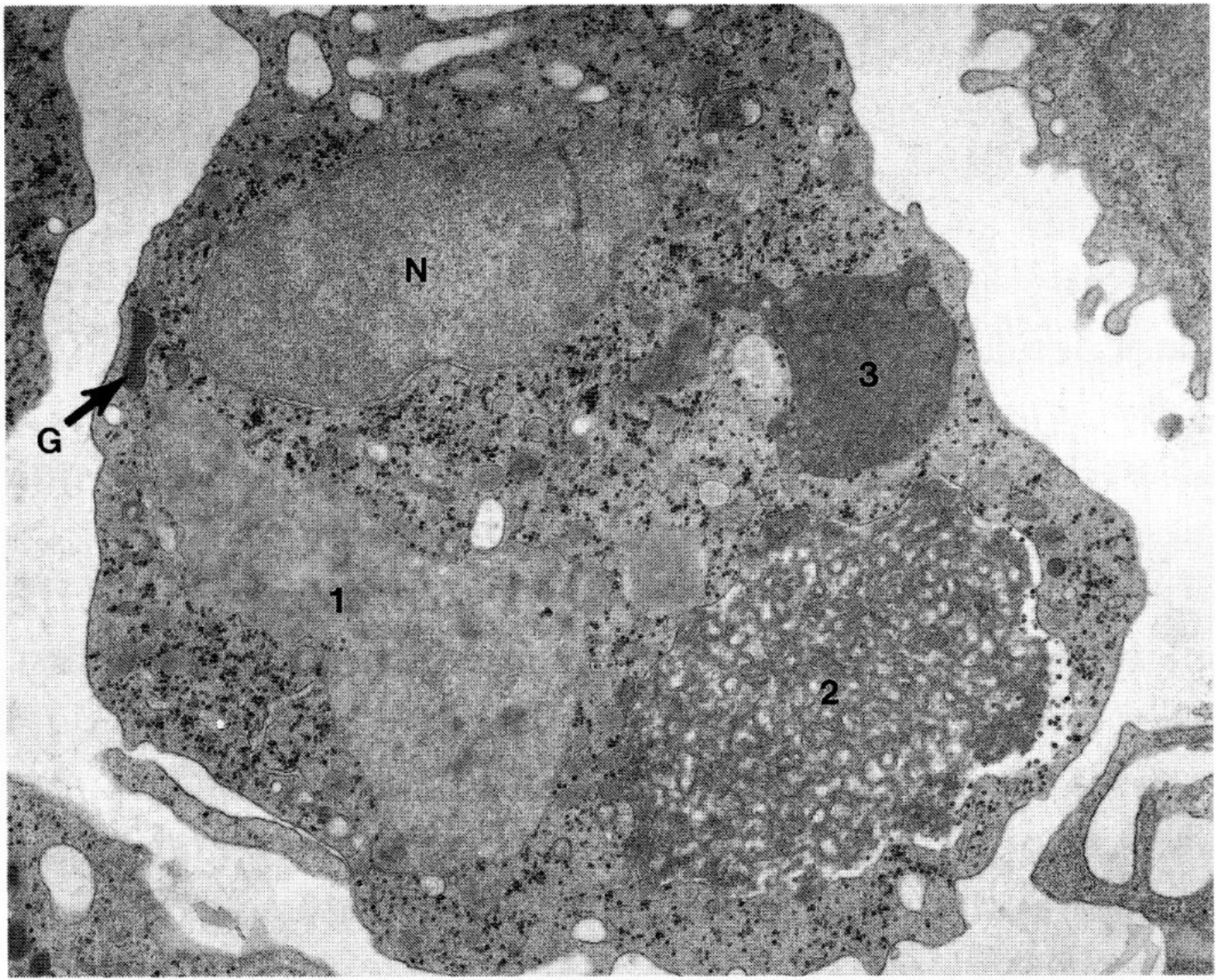

Fig. 25.9 Chediak–Higashi syndrome (CHS). Neutrophil from a patient with CHS. A nuclear lobe (N) and normal-sized granule (G) are dwarfed by greatly enlarged lysosomes (1,2,3). ×16 000.

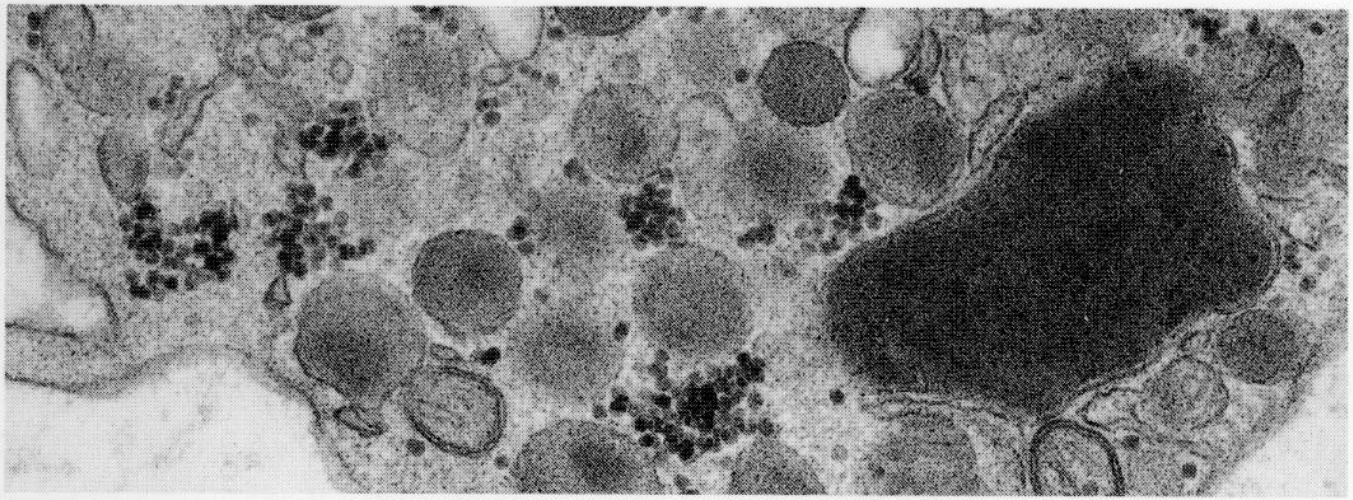

A

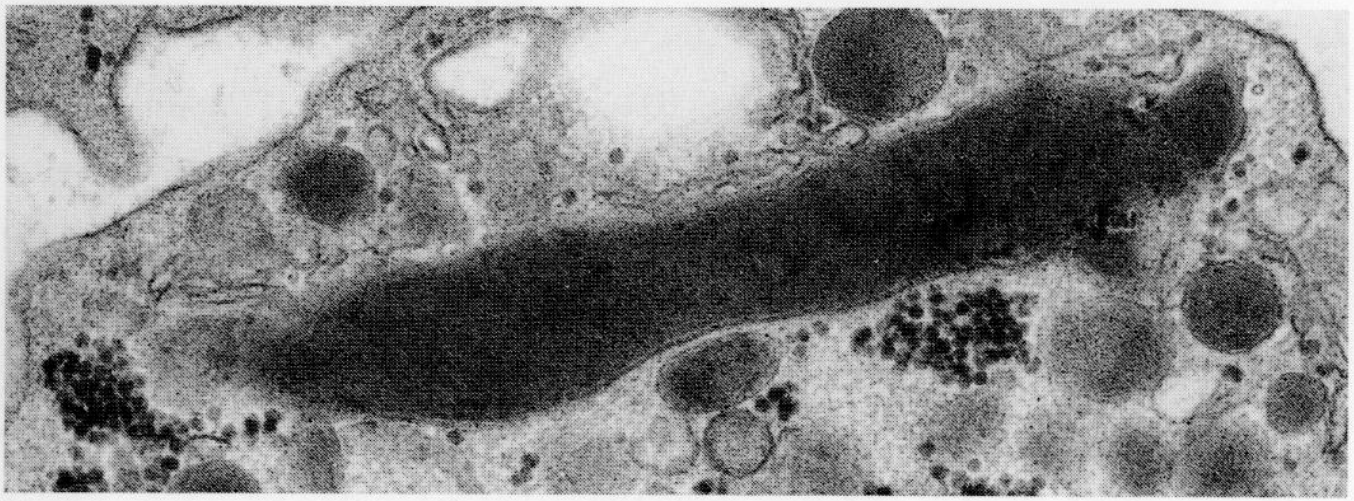

B

Fig. 25.11 (A,B) Chediak–Higashi syndrome (CHS). About 5% of platelets from patients with CHS contain giant granules. Incubation for acid phosphatase activity has shown that the giant granules in CHS platelets are lysosomes. A,B × 44 000.

Fig. 25.21 Chediak–Higashi syndrome (CHS). Platelet from patient with CHS reacted for acid phosphatase with cerium as the capture agent. A giant lysosome in the cell cytoplasm is positive for the hydrolytic enzyme activity. × 35 000.

New platelet pseudo-disorder

- Pseudo-ichthyosiform thrombocyte disorder or

Pilchard disease

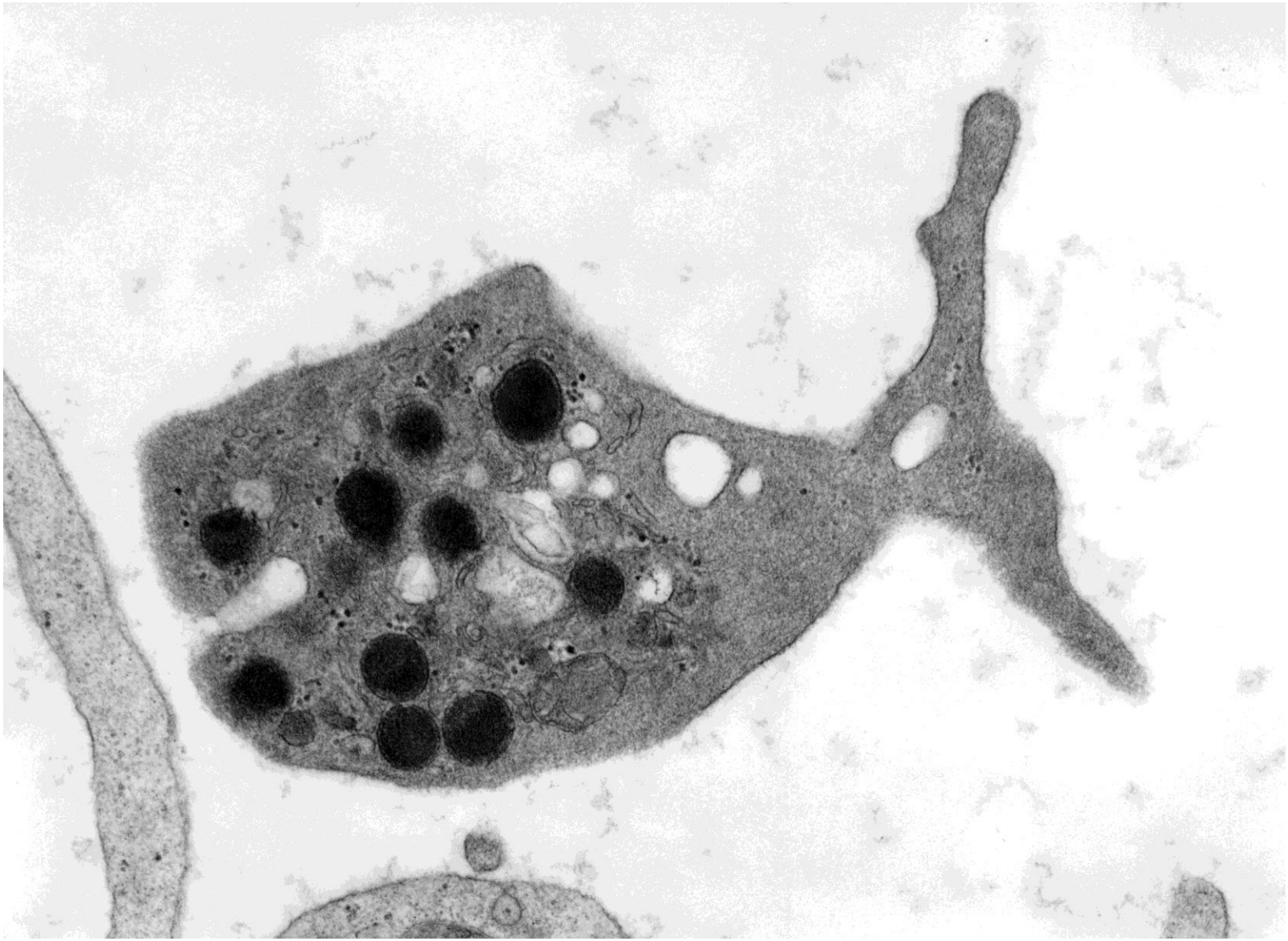

Pilchard disease